Investigation of the Influence of the Condition of Asphalt Pavement Surface on Road Safety of Rural Ontario Highways

by

Luciana Girardi Omar

A thesis submitted to the Faculty of Graduate and Postdoctoral Affairs in partial fulfillment of the requirements for the degree of

Doctor of Philosophy

in

Department of Civil and Environmental Engineering

Carleton University
Ottawa, Ontario

Abstract

Road collisions are complex events that are influenced by a combination of factors, including driver behaviour, environmental condition (e.g., icy and wet roads), road geometry, roadside elements, vehicle speed, tire deficiencies, traffic, and pavement condition. While the influence of some of these factors has been studied extensively for decades, the influence of pavement condition on road safety is relatively under-researched. This research investigated the influence of pavement surface condition on road safety by developing statistical models that correlate pavement surface condition and collisions. This research also examined the possibility to integrate skid resistance into pavement management by investigating the correlations between skid resistance, pavement distress, and operational conditions of the roads.

This study was limited to rural arterial and freeways of the Ontario asphalt pavement road network. Data of pavement condition, operational condition, and collision was obtained from the Ontario Ministry of Transportation for 6879 kilometers across 37 provincial rural highways for the period of 2012 to 2014. Pavement condition data was collected at network level with an automatic road analyzer road and included information about roughness, rutting, cracking, and macrotexture. Skid resistance data was collected with a locked wheel tester. The collected data was combined into a spatial data model, also known as a vector-based geographic information system.

The results of the investigation using regression analysis showed that pavement friction is affected by traffic, pavement age, and pavement distress. Skid resistance decreased with the increase of traffic and increased with the increase of pavement distress. Macrotexture increased with the increase of traffic and pavement distress.

The influence of pavement condition on road safety using statistical analysis and regression models indicated that collisions were lower for pavements in fair condition and greater for pavements in poor and good condition. Pavement texture also showed to be an important factor for collision classes that demanded satisfactory levels of macrotexture and pavement friction. In particular, greater levels of macrotexture contributed to a reduction in sideswipe and wet surface collisions.

Acknowledgments

I would like to express sincere gratitude to my supervisor Dr. Abd El Halim Omar Abd El Halim for his supervision, guidance, and financial support throughout this thesis. Without his support, this research would not have been possible.

I would also like to thank my professors, especially Dr. Yasser Hassan for his valuable collaboration about my research. I would also like to thank Mr. Steven Lee, Mrs. Susanne Chan, Mr. Sam Cui, Mrs. Magda Skinner, and Mrs. Sulaf Alkarawi of the Ontario Ministry of Transportation for providing the data necessary for this research.

I would like to thank my colleagues and members of the Department of Civil and Environmental Engineering, in particular my colleague Mr. Anandkumar Chelliah for his contributions to data collection for my research.

This research was supported financially by funds from the Ontario Ministry of Transportation, the Natural Sciences and Engineering Research Council, and Carleton University.

Finally, I would like to thank my family, especially my husband and sons for their support and understanding.

Table of Contents

List of Tables

List of Figures

1 Chapter: Introduction

This chapter presents background information about the research problem statement, gaps in the literature related to pavement condition and road safety, objectives, and scope of this study. This chapter also outlines the research plan and thesis organization.

1.1 Background

Canada is a large country with rural regions and urban centres separated by great distances. Highways and roads play a crucial role in delivering numerous social and economic benefits, including: integrating communities, facilitating access to education and health care, increasing mobility of people and goods, reducing transport costs, improving access to markets, increasing business and industrial opportunities, and increasing employment opportunities generated by the construction and maintenance of roads (Burningham and Stankevich, 2005). However, in order for these benefits to be sustainable, the serviceability of roadway pavements must be preserved. Serviceability considers that roadways are built for the comfort, convenience, and safety of road users (Canadian Strategic Highway Research Program, 1999; Lavin, 2003; Abd El Halim, 2009), and therefore reduced serviceability compromises ride quality and road safety (Canadian Strategic Highway Research Program, 1999; Haas *et al*., 2015).

In the last two decades, the Canadian government has begun to implement a long-term national strategy to make Canada's roads the safest in the world (Transport Canada, 2012). Despite this ambitious program, in the year 2012 there were 2,006 fatal collisions and 115,503 injuries reported across the country, which cost a total of CAD$37.4 billion, or the equivalent of 2.2% of Canada's gross domestic product (GDP) (International

Transport Forum, 2015). In the same year, in Ontario alone there were 505 fatal collisions and 43,484 injuries, of which 373 fatal collisions and 31,969 injuries occurred on dry surfaces, and 93 fatal collisions and 8,084 injuries occurred on wet surfaces (Ontario Road Safety Annual Reports, 2012). Run-off-the-road and skidding/sliding events were the most frequent types of events (Ontario Road Safety Annual Reports, 2012). This finding is relevant in light of studies that have found that poor road surface textures contribute to 20% to 35% of all wet-weather vehicle collisions (Hoerner and Smith, 2002; Ahammed, 2009; Ahammed and Tighe, 2012), while also influencing collisions in dry conditions, especially in situations that require braking and cornering (Swanlund, 2005; Snyder, 2006).

Pavement condition is not the only factor involved in road collisions, which are caused by a combination of factors, such as driver behaviour, environmental factors (e.g., icy and wet roads), road geometry, roadside elements, vehicle speed, tire deficiencies, and traffic (Tighe *et al.*, 2000; Henry, 2000; Hall *et al.*, 2009; Rezaei, 2010). While the influence of some of these factors on road safety has been studied extensively for decades, few studies examine the influence of general pavement condition on road safety (Chan *et al.*, 2009; Elghriany, 2016; Li and Huang, 2014). The majority of existing literature on road safety and pavement surface condition is restricted to studies comparing collision frequency and severity before and after maintenance activities (e.g., resurfacing), and studies examining a specific type of pavement surface distress – for example, differences in elevation between the pavement surface and the shoulder (pavement edge drop-off), depression in the wheel path (rutting), and irregularities in the pavement surface that affect ride quality (roughness) (Zeng *et al.,* 2014; Lee *et al.,* 2015).

1.2 Problem Statement

Road transportation is the most important mode for freight and passenger travel in Canada (Government of Canada, 2017). Despite the economic importance of the road transportation system and continuously increasing traffic volume, the Canadian roadway system has not grown significantly since last decade (Government of Canada, 2017). This is due to various factors, including environmental considerations, safety concerns, and limited financial funds for the maintenance of existing road infrastructure (Hein and Croteau, 2004; Government of Canada, 2017).

As the existing road infrastructure ages and deteriorates, the challenge to the Canadian government becomes maintaining an efficient road transportation system to support Canada's competitiveness using limited funds and without compromising road safety. Pavement deterioration decreases road serviceability and arguably influences road safety, although further evidence is needed to support this claim. The questions to be answered are: “Does the condition of pavement influence safety?”, “Are roads safer by maintaining pavement in excellent and good conditions?”, “Is it possible to incorporate safety into pavement management?”. The answers to these questions will help to guide transportation agencies to optimize expenditures for maintenance while reducing fatalities and serious injuries caused by road collisions.

1.3 Gaps in the Literature

Pavement surfaces deteriorate over time due to traffic loading and environmental conditions. The result is increased pavement roughness, pavement distress, and the polishing of aggregates that reduces skid resistance. However, the influence of pavement condition on road safety is not yet fully understood and relativelly under-examined

(Noyce *et al.*, 2007; Lee *et al.*, 2015).

Several studies investigated the effect of pavement condition on road safety with conflicting results. Some studies reported that collisions can be minimized by improving or maintaining adequate pavement conditions and those collisions were lower for pavement in good condition (Chan *et al.*, 2009; Li and Huang, 2014; Lee *et al.*, 2015; Elghriany, 2016). Yet, other studies reported that pavements in good condition were correlated with higher collision rates and severe and fatal collisions (Al-Masaeid, 1997; Buddhavarapu *et al.*, 2013; Li *et al.*, 2013; Li and Huang, 2014). Therefore, there is a need to investigate how the condition of pavements influences road safety in order to establish timely and cost-effective improvements that could reduce the number of vehicle collisions and fatalities.

There is also a gap in the literature related to the influence of pavement friction (skid resistance and macrotexture) on road safety. In particular, pavement friction-related data is often not fully integrated into pavement performance databases or into pavement performance models that are used for pavement management (Abd El Halim, 2009; McDaniel and Kowalski, 2012). The lack of integration of friction-related data in the pavement performance models is partly due to field measurements of skid resistance that require laborious tests using specific semi-automated devices, for example a locked wheel trailer; while the other indicators of pavement condition, including macrotexture, are measured with more consistency and frequency by semi-automated or automated devices.

Pavement performance databases and pavement performance models are composed of field measurements of indicators of pavement condition (e.g., roughness,

rutting, and cracks) collected at the network level using semi-automated and automated methods of pavement data collection. An example of a pavement condition data collection device that has been used by the Ontario Ministry of Transportation (MTO) since 2012 is the automatic road analyzer (ARAN). Despite its strengths, ARAN is not readily used for conducting comprehensive evaluations of pavement surface friction because it is not capable of measuring skid resistance. ARAN is capable of measuring only one of the surface textures that affects pavement friction, macrotexture, which is not included into pavement performance models.

Therefore, an investigation of the relationships between collisions and macrotexture, skid resistance, and other indicators of pavement condition could provide a way to integrate pavement friction into pavement management. This integration could contribute to management, decision-making in maintenance services, and road safety. Further, if skid resistance could be correlated to macrotexture and operational condition of roads, pavement friction management would be simpler and less costly for transportation agencies.

1.4 Research Objectives and Scope

Based on the above gaps, the main goals of this research are to improve road safety and to provide knowledge base to guide transportation agencies in roadway management and decision-making in maintenance services. This research investigated whether pavement condition influences road collisions and whether macrotexture could be used to integrate pavement friction into pavement management.

To achieve these goals, the following objectives were identified:

1. Investigate the relationship between skid resistance and macrotexture,

2. Investigate the influence of the type of mix and operational condition of the roads (e.g., traffic and loads, pavement age) on skid resistance and macrotexture,
3. Investigate the influence of pavement distress on skid resistance and macrotexture,
4. Based on the results of the above investigations, develop regression model (s) to predict skid resistance for Ontario roads,
5. Investigate the influence of the condition of pavement and macrotexture on collisions for rural arterials highways and freeways, and
6. Develop regression models to predict collision frequency for rural arterial highways and freeways using indicators of pavement condition as explanatory variables.

This research is limited to the Ontario asphalt concrete pavement road network and to a variety of functional classes of rural arterial highways and freeways that have speed limits of 80 km/h and 100 km/h. Intersections, rigid (e.g., Portland cement concrete pavements), and composite pavements are not included in this study.

The variables involved in the analysis are limited to those that were measured in the field by automated devices at the network level and readily available in MTO's inventory, such as operational condition of the roads, geometric features, indicators of pavement condition of the roads, and collision data. Variables related to driver and pedestrian behaviours and characteristics (e.g., age, health, and gender) were not included because they were considered beyond the scope of this study.

1.5 Research Plan

To achieve the objectives of this research, a working plan was established. The first step was to conduct a comprehensive literature review on the influence of pavement condition on road safety and development of prediction models for pavement skid resistance. The literature review provided an overview of concepts, theory, methodologies, and reference values of the principal indicators of pavement condition used by road agencies to assess pavement condition. The literature review demonstrated inconsistencies among the studies that became the motivation of this thesis.

Subsequently, data was collected and used to develop thesis framework consisting of three modules. The three modules included data integration, pavement friction, and road safety. The following sub-sections concisely describe each research module.

1.5.1 Module 1: Data Integration

The objective of Module 1 was to integrate data collected from different sources and formats and create a single data file. The data was obtained from several departments within the MTO and included operational condition of the roads (e.g., pavement type, traffic, loads, and years of service), geometric features of the roads (e.g., segment length and grade), measurement of indicators of pavement distress (e.g., roughness, rutting, and cracks), pavement friction (skid resistance and macrotexture), and collision data.

The measurements of pavement distress and roughness were used to calculate the overall condition of pavement, the pavement condition indicator (PCI). The measurements of macrotexture and skid resistance were used to calculate the international friction indicator (IFI). The parameters of operational condition and

geometric features of the roads were included in the investigation of correlations between pavement distress, pavement friction, and collisions.

The data from MTO was recorded using the linear highway referencing system (LHRS), which is a system that enables MTO to record information about the Ontario road network in a consistent format. The LHRS was used as reference to create a single database. This single database was created using the geographic information system (GIS), which permitted integration of spatial data (e.g., pavement condition measurements and collision data) and non-spatial data (e.g., traffic, type of pavement, and pavement age).

The single GIS data file was exported as *xls* file extension for use with Microsoft Excel. In this format, the data file was manipulated and exported to other formats to be used in data analysis and modelling.

1.5.2 Module 2: Pavement Friction

The objective of Module 2 was to investigate whether pavement friction could be integrated into pavement management by examining factors that affect pavement friction and to develop multivariate model (s) to predict skid resistance. First, it was examined if there were correlations between skid resistance, macrotexture, pavement distress (roughness, rutting, and cracks), and the operational condition of roads (traffic, type of mixes, and pavement ages). Further, the variables that showed a statistically significant influence on skid resistance were used to develop multivariate regression model (s) for skid resistance prediction.

To examine the relationships between variables, several statistical analyses were employed. The relationships were examined using simple linear and nonlinear

regressions and tests for the comparison of means (one-way ANOVA, t-test, and Tukey post hoc test). Regression models were developed using the ordinary least squares method (OLS). The models were evaluated through an analysis of residuals and multicollinearity and tested using the bootstrapping statistical technique.

1.5.3 Module 3: Road Safety

The objective of Module 3 was to investigate the influence of pavement condition on road safety. The condition of pavement was defined by the indicators of pavement distress, skid resistance, and macrotexture.

The pavements were categorized into three groups according to their level of pavement condition ("poor", "fair", and "good") and macrotexture ("low", "medium", and "high"). The collisions were categorized by severity (property damage only, fatal and injury), impact (single vehicle, sideswipe, rear-end), surface condition (wet, dry), and total number of collisions (all collisions regardless type of surface, impact, and surface condition).

The collision and traffic data were used to calculate the collision rates for each class of collision. The relationships between collision rates and the groups of pavement condition and macrotexture were examined using statistical tests for comparison of medians. The medians of the groups of pavements were compared and pairwise post hoc tests were performed to identify groups that differed statistically. The results of the statistical analysis were presented by class of roads (arterial rural highways and freeways).

Multivariate regression models were developed for collision frequency prediction using the negative binomial regression and the zero-inflated negative binomial

regression. The models were tested using the bootstrapping statistical technique.

1.6 Thesis Organization

This thesis is organized into six chapters, as can be seen in Figure 1.1. Chapter 1 presented the rationale of the present work and introduced the research objectives and the research plan. Chapter 2 provides a literature review relevant to this research. Chapter 3 expands on research design, data collection, and data integration. Chapter 4 presents and discusses (1) the results obtained from the analysis of factors that affect pavement friction and (2) the development of predictive models for skid resistance. Chapter 5 presents and discusses the results obtained from the investigation of the influence of pavement condition on road safety. Finally, Chapter 6 includes conclusions, recommendations, and suggestions for future research and consideration.

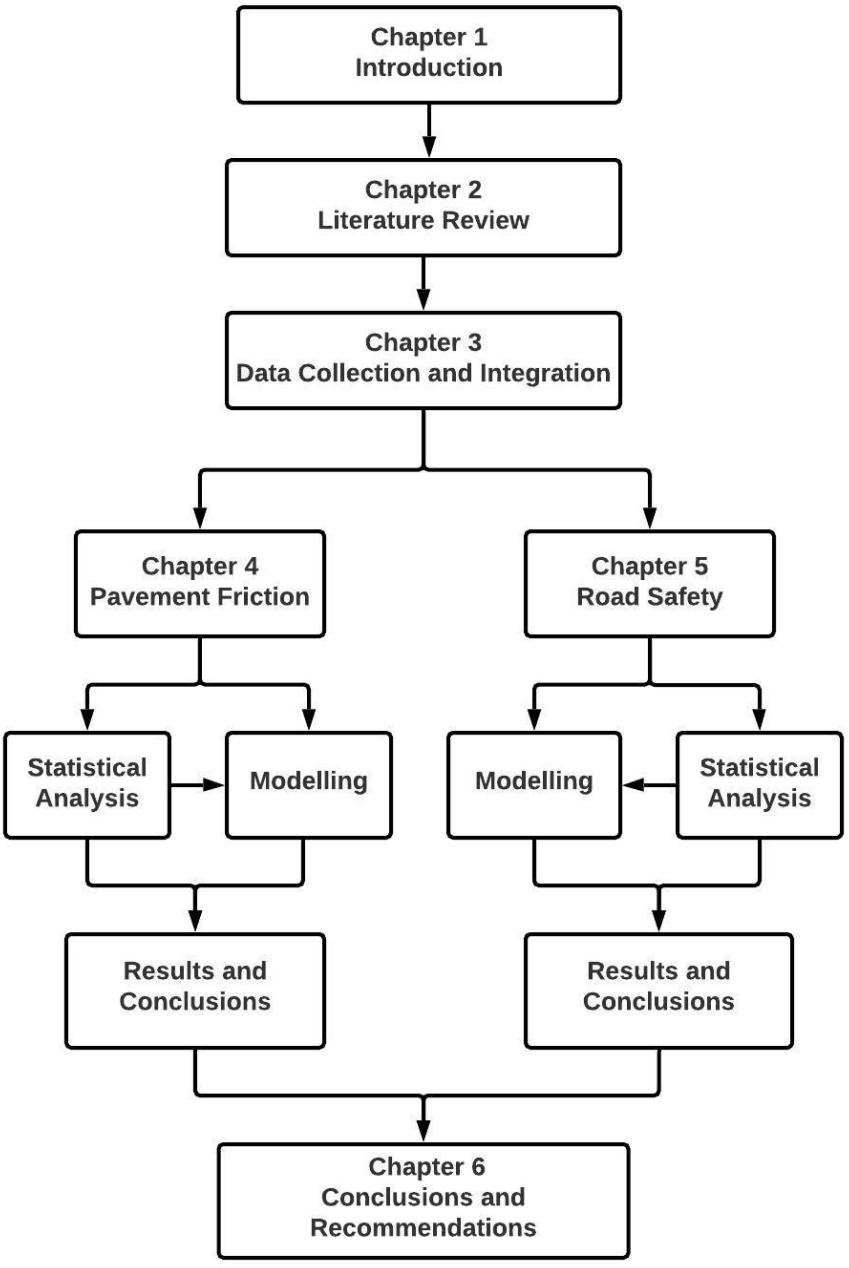

Figure 1.1 Thesis Organization

2 Chapter: Literature Review

This chapter begins with an overview of the indicators of pavement surface condition – roughness and pavement distress – and a more in-depth review of the concept of pavement surface friction. This is followed by a comprehensive literature review of studies that estimated skid resistance based on pavement characteristics and operational condition of the roads. The chapter closes with a review of studies that examine the relationship between pavement condition and road safety.

2.1 Pavement Surface Condition

Research in pavement surface condition considers the performance and physical condition of a pavement section or an entire network. Road agencies perceive the pavement surface condition as an indicator of the overall condition of the road and use a condition rating to determine road deficiencies and inadequacies in programming maintenance and rehabilitation services. In Ontario, surface condition ratings are based on two measures: roughness and distress (MTO, 2007; Jannat and Tighe, 2015). These two measures are described in the following sections, followed by a description of pavement surface condition indicators. Friction, a third measure of pavement surface condition, is considered an independent indicator of pavement condition since it is not integrated into the pavement condition index (PCI), the principal indicator used by the road agencies to define the condition of pavements.

2.1.1 Roughness

The Federal Highway Administration (FHWA) recognizes roughness as an important pavement performance indicator in pavement maintenance and rehabilitation process, and the principal indicator of ride quality (FHWA, 2014; Haas and Hudson,

2015). In addition, studies found that pavement roughness is a contributing factor to road safety (Al-Masaeid, 1997; Anastasopoulos *et al.*, 2008; Chan *et al.*, 2009; Sharif *et al.*, 2017).

In technical terms roughness is defined by the American Society for Testing and Materials (ASTM) as "the deviation of a surface from a true planar surface with characteristic dimensions that affect vehicle dynamics and ride quality" (ASTM, 2012b). Roughness refers to irregularities in the pavement surface that exhibit texture wavelengths longer than 500 mm (wavelength measurement thresholds are used to define different levels of pavement surface texture).

There are several methods and techniques for measuring pavement roughness. Currently, for roughness evaluations at the road network level, road agencies use laser-sensors attached to a bar located in the front of a truck to measure the longitudinal profile of the pavement. The laser-sensors capture the pavement surface deviation in both the left and right wheel paths. The measurements are used as input for an algorithm that calculates the deviations in either m/km or in/mi. Pavement roughness is then computed from a single longitudinal profile using computer programs (FHWA, 2014).

Various indicators are used to define pavement roughness. The most common indicators are the Present Serviceability Index (PSI), the Ride Comfort Index (RCI), and the International Roughness Index (IRI). Of the three, the IRI is the most widely used in North America (Ashraf and Jurgens, 2000). Figure 2.1 shows lower IRI values for new pavements (from 1.5 to 3.5 m/km) and higher IRI values for older pavements (from 2.5 to 6.0 m/km).

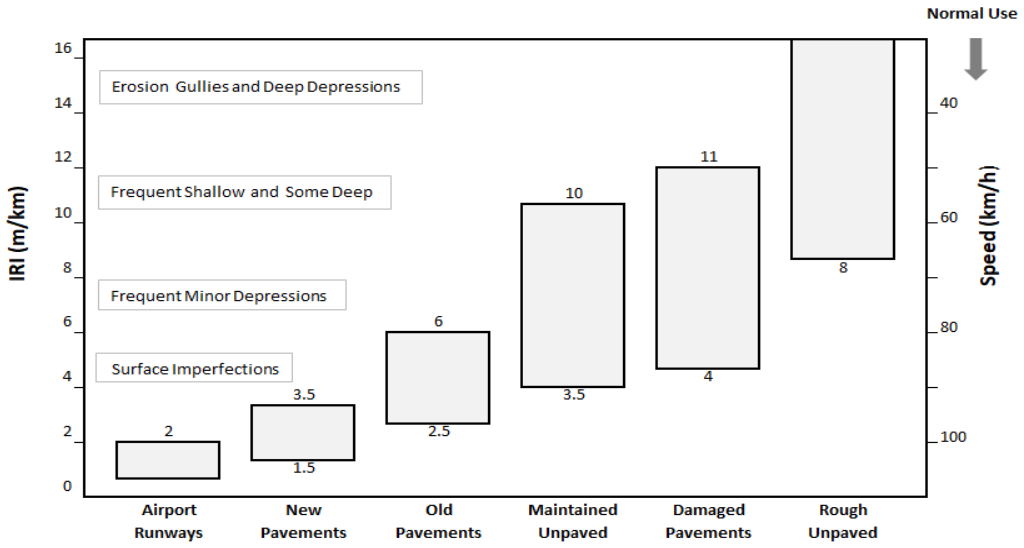

Figure 2.1 Range of IRI Values (Adapted from Sayers *et al.*, 1986)

2.1.2 Pavement Distress

Pavement distresses are visible signs of pavement surface deterioration and indicate various types of pavement damages caused by construction, environmental and climatic conditions, and traffic loading. Pavement suffering severe distress can compromise road safety by affecting drivers' control of their vehicles (Jo and Ryu, 2015; Madli *et al.*, 2015). For example, surface irregularities may influence a driver's behaviour that may change his/her trajectory, for example, swerving to avoid a pothole. This maneuver can result in vehicle collisions and run-off-the-road events (Jiang *et al.*, 2013). Rutted wheel paths can also be a safety problem when, for example, water accumulates in the rut paths and creates a layer of water between the tires and the pavement, which can cause a driver to lose control in what is known as hydroplaning (Fwa *et al.*, 2011; Cenek *et al.*, 2014). Deep rut paths can be additionally dangerous if it requires extra effort to get

out of the rut channel, which may affect overall vehicle manoeuvrability and stability (Chan *et al.*, 2009; Elvik *et al.*, 2009).

Pavement distress manifestations are categorized into three groups: 1) surface defects (e.g., aggregate loss such as ravelling, 2) surface deformation (e.g., rutting), and 3) cracking (e.g., fractures of the pavement surface) (MTO, 2016b). The Manual for Condition Rating of Flexible Pavement prepared by the MTO provides standards for each type of distress manifestation (MTO, 2016b). As stated in the MTO's guidelines, each type of distress is evaluated and rated according to the degree of severity and density of occurrences. The severity of observed distress is based on a five-level rating system: very slight, slight, moderate, severe, and very severe (MTO, 2016b). Density, meanwhile, describes the extent of the occurrence based on the percentage of area affected or the length of distress – specifically, according to the width, depth, and/or diameter of each different type of distress manifestation (MTO, 2016b). Density also has a five-level rating system based on the percentage of the area affected:

1. Few (less than 10% of the pavement surface affected)
2. Intermittent (between 10% and 20% of the pavement surface affected)
3. Frequent (between 20% and 50% of the pavement surface affected)
4. Extensive (between 50% and 80% of the pavement surface affected)
5. Throughout (greater than 80% of the pavement surface affected)

For example, the severity of rutting of a wheel path would be considered moderate if the rut depth ranged between 14 mm to 19 mm. The density of this wheel path rutting would be extensive when the length of the rutting extended for 50% to 80% of the total length of the segment.

2.1.2.1 Surface Defects

The three types of surface defects are ravelling, segregation, and flushing. Ravelling is the loss of bond between the aggregate and asphalt binder (Chong *et al.*, 1989). Ravelling can be caused by the penetration of moisture into the pavement that affects the adhesion between aggregates and binder, poor adhesion of asphalt content, high air voids, insufficient asphalt content, poor compaction, poor construction, disintegration of particles, fracture of the particles caused by traffic or natural causes (Chong *et al.*, 1989; MTO, 2016b).

Segregation is related to construction deficiencies resulting in areas with an irregular distribution of coarse and fine aggregates. Segregation can be caused by poor construction, placement of segregated hot mix, and thermal segregation (MTO, 2016b).

Flushing, also known as bleeding, is characterized by the excess of bituminous binder on the pavement surface. It often occurs in the wheel paths during the hot weather (MTO, 2016b). Flushing can be caused by excessive asphalt content relative to void in the mineral aggregate and paving over excess primed surfaces (MTO, 2016b).

2.1.2.2 Surface Deformation

The three types of surface deformation are shoving, rutting, and distortion. Shoving is characterized by longitudinal displacements (i.e., undulations) of a specific area of the pavement. Shoving is common in areas of heavy traffic on a steep downgrade or upgrade, horizontal curves, and intersections. Shoving can be caused by a lack of bond between the asphalt surface and underlying layers, heavy traffic, an unstable granular base, poor construction, inadequate asphalt mix, movements of braking, acceleration and turning at intersections (MTO, 2016b).

Rutting is characterized by longitudinal depressions in the pavement that occur within the wheel path of vehicles (FHWA, 2009). Rutting usually appears as single or double longitudinal ruts in the wheel paths, accompanied by small projections to the sides. They result in permanent deformation combined with a displacement of pavement. Rutting can be caused by a lack of lateral support (i.e., unstable shoulder), poor compaction, an unstable granular base and subbase, an unstable asphalt mix, overstressed subgrade, and wear from studded tires (MTO, 2016b).

The last subgroup classification of surface deformation, distortion, is characterized by any deformation of the pavement surface shape not classified as shoving or rutting. Distortion can be due to lack of subgrade support, differential frost heave, differential settlement of subgrade, slope defects, culvert deficiencies, and loss of granular into rock fill (MTO, 2016b).

2.1.2.3 Cracking

Cracking is the third type of pavement surface distress and includes seven main subgroups (MTO, 2016b):

- Longitudinal wheel cracking – cracks that follows a path parallel to the centre line of the pavement and close to the centre of the wheel paths.
- Longitudinal meander cracking – single cracks that wander from one edge of the road to the other, or cracks parallel to the centre line of the lane.
- Centre line cracking – cracks that run in the joints close to the road centre line.
- Edge cracking – cracks longitudinal cracks that develop within 30 cm and 60 cm of the pavement edge line.
- Transverse cracking – cracks that occur perpendicular to pavement centre line.

- Map cracking – cracks that combine transverse and longitudinal cracks to form a series of large polygons that resemble a map.
- Alligator cracking – cracks that present an interconnected network of polygon blocks resembling the skin of an alligator.

Cracking can be caused by several factors, including repeated traffic loading, fatigue of thin asphalt, frost actions, thermal shrinkage, deficiencies in the base stability, reflection cracks, deficiencies in the mix design, poor construction, poor drainage, moisture infiltration, inadequate road width, and compaction (Said *et al*., 2008; MTO, 2016b).

2.1.3 Pavement Condition Indicators

This section describes the two pavement condition indicators, the Distress Manifestation Index (DMI) and the Pavement Condition Index (PCI). Both are used by MTO to rate the surface condition of asphalt pavement.

The Distress Manifestation Index (DMI) indicates a pavement's surface distress level based on pavement distress information collected in the field. The DMI is calculated using the type of distress, severity, density, and a set of predefined weight values for each distress (Kazmierowski *et al.*, 2001; Ningyuan *et al*., 2011). The weight values represent the importance given to a specific distress defined by the maintenance personnel (Grivas *et al*., 1992).

In Ontario, the DMI is typically calculated for an individual pavement section of 10 km length and uniform performance (Ningyuan, 2009). The DMI scale ranges from 0 to 10, where 0 indicates the worst condition and 10 is the excellent condition (Ningyuan, 2009). Since 2006, the traditional way of to calculate DMI has been reviewed by a team

of researchers from the Centre for Pavement and Transportation Technology at the University of Waterloo and MTO. The objective of the study was to review existing pavement distress practices and rationalize amount of distress to be use for surveying pavement distress at network level using semi-automated and automated technologies (Chamorro *et al.*, 2009; Chamorro *et al.*, 2010; Chan *et al.*, 2016).

As a result of years of research, the traditional DMI used by the MTO for manual data collection was modified and new approaches to calculate DMI for network level were introduced (Chamorro *et al.*, 2009; Chamorro *et al.*, 2010; Chan *et al.*, 2016). The traditional DMI contrasts with the new DMIs in three main adjustments. First, the number of distress considered in the traditional DMI was reduced depending of surface type (asphalt, concrete, composite, and treated) (Chamorro *et al.*, 2010; Chan *et al.*, 2016). Second, the extent of distress was considered as the percentage of damaged pavement surface considering that 1 m of cracking is equivalent of to 1 m^2 of damaged surface (Chamorro *et al.*, 2009; Chamorro *et al.*, 2010). The distress densities were presented as areas, which makes possible to compute the percentage of the total area of the section affected by each distress on the basis of the section length and section width (*Chan et al.*, 2016). Third, the severity levels were classified on a three-level scale: slight, moderate and severe (Chamorro *et al.*, 2009; Chamorro *et al.*, 2010; Chan *et al.*, 2016).

The traditional DMI and an example of a new DMI (DMI_{NT}) for application at the network level using semi-automated and automated technologies are given in Equation 2.1 and 2.2 (Ningyuan *et al.*, 2011; Chamorro *et al.*, 2010). The individual distress weight, level of severity, and density given by MTO guidelines for the traditional DMI and for the adjusted DMI (DMI_{NT}) are shown in Appendix A (Ningyuan *et al.*, 2009;

Chamorro *et al.*, 2009; Chan *et al.*, 2016).

$$DMI = 10 \times \frac{DMI_{MAX} - \sum_{i=1}^{n} w_i \ (s_i + \ d_i)}{DMI_{MAX}} \quad \textbf{(2.1)}$$

$$DMI_{NT} = 10 - \sum_{i=1}^{n} \beta_i \times Disstress\ \%_i \quad \textbf{(2.2)}$$

Where i = distress type *i,* n = number of distress, w_i = weighting factor assigned to distress i, s_i = severity level of distress i, d_i = distress extent of i^{th} distress (%), DMI_{MAX} = maximum value theoretically assigned to an individual pavement distress. The DMI_{MAX} is a constant value based on different pavement types, β_i = parameters defined per distress type, and Distress% *i* = distress percentage per distress type (*i*).

The Pavement Condition Index (PCI) was originally developed by the U.S. Army Corps of Engineers and later standardized in the ASTM D5340 (ASTM, 2012a). The PCI rates the condition of the surface of a road network and identifies roads that are exhibiting distress. This rating is used to: (1) identify maintenance and rehabilitation needs, (2) monitor the pavement condition over time, (3) develop a network preventive maintenance strategy, (4) develop road maintenance budgets, and (5) evaluate pavement materials and designs.

Specifically, the PCI measures the type, extent, and severity of pavement surface distress (typically cracks and rutting), and the roughness (ride comfort) of the road. The PCI provides a numerical rating between 0 and 100 (where 0 is the worst condition and 100 is the excellent condition) for the condition of road segments within the road network using pavement distress surveys on a sample of the network. The PCI score is calculated using IRI and DMI values. In Ontario, the formula used to calculate the PCI for asphalt

pavement is given by Equation 2.3 (Jannat and Tighe, 2015; Chan *et al.*, 2016).

$$PCI = 13.75 + 9 \times DMI - 7.5 \times IRI \quad \textbf{(2.3)}$$

Where PCI = Pavement Condition Index ranging from 0 to 100, IRI = International Roughness Index, and DMI = Distress Manifestation Index (ranging from 0 to 10).

2.2 Pavement Surface Friction

Pavement surface skid resistance, or pavement friction, is considered one of the most important indicators of road safety (Hall *et al.*, 2009). In general, driver control is related to the friction available at the tire-pavement interface; the higher levels of friction lead to greater vehicle control (Hall *et al.*, 2009). Briefly, friction refers to the force that opposes the movement between tire and pavement surface (Hall *et al.*, 2009).

The next sections expand on the frictional force analysis and on the mechanisms of friction, followed by a more in-depth treatment of the concept of pavement surface texture, factor affecting friction, and approaches to its measurement. Finally, friction indicators will be described.

2.2.1 Frictional Forces at Tire-Pavement Interface

Pavement friction is defined as "the force that resists the relative motion between a vehicle tire and a pavement surface" (Hall *et al.*, 2009). The resistive force is generated at the tire-pavement interface to oppose longitudinal rolling or sliding when braking forces are applied to the tires and sideways when a vehicle steers around a curve (Wang, 2006). The resistive force is expressed as the non-dimensional coefficient of friction expressed by the ratio of the frictional force between the tire and the pavement surface to the perpendicular force (normal force).

For highway design and pavement managements, frictional forces are analyzed in two components, longitudinal and transverse, as described below. The longitudinal friction component represents the forces that occur between the pavement surface and the rolling tire when operating in the free rolling or constant-braked mode (Hall, *et al.*, 2009). In the free-rolling mode, the relative speed between the tire circumference and the pavement surface, also referred as the slip speed, is equal zero because the average peripheral speed of the wheel is equal to vehicle speed. In the constant-braked mode, the slip speed increases from zero to a maximum of the vehicle speed. The slip speed is calculated by Equation 2.4 (Hall *et al.*,2009).

$$S = V - Vp = V - (\omega \times r) \quad \textbf{(2.4)}$$

Where S = slip speed, V = vehicle speed, Vp = average peripheral speed of tire, ω = angular speed of the tire, and r = average radius of tire.

The relationship between the vehicle speed (V) and the average peripheral speed (Vp) of the tire can be also expressed as slip ratio (SR). The slip ratio is expressed in a percentage, as calculated by Equation 2.5 (Hall *et al.*, 2009).

$$SR = \frac{(V - Vp)}{V} \times 100\% \quad \textbf{(2.5)}$$

In the free rolling mode, the average peripheral speed of the tire is equal to the vehicle speed and the slip ratio is equal to zero. In the locked-wheel mode, the average peripheral speed of the tire is equal to zero and the vehicle speed is not equal to zero and the slip ratio is 100%. This condition occurs during sudden braking, where the vehicle

loses traction and does not respond to the driver's command.

Variation in the tire slip affects the coefficient of friction at the tire-pavement interface. The coefficient of friction increases rapidly with increasing slip to a peak value (Hall *et al.*, 2009; Flintsch *et al.*, 2012). The peak value normally occurs when the tire slip is between 10 to 20% (critical slip) (AASHTO, 2008). After that, the coefficient of friction starts to decrease to a value known as the coefficient of sliding friction. At the maximum slip of 100%, the tire is fully locked, and the vehicle is skidding, see Figure 2.2 (AASHTO, 2008; Flintsch *et al.*, 2012).

Vehicles with an anti-lock braking system (ABS) are designed to activate the brakes on and off repeatedly before the coefficient of friction reaches the peak friction. The ABS is designed to turn off before the peak friction is reached and below critical slip.

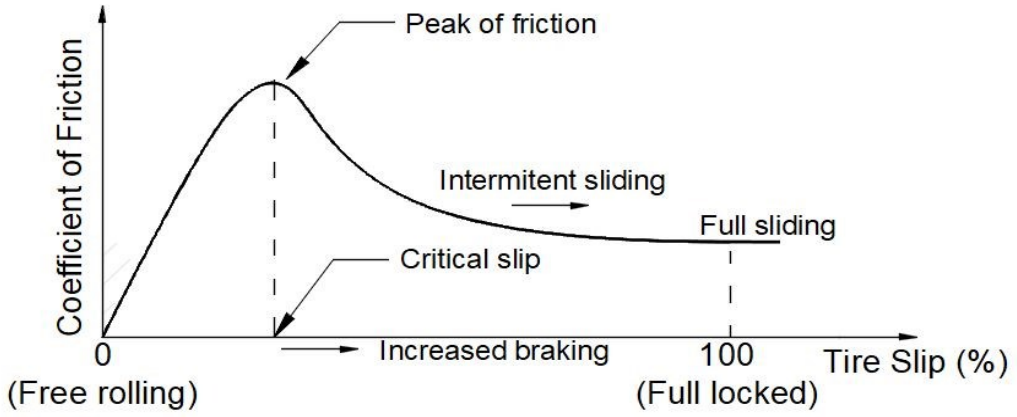

Figure 2.2 Pavement Friction and Tire Slip (Adapted from AASHTO, 2008)

The transverse friction force, also called side-force friction, affects the dynamic stability of vehicles, especially on horizontal curves in which the demand for friction

increases with an increase in speed. Side-force friction is generated when a vehicle changes direction, e.g., steering around a curve or changing lanes. It also occurs to compensate for limited pavement superelevation and/or crosswind effects (Hall *et al.*, 2009).

Side-force friction is the ratio of the transverse force (Ff) and the weight force (W) perpendicular to the pavement. In a curve, side-force friction acts to counterbalance the centripetal force (Fc) that develops as the vehicle steers a curve. Figure 2.3 shows a diagram of the forces acting on the vehicle as the vehicle steers a curve without and with superelevation.

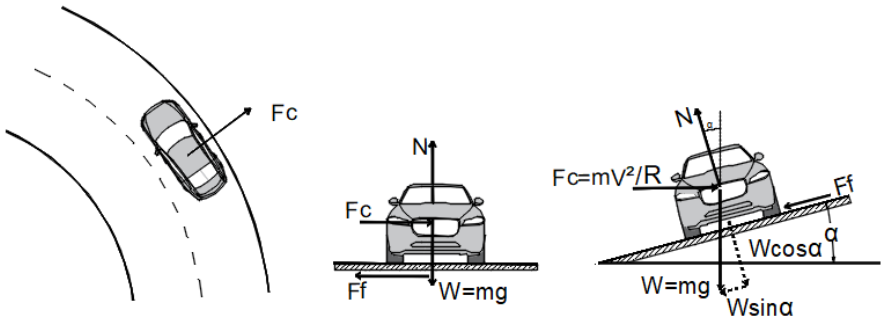

Figure 2.3 Forces Acting on a Vehicle on a Curve without and with Superelevation

Side-force friction is a function of several factors, including pavement surface texture, vehicle speed, and superelevation. The side-force friction provides safety by maintaining the vehicles from sliding (Bonneson, 2000; Voigt *et al.*, 2003). The vehicle may slide when the coefficient of friction is relatively low, as on wet and icy roads.

The relationship between the forces acting on the vehicle tire as the vehicle steers

a curve is given by coefficient of side friction, Equation 2.6 (TAC, 1999; Garber and Hoel, 2015).

$$ft = \frac{V^2}{127 \times R} - e \qquad \textbf{(2.6)}$$

Where ft = coefficient of side friction, V = vehicle speed in km/h, R = radius of horizontal curve (m), and e = road superelevation.

2.2.2 Pavement Surface Texture and Mechanisms of Friction

The two main mechanisms involving pavement friction in tire-pavement interface are adhesion and hysteresis (Kummer, 1966; Hall *et al.*, 2009). The two mechanisms are illustrated in Figure 2.4.

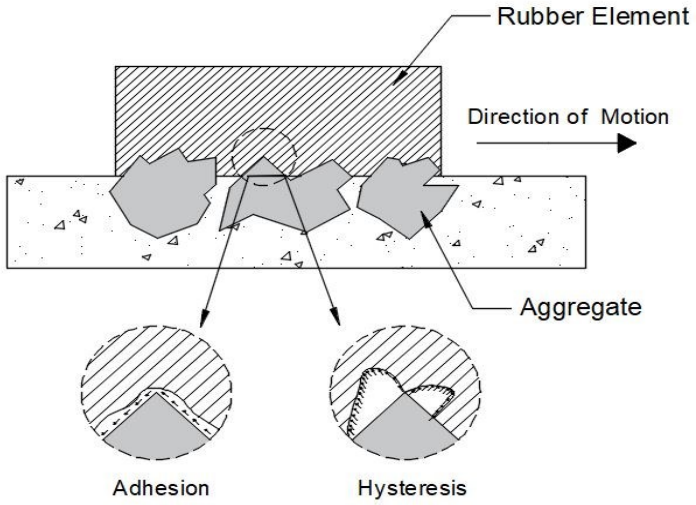

Figure 2.4 Mechanism of Pavement-Tire Friction (Adapted from FHWA, 2015)

Adhesion and hysteresis forces are fundamentally dependent on pavement surface characteristics, tire-pavement contact, and the properties of the tire (Hall *et al.*, 2009). In

addition, both forces are affected by temperature and sliding speed due to the visco-elastic property of rubber tires (Hall *et al.*, 2009). Adhesion is due to the contact between the tire and the surface of the pavement and is a function of shear strength and contact area. Hysteresis force is the result of energy loss (dissipated heat) due to bulk deformation of a rubber tire; this deformation is referred to as enveloping of the tire around the texture (Hall *et al.*, 2009).

Adhesion and hysteresis are not necessarily independent. On wet pavements, adhesion force decreases with the increase of speed, while hysteresis force increases with the increase of speed (Smith, 2008; FHWA, 2015). An increase in hysteresis force due to the increase of speed may account for over 95% of the friction at speeds above 105 km/h (Hall *et al*., 2009).

A situation in which adhesion is reduced and friction is predominantly governed by hysteresis forces occurs when an enormous heat is generated at the tire-pavement contact under severe conditions of tire rubber sliding (Sakai and Araki, 1999). In this case, a thin layer between the asphalt and the tire is created by the melting rubber, which affects tire-pavement contact by reducing adhesion forces and increasing hysteretic forces (Sakai and Araki, 1999).

2.2.3 Factors Affecting Tire-Pavement Friction Interaction

There are many factors that can influence pavement-tire friction interaction (Wallman and Astrom, 2001; Hall *et al.*, 2009). These factors can be categorized into five main groups: (1) pavement surface texture, (2) vehicle speed, (3) tire characteristics, (4) traffic, and (5) environmental factors. The influence of each of these factors is discussed in the following sections.

2.2.3.1 Pavement Surface Texture

Pavement surface texture is defined by the International Organization for Standardization (ISO) and the American Association of State Highway and Transportation Officials (AASHTO) as "the deviations of the pavement surface from a true planar surface" (ISO, 2002; AASHTO, 2008) Texture wavelength describes the horizontal dimension of the roughness of a texture profile, which is expressed in meter (m) or millimeter (mm) (ISO, 2002). Pavement deviations are categorized into four levels according to texture wavelength, where:

- Microtexture: wavelength < 0.5 mm, amplitude 0.001 mm to 0.5 mm
- Macrotexture: wavelength > 0.5 mm to 50 mm, amplitude 0.1 mm to 20 mm
- Megatexture: wavelength > 50 mm to 500 mm, amplitude 0.1 mm to 50 mm
- Roughness or unevenness: wavelength > 500 mm

Pavement texture affects the interface between the tires of a vehicle and the pavement surface. For instance, pavement friction is provided through a combination of two surface texture properties, microtexture and macrotexture (Kummer, 1966; Hall *et al.*, 2009; AASHTO, 2008). Megatexture and roughness are associated with pavement distress and ride-related qualities, such as, splash spray, rolling resistance, level of noise, vibration, fuel consumption, and tire wear (Noyce *et al.*, 2007; AASHTO, 2008).

Microtexture is associated with the scale texture of the individual aggregate and is dependent on the physical nature of the aggregates (i.e., surface texture). Microtexture is provided by the surface of coarse aggregates or by the fine aggregates for concrete and bituminous surfaces (Flintsch *et al.*, 2012). Poor levels of microtexture imply a low level of skid resistance at most speeds (Glennon and Hill, 2004). Excellent levels of

microtexture allow a good level of skid resistance at low and high speeds, except on flushing surfaces, where there is no macrotexture (Glennon and Hill, 2004).

Macrotexture is related to the height, width, angularity, and density of macro projection above the surface. Macrotexture is usually assessed by the depth of the peaks of large aggregates. Macrotexture allows the drainage of water through channels formed by large aggregates or by grooves cut into the pavement surface. The level of pavement macrotexture is arguably correlated with the level of skid resistance, where a good level of macrotexture tends to give good levels of skid resistance at high speeds. Limited macrotexture associated with polished aggregate and combined with speed, tire pressure, and water depth affects the susceptibility of a vehicle to hydroplaning (Glennon and Hill, 2004). Hydroplaning occurs when the tire and the pavement are separated by a thin film of water, causing the vehicle to skid without any resistance.

2.2.3.2 Influence of Aggregate on Pavement Texture

The microtexture and macrotexture of the pavement surface are influenced by aggregates, binder, mix properties, and the type of texturing applied over the surface. Several studies demonstrated that the skid resistance of pavement texture differs based on its microtexture and macrotexture: microtexture is mainly affected by the coarse aggregate shape and mineralogy characteristics, while macrotexture is affected by other factors, such as maximum aggregate size, type of coarse and fine aggregates, mix gradation, compaction method, air content, and binder (Leu and Henry, 1978; Kandhal and Parker, 1998; Henry, 2000; Zaniewski and Mason, 2006; Masad *et al.,* 2007).

Greater levels of pavement surface texture are obtained when fine and coarse aggregates present irregular shapes and angular and cubical edges (Rado, 2009). This

improvement is due to the fractured faces of coarse aggregates that improve the stability of the mixture and produce a deeper macrotexture (Shaffer *et al.*, 2006). Whether the aggregates remain angular during wearing and polishing from traffic is determined by the mineral composite of the aggregates' source (Zaniewski and Mason, 2006). In asphalt mixes, the presence of flat and elongated aggregates results in lower macrotexture depth because the aggregates tend to orient themselves horizontally (AASHTO, 2008; Rado, 2009).

2.2.3.3 Vehicle Speed

Pavement friction on wet surfaces decreases with an increase in vehicle speed (Flintch *et al.*, 2012). As the speed increases, the contact between the tire and the pavement is reduced, which affects the adhesion force. A decreased rate of friction is further influenced by the type of pavement surfaces and their characteristics, such as tire tread pattern, tire width, tire compound, tire inflation pressure and loads.

The influence of a pavement surface's microtexture and macrotexture on pavement friction differs with different sliding speeds (Flintch *et al.*, 2002). Figure 2.5 shows how different levels of microtexture and macrotexture have different effects on the coefficient of friction. At a low speed, a high level of microtexture shows a greater influence on the coefficient of friction (Point A and Point C); however, as the speed increases at the speed limit, a higher level of macrotexture shows more influence on the coefficient of friction than higher levels of microtexture (Point B and Point D).

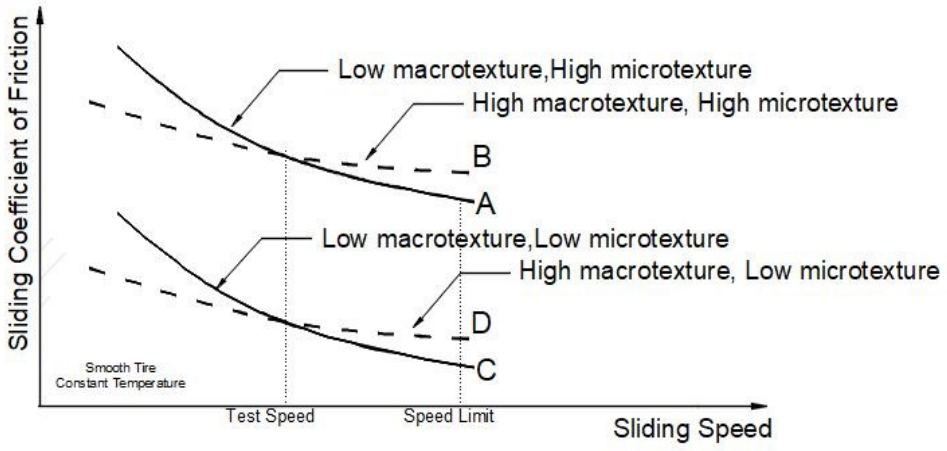

Figure 2.5 Effect of Microtexture and Macrotexture on Pavement Friction at Different Sliding Speeds (Adapted from Flintch *et al.*, 2002)

2.2.3.4 Tire Characteristics

Tire characteristics and tire condition play an important role on skid resistance because the tires provide the connection between the vehicle and the pavement surface. Tire characteristics are defined by tread patterns, inflation pressure, and tire stiffness.

The contact area, or the footprint of a tire, is defined by the area of the tread in contact with the pavement (Guiggiani, 2014). It is in this area that forces are transmitted between the tire and the pavement. A tire's tread contributes to draining water and removing contaminants from the pavement surface. Tire treads have a similar function to macrotexture, where a tire with low tread depth increases the vehicle's risk of hydroplaning and reduces traction on wet and snowed surfaces (Gunaratne *et al.*, 2012).

Tire inflation pressure also influences the tire contact area with the pavement surface. The contact area is proportional to inflation pressure, loads, and temperature (Transportation Research Board, 2006; Guiggiani, 2014). The tire contact area decreases

with an increase in tire inflation pressure and increases with an increase in tire loads (Fernando *et al.*, 2006). Further, tire pressure changes with temperature, where lower temperatures lead to lower tire pressure and higher temperatures to higher tire pressure. This is because the air in tires expands with warmer temperatures and contracts with colder temperatures.

Low tire pressure affects the distribution of the load on the tire, which may contribute to increased tire deformation, increased lateral forces on the contact area, and increased rolling resistance (Cordos *et al.*, 2017). An increase in contact due to increased rolling resistance can have negative effects on the tire, such as excessive tire heating and premature wear of the tires (Cordos *et al.*, 2017). In contrast, in a high tire pressure the contact area is reduced and the wheel load is concentrated in the central area of the tire, which can cause excessive wear of the central section of the tire and, under extreme conditions, lead to the delamination of the tire (Cordos *et al.*, 2017). The ideal pressure for a specific tire is recommended by the manufacturer.

Tire inflation pressure also affects the stiffness, or elasticity, of a tire. An increase in the stiffness of a tire caused by an increase in the tire pressure affects the contact area between the tire and the pavement. This, in turn, affects the lateral force developed at the contact area, where the lateral force is the force required to maintain the vehicle on the cornering trajectory (Doumiati *et al.*, 2010; Cordos *et al.*, 2017). The increasing of tire pressure above the recommend limit specified by the manufacturer will cause a decrease in tire stiffness and reduction of the tire-pavement contact area.

2.2.3.5 Traffic and Pavement Age

Studies of variation of friction due to traffic and age in asphalt pavements have shown that traffic was the principal factor in the deterioration of pavement surface textures (AASHTO, 2008; Goodman, 2009; Ech *et al.*, 2009). Heavy load trucks and high traffic volume cause faster deterioration of frictional properties because under traffic loading the surface microtexture of the aggregates becomes polished (AASHTO, 2008; Ech *et al.*, 2009). Further, heavy loads may dislodge coarse aggregates or over-compact the wheel paths, resulting in less macrotexture that ultimately prevents water from draining or the formation of rut channels that retain water and may cause hydroplaning (National Cooperative Highway Research Program, 1972).

In general, pavement friction is low in the first year after the construction of the asphalt pavement because the aggregates were covered in a binder coat (Kowalski *et al.*, 2009; Mayora and Pina, 2009; Vaiana *et al.*, 2012). In the following two years, friction increases and reaches its maximum values due to the wearing of the pavement surface caused by traffic and the exposure of rough aggregate surfaces (Kowalski *et al.*, 2009; Mayora and Pina, 2009). After the third year, friction is expected to decrease at a constant rate over the remaining pavement life as aggregates become more polished due to traffic and loads until the pavement surface reaches an equilibrium state of polishing (Kowalski *et al.*, 2009; Mayora and Pina, 2009).

Although it is logical to accept that pavement friction decreases with increased traffic and loads, studies have observed that friction variation is also affected by surface conditions and different types of pavement distress. A study conducted Li *et al.* (2003) in Indiana, USA, measured the skid resistance values of two asphalt sections with different

surface conditions over eight years. The study found that skid resistance values decreased at a constant rate after the fifth year in the road section that solely exhibited rutting on the surface. However, in the road sections that exhibited distress such as cracking and ravelling, friction values increased after the fifth year.

In another study in Indiana, McDaniel and Kowalski (2012) investigated skid resistance changes over time using four years of skid resistance data collected with a locked wheel trailer. The data included 16 road sections located on interstate and non-interstate roads in the USA. The authors observed that 14 out of the 16 road sections did not show a trend of decreasing skid resistance over time. For the other two road sections, one of the sections showed a decrease in skid resistance in the first two years and remained stable until the fourth year; in the other section, friction values were greater in the third and fourth year.

Variation of skid resistance over time for asphalt and concrete pavements was also examined by Ahammed and Tighe (2008), who used field data collected with a locked wheel skid trailer in Canada and the United States. For asphalt pavements, the study found an increase in friction in asphalt pavements during the early ages of the pavement. Maximum skid resistance was attained after 1.5 year for asphalt pavements and 2.5 years for concrete pavements. After the initial period of increase, skid resistance decreased for a period of six years for asphalt pavements and 12 years for concrete pavements. The authors attributed the decrease in skid resistance to increased traffic exposure. After the period of decreasing, skid resistance then showed a trend of increasing, which the authors attributed to an increase in pavement distress, such as ravelling.

2.2.3.6 Environmental Factors

Pavement friction levels fluctuate according to environmental conditions, e.g., wet and dry pavement surfaces. Pavement friction is typically higher on dry roads than on wet roads because of the decreased friction caused by the water layer between the tire and the pavement surface (Mayora and Pina, 2009). On wet pavements, pavement friction not only decreases with an increase in vehicle speed but is also influenced by the characteristics of the tire, the amount of water and contaminants on the pavement, and the properties of the surface microtexture and macrotexture (Wallman and Astrom, 2001; Flintsch *et al.*, 2012).

Pavement friction is also affected by the ambient temperature and the pavement surface temperature. Both temperatures determine the tire rubber temperature, which ultimately affects the viscoelastic temperature of rubber (Oliver, 1989). An increase in the tire rubber temperature reduces the coefficient of friction (Kummer and Meyer, 1962). This reduction occurs because at higher temperatures the rubber becomes more flexible, leading to less energy loss and results in a lower hysteresis force (Jayawickrama and Thomas, 1998; Anupam *et al.*, 2013). Thus, higher temperatures lead to a decrease in pavement surface friction.

Further, pavement friction fluctuates seasonally. Elkin *et al.* (1979) observed that skid resistance is lower in the summer and higher in the spring. Noyce *et al.* (2007) observed that friction is greater on dry surfaces in the winter than in the summer because the binder in the asphalt pavements tends to contract as the temperature drops, causing more exposure of the aggregates.

Pavement friction also fluctuates from year to year and during different periods,

depending on the predominant weather conditions and contaminants on the roads such as oil, rubber, and dust (Wallman and Astrom, 2001). Ahammed and Tighe (2008) observed that skid resistance decreases with an increase in temperature regardless of the type of pavement, though asphalt pavements proved to be more sensitive to environmental conditions than concrete pavements.

The seasonal variation of skid resistance is acknowledged in the Skidding Resistance section of the Design Manual for Roads and Bridges (DMRB) published by Highways England (DMRB, 2015). The design manual observed that after the initial period of wearing of the aggregates, when the roads reach an equilibrium state of polishing, skid resistance levels fluctuate through seasonal variations in weathering and polishing cycles. The lowest skid resistance levels were observed in the summer (May to September) and the greatest levels of skid resistance occurred in the winter (October to March), regardless the year. The manual attributed the seasonal fluctuation of skid resistance to the presence of contaminants on the road surfaces. In the winter, detritus on the road surfaces in the United Kingdom is mainly coarse, which alters the road surface and contributes to increased skid resistance. In the summer, the detritus is mainly dusty, which contributes to decreased skid resistance (DMRB, 2015).

2.3 Characterization of Surface Texture

The surface texture can be characterized by various parameters defined by the International Organization for Standardization (ISO, 1984). These parameters are based on vertical and horizontal deviations of the roughness profiles measured according to the height difference between the vertical deviation (profile depth) and horizontal line (average level) (ISO, 2002). These parameters are used for quantitative texture

measurements of macrotexture. Since, there is no specific standard that defines the parameters and quantitative texture characterization method for microtexture, many researchers used similar parameters to those used for macrotexture characterization to develop new methods for measuring microtexture and estimating friction using image processing and laser measuring systems (Ergun *et al.,* 2005; Kebrle and Walker, 2007; Goodman, 2009; Li *et al.*, 2010).

The most common parameters used for quantitative macrotexture measurements are mean the texture depth, mean profile depth, arithmetic mean, and root mean square of the profile. These parameters are described in the sections that follow.

2.3.1 Mean Texture Depth

The measurement of mean texture depth (MTD) is based on the volumetric patch method in which a given volume of fine material, usually sand or glass spheres is spread out on a surface with a rubber pad to form a circular patch. The circular patch is measured on four axes and the values are averaged to calculate the average diameter of the circle. The MTD is obtained by dividing the volume of the material by the area of the circular path. The sand patch method is standardized in the ASTM N E965-15 (ASTM, 2015j).

2.3.2 Mean Profile Depth

The mean profile texture (MPD) is the average value of the profile depth over a 100 mm long baseline. The MPD is calculated as the difference between the arithmetic mean of the peak levels of two baselines halves and the average level over the baseline. The method for estimating the mean profile depth is standardized in the ISO 13473-2 and the ASTM E1845-151 (ISO, 2002; ASTM, 2009).

2.3.3 Root Arithmetic Mean and Root Mean Square

The other two measurements of surface roughness are the arithmetic mean (RA) and the root mean square (RMS). The RA is the arithmetic average of the absolute values of the profile deviations from the mean line, measured within the evaluation length. The RMS is the root mean square average of the profile deviations from the mean line, measured within the evaluation length. The method for estimating the mean profile depth is standardized in the ISO and the ASTM (ISO, 2002; ASTM, 2009). The RA and RMS unit is mm.

2.3.4 Measuring Pavement Textures

There are a variety of devices that can be used to measure pavement textures in the field or in the laboratory, both stationary and dynamic methods at low and high speeds. Stationary, or static, methods can be used for project-level measurements because they are slow and the area surveyed represents only a minor portion of the entire pavement surface section (Flintsch *et al.*, 2012). Dynamic methods, however, are more appropriate for network-level data collection because they can be conducted at high speed and thus survey great portions of the road network (Hall *et al.*, 2009).

Currently, there is no device capable of measuring macrotexture and microtexture simultaneously. Macrotexture can be readily measured using laser-based sensors and volumetric tests, but microtexture is currently estimated as a surrogate indicator using devices to measure skid resistance. No commercial laser sensor has yet been reported to be able to capture microtexture at high speeds (Li *et al.*, 2010; McDaniel and Kowalski, 2012).

2.3.4.1 Microtexture Measurements

Microtexture measurements can be estimated using a wide variety of devices that measure skid resistance. These devices are fundamentally based on the principle of estimating friction by measuring the reacting forces that develop between the surface and a sliding rubber tire (Flintsch *et al.*, 2012). Stationary methods of skid resistance measurement include slider devices that measure the energy loss when a rubber slider edge is propelled over a surface (Lavin, 2003). The traditional device in which this principle is applied is the British Pendulum Tester (BPT). Another device that applies the same principle is the Dynamic Friction Tester (DFT). The standard practice for calculating friction using the BPN and DFT are established by the ASTM E303-93 and ASTM E1911-09, respectively (ASTM, 2018; ASTM, 2009).

Dynamic methods for skid resistance measurement at high speed include four categories of devices. First category of dynamic includes the longitudinal friction measuring devices that measure the longitudinal friction coefficient to break a rubber tire mounted in line of the direction of travel. The locked wheel trailer (LWT) is the most widely used such device in North America (Hall *et al.*, 2009). LWT measurements are reported in the form of Skid Number (SN) or Friction Number (FN). A higher SN indicates greater friction resistance. The standard practice for calculating the SN and the standard specification for smooth, full scaled and ribbed tires are established by the ASTM E524-08, E274/E274M-15, and E501-08 (ASTM, 2015b, g, h).

Second category includes the side force measuring devices that measure the side-force coefficient friction (SFC). The SFC represents the side force generated between the pavement surface and a freely rotating test wheel estimated with a standard tire angled at

20° to the direction of travel. The SFC is the ratio of the force developed at right angles to the plane of the axis of the wheel to the load on the wheel. The most common devices are the MU-Meter trailer and the British Sideway Force Coefficient Routine Investigation Machine (SCRIM). MU-Meter and SCRIM measurements are reported in the form of a MU value and a SCRIM value, respectively. The standard practice for calculating friction using side force devices is established by the ASTM E670-09 (ASTM, 2015i) and the BS 7941-1 (British Standard, 2006).

Third category includes the fixed-slip and variable-slip measuring devices that measure friction as a function of the slip between the tire and the pavement. Fixed-slip devices maintain a constant slip between 10% and 20% as the vertical load is applied to the test tire. In variable-slip devices the slip may range from 0 to 100% (Hall *et al.*, 2009). The most common fixed-slip devices are the roadway and runaway friction testers (RFTs), the Saab friction tester (SFT), the U.K. Griptester, the Finland BV-11, and the road analyser and recorder (ROAR). The most common variable-slip testers are the French IMAG and the Norwegian Norsemeter RUNAR. The standard practice for friction using calculating fixed-slip and variable-slip are established in the ASTM E1859 (ASTM, 2015c).

Fourth category includes devices that measure deceleration rates. These devices estimate road friction based on the deceleration rate for vehicles travelling at a constant speed (32 km/h to 48 km/h) from the instant brakes are applied to the instant the wheels are locked. A decelerometer device is mounted in a vehicle test. The standard practice for friction using calculating decelerometers is established in the ASTM E2101 (ASTM, 2015d).

2.3.4.2 Macrotexture Measurement

There are three stationary methods for measuring macrotexture: the volumetric test using the sand patch apparatus, outflow meters, and laser-based devices such as the circular texture meter (CTM). The first method, the sand patch test, delivers an estimate of macrotexture through mean texture depth. The standard practice for the sand patch test was previously described in the above section "The mean texture depth".

The second method uses outflow meters, measures the drainage characteristics of a surface. A cylindrical liquid reservoir with a neoprene gasket attached to its base has an orifice for permitting the liquid to flow out of the cylinder over a period of time. In this approach, very short outflow times indicate rough surface texture and long outflow times indicate smooth surfaces. In this method is assumed that none of the liquid penetrates into the pavement and instead flows laterally across the pavement, which is likely to occur in open graded asphalt concrete surfaces. The standard practice for measuring pavement texture drainage using an outflow meter is established in the ASTM E2380 (ASTM, 2015f).

The third method for macrotexture measurement uses the CTM device, which uses a high frequency laser to measure the surface profile. The laser head scans a circle with a radius of 142 mm. The circumference is divided into eight segments of 100 mm that are used for the estimation of MPD and RMS. The standard practice for the CTM test is established in the standard ASTM E 2157-15 (ASTM, 2015e).

Macrotexture measurements using dynamic methods include use of non-contact profiling techniques that employs cameras, sensors, and advanced laser scanners mounted on a data collection vehicle that travels at highway speeds.

2.3.4.3 Alternative Methods

Advances in technology have contributed to the development of new methods for data acquisition and data analysis of pavement textures. In particular, the use of laser technologies, image processing, and computational simulation have advanced significantly in the last decades. These are further discussed below.

The use of laser-based devices to measure pavement microtexture and macrotexture were reported by Xie (2010) and Li *et al.* (2010). Xie (2010) used a laser surface imaging system developed by the University of Houston to collected skid resistance data on Texas roads. The imaging system consisted of a device that used laser triangulation techniques to measure pavement textures and software to analyse and process data. The laser system had a 12-bit digital resolution and a 150 kHz operating frequency, and it was mounted in a vehicle that travelled at a speed of 60 mph (96 km/h). Xie (2010) analyzed skid resistance values measured with LWT and with the laser device. The results showed that skid resistance values were comparable with 88% of accuracy.

In another study, Li *et al.* (2010) tested different laser measuring systems mounted in a vehicle to measure microtexture and macrotexture in the field. For macrotexture measurements, the authors compared macrotexture profiles measured with three devices: a CTM, a 1 kHz laser, and a 62.4 kHz laser. The analysis showed that only the 1 kHz laser was capable of capturing macrotexture textures for asphalt surfaces, and the 62.4 kHz laser was capable of capturing macrotexture on tined concrete surfaces. For microtexture measurements, Li *et al.* (2010) observed that the 1 kHz laser was capable of capturing texture with wavelengths from 0.03 mm to 50 mm and showed a good correlation with the

observed pavement skid resistance measured with LWT at 30 mph (48 km/h) with a smooth tire.

The use of digital image processing to estimate pavement texture has been reported by various researchers. El Gendy (2008) used a digital camera to record pavement texture images and algorithms to develop a three-dimensional model that could be employed to estimate the surface macrotexture indicators MPD and RMS, and skid resistance measured with Griptester. Ergun *et al.* (2005) developed a contactless method for measurement of microtexture using a new image analysis system (NIAS) that employs a series of image analysis techniques and a camera capable of capturing a surface microprofile. Masad *et al.* (2007) developed a new method of image analysis, the Aggregate Imaging System (AISM), using an autofocus microscope and a digital camera to quantify angularities of aggregates' textures (microtexture and macrotexture) and changes in texture due to polishing. In another study, Goodman (2009) developed a portable data acquisition and analysis system, the Pavement Surface Imager, based on digital imaging techniques to estimate pavement frictional and textures properties.

The use of computer simulation is another approach that has been developed to estimate pavement surface texture and the effects of microtexture and macrotexture on the tire-pavement interface. Cummings (2010), for example, developed a theoretical model for predicting skid resistance that simulates the LWT behaviour and skid resistance values. Chen *et al.* (2014) similarly estimated skid resistance based on computer simulation of the physical mechanism of hysteresis originating from the contact between a rubber tire and the pavement surface.

2.3.5 International Friction Indicator

In Europe in 1992, the Permanent International Association of Road Congresses (PIARC) developed the International Friction Index (IFI) for the purposes of comparing and harmonizing friction measurements obtained from different measuring devices to a common calibrated friction index (Fuentes *et al.*, 2012). The IFI, also called F60, was determined using measurements of microtexture and macrotexture of wet surfaces and based on the assumption that friction is a function of speed (Lu and Steven, 2006). In the IFI model, microtexture determines friction at low speed, while macrotexture determines friction slip speed variation and the rate at which skid resistance decreases with the slip speed (Fuentes *et al.*, 2012). This method is also covered by the ASTM E 1960-07 (ASTM, 2015a). The IFI friction index equation is shown in 2.7 and 2.8.

$$IFI = A + B \times F \times e^{\frac{S-60}{Sp}} + C \times TX \quad \textbf{(2.7)}$$

$$Sp = a + b \times TX \quad \textbf{(2.8)}$$

Where IFI = International Friction Index at slip speed of 60 km/h, A, B, and C = calibration constants for specific friction measuring device, as per ASTM E1960-07 (ASTM, 2015a), TX = macrotexture measurement given by the device in mm, F = measured friction, S = slip speed at which the friction was measured, Sp = speed constant given or golden value speed, and a, b = constants depending on macrotexture measuring device as per ASTM E1960 (ASTM, 2015a).

2.3.6 Skid Resistance and Macrotexture Reference Values

Skid resistance and macrotexture reference values are used as parameters by road

agencies for investigatory and intervention levels of pavement friction. The investigatory and intervention levels are used to define maintenance strategies and safety purposes. However, the minimum acceptable friction values are not consistent among individual agencies (Noyce *et al.*, 2007). For instance, the Washington Department of Transportation recommends a skid resistance (SN) of below 30 to take actions to correct pavement friction and between 31 to 34 to monitor the pavement frequently, while an SN greater than 35 indicates no further action is required (Washington State Department of Transportation, 2004). Using the same categories of action, the states of Maine, Minnesota, and Wisconsin use SN of 35, 38, and 45, respectively (Noyce *et al.*, 2007).

For Canadian roadways, the Transportation Association of Canada (TAC) recommends an SN of 31 as investigatory level of friction; intervention, surveillance, and corrective action should take place if the SN is between 31 and 40; no further action is required if the SN is greater than 40 (TAC, 1999). In Ontario, a tentative friction classification system guideline is used by MTO (Kamel and Gartshore, 1982). Table 2.1 shows friction levels represented by skid number measured at a speed of 64 km/h with LWT using a full-scale tire as per ASTM E274/E274M-15 (ASTM, 2015g). The Ontario guidelines do not include reference values for macrotexture.

Table 2.1 Tentative Guidelines for a Friction Classification System for Ontario Roads

Road Type	Speed Limit (km/h)	Friction Level (SN)		
		Good	Borderline	Low
Freeways and main highways	100	≥ 31	25 to 30	< 25
2-lane and 4-lane	80	≥ 32	27 to 31	< 27
Intersections	80 60	≥ 40 ≥ 45	31 to 39 36 to 44	< 31 < 36

In Australia and New Zealand, pavement friction maintenance includes investigatory levels of skid resistance and macrotexture. For instance, the Australasian road transport and traffic agencies (Austroads), measures skid resistance with Griptester (GPN) at the network level and with British pendulum tester (BPN) for special projects and research. Macrotexture (MPD) is measured with an automated laser profilometer. The Austroads investigatory levels of skid resistance for different road categories are shown in Table 2.2 and the investigatory levels and new surfacing levels of macrotexture are shown in Table 2.3 (Austroads, 2003).

Table 2.2 Investigatory Levels of Skid Resistance

Road Categories	Minimum GPN	Maximum Vehicle Speed (km/h)
Difficult sites (steep grades, traffic light approaches, tight bends, roundabouts)	0.50 to 0.55	60 to 80
Urban arterial roads	0.45	60
Rural arterial roads	0.45	110
Urban/lightly trafficked	0.40	60
Urban arterial expressway	0.45	90 to 100
Note: Conversion between BPN and GPN = 0.01 x BPN		

Table 2.3 Investigatory and New Surfacing Levels of Macrotexture

Road Type	Texture Depth (mm)
Freeways, high class facilities with free-flowing traffic condition, and local roads	0.4
Highways (> 80 km/h) and other major main roads to stopping and turning (< 80 km/h)	0.6
Surfacing Type	
Spray seals, 10 mm or larger	> 1.5
Spray seals, 7 mm	0.6 to 1.0
Dense graded asphalt, 10 mm or larger	0.4 to 0.8
Dense graded asphalt, 7 mm	0.3 to 0.5
Open graded asphalt	> 1.2
Stone mastic asphalt	> 0.7
Fine gap graded asphalt	0.2 to 0.4
Tined concrete	0.4 to 0.7
Exposed concrete	> 0.9

In the United Kingdom, a revised standard for skid resistance measurement was introduced in 2004 and revised in 2015. The revised standards of skid resistance are specified in the Design Manual for Roads and Bridges (DMRB) and were defined based on studies that investigated the relationship between skid resistance, accident history, and nature of the specific site (DMRB, 2015). The current investigatory levels of skid resistance (SCRIM, SC50) for roads in Great Britain range from 0.35 to 0.55 according to road category, gradient, curve radius, and risk of accidents. The DMRB also recommends investigatory levels for skid resistance on road surfaces that show macrotexture levels below 0.8 mm in order to avoid the combination of low skid resistance and low texture depth (DMRB, 2015).

2.3.7 Pavement Friction and Probability of Collisions

Various studies have attempted to determine road friction threshold values to address the probability of collisions. For instance, McCullogh and Hankins (1966) examined the relationship between skid resistance and collisions in Texas. The study found that collisions tend to decrease on pavements that exhibited an SN of 40. Studies conducted by Wambold (1988) and Noyce *et al.* (2007) suggested an SN of 35 should be adopted for rehabilitation and reconstruction activities to reduce the probability of collisions. Abd El Halim (2009) examined the relationship between SN and collision rates in Ontario, observing that decreasing the skid resistance threshold resulted in an increase in the collision rate by an average of 100% when the SN dropped from of 35 to 32.

The relationship between macrotexture and accidents was also investigated. In a study in Great Britain, Roe *et al.* (1991) examined the relationship between macrotexture

and collisions on three different types of roads: motorways, major roads, and minor roads. Roe *et al.* observed that the probability of collisions increased on road segments where the level of macrotexture (MTD) was lower than 0.6 mm for minor roads, 0.7 mm for major roads, and 0.8 mm for motorways, irrespective of the level of skid resistance. The study also indicated that the number of collisions increased approximately twofold when the macrotexture was below 0.4 mm.

Pulugurtha *et al.* (2010) examined the influence of macrotexture measured on asphalt pavements of four highways in the state of North Carolina in the United States. The study found that the probability of collisions could be reduced by maintaining a macrotexture (ETD) greater or equal to 1.524 mm for asphalt pavements (Pulugurtha *et al.*, 2010).

2.3.8 Estimating Friction from Pavement Texture

This section presents a summary of studies that estimated pavement friction using statistical models that correlated pavement textures with other variables related to aggregate properties, mix design parameters, macrotexture, and road characteristics (e.g., traffic, loads, road design, and environmental conditions).

Several studies have developed friction models in terms of IFI using skid resistance measurements as a surrogate measurement of microtexture and macrotexture measurements (Flintsch *et al.*, 2003; Rezaei *et al.*, 2011; Kassem *et al.*, 2013). Flintsch *et al.* (2003) investigated pavement friction on seven types of hot-mix asphalt roads in Virginia, USA. The researchers developed a model to estimate IFI, where macrotexture (MPD) was measured using laser profiles and microtexture was estimated from measurements of skid resistance measured with LWT at three different speeds with

ribbed and smooth tires. The friction model included type of tire, total the voids in the mixture, percentage of material passing sieve on 200 mm, binder type, and content. The IFI model exhibited an R-square of 0.412. The model is given by Equation 2.9.

$$IFI = 0.382 - 0.029\,Tire + 0.013\,Binder + 0.009\,PP200 + 0.009\,VTM \quad \textbf{(2.9)}$$

Where IFI = International Friction Index, Tire = 0 for smooth tire and 1 for ribbed tire, Binder = binder code (-1 for PG 64-22, 0 for PG 70-22, and 1 for PG 76-22), PP_{200} = percentage of material passing sieve # 200 mm, and VTM = total voids in the mixture.

Kassem *et al.* (2013) developed a model for predicting friction loss of asphalt pavements by using aggregate shape characteristics, aggregate resistance to abrasion and polishing, aggregate gradation, and polishing cycles. Kassem *et al.* (2013) used square-shaped slabs of different asphalt mixtures that were prepared in the laboratory by using a linear kneading compactor and polished with a wheel-polishing device. A DFT was used for skid resistance measurements, a CTM was used for macrotexture measurements, and the AIMS was used to measure aggregate polishing resistance before and after the Micro-Deval abrasion test. Regression parameters were obtained using nonlinear regression analysis. The model to predict IFI exhibited an R-square of 0.92. The IFI model is given by Equation 2.10.

$$IFI_N = (a_{mix} + b_{mix})e^{\left(-c_{mix}/N\right)} \quad \textbf{(2.10)}$$

Where $IFI_{(N)}$ = International Friction Index, N = Number of polishing cycles using the polisher (in thousands), amix = 0.20 (terminal aggregate texture), bmix = 0.39 (initial aggregate texture), and cmix = 0.052 (rate of change in aggregate texture).

Other studies have attempted to develop models to predict skid resistance and macrotexture using mix design parameters that included aggregate distribution, percentage asphalt concrete, percentage of air voids, and percentage of voids in the mineral aggregates (Goodman *et al.*, 2006; Ahammed and Tighe, 2008, Ahammed and Tighe, 2012).

Goodman *et al.* (2006) developed a model to predict initial pavement friction, skid resistance given by British pendulum number (BPN) and macrotexture (MTD) using mix design properties such as bulk relative density, the percentage of aggregates passing at 4.75 mm sieve, asphalt content, and the fineness modulus that was calculated by summing the fractions of the percentage of aggregates distribution of fine and coarse aggregates by sieving and dividing by 100. Goodman *et al.* (2006) tested a series of specimens of asphalt mixes collected in the field from projects in the city of Ottawa, as well as specimens prepared in the laboratory. The model used to predict skid resistance exhibited an R-square of 0.69; the model to predict macrotexture exhibited and R-square of 0.95. The models are given by Equation 2.11 and 2.12.

$$BPN_i = 42.32 + 2.95 \left(\frac{P4.75 \times BRD}{FM \times AC}\right) \quad \textbf{(2.11)}$$

$$TD = -0.24\ 0.981 \left(\frac{FM \times VMA}{P4.75 \times BRD}\right) \quad \textbf{(2.12)}$$

Where BPNi = initial British pendulum number, MTD = mean texture depth in mm; P4.75 = percentage of aggregates passing at sieve 4.75 mm, BRD = bulk relative density, FM = fineness modulus, and AC = percentage of asphalt concrete.

Ahammed and Tighe (2008) developed models to predict skid resistance for

asphalt concrete (AC) and Portland cement concrete (PCC) pavements using specimens prepared in the laboratory and specimens obtained from Canadian road sections. The specimens prepared in the laboratory were exposed to a natural environment and the surface textures were measured monthly using a BPT to measure skid resistance. In addition to the data analyzed in the laboratory, Ahammed and Tighe (2008) included field data collected with LWT with a ribbed tire from road sections across different provinces and states of Canada and the United States. The data analyzed included information of mix design, pavement age, speed test, temperature during the testing, surface texture, cumulative traffic passes, pavement age, vehicle speed, and environmental factors for each road section. Results showed that the predictor variables related to mix design parameters were not statistically significant (p-value > 0.05) and variables related to traffic, pavement age, and environment were statistically significant (p-value < 0.05). The R-square values of the models for AC and PCC pavements were 0.484 and 0.412, respectively. The models for AC and PCC pavements using data collected by LWT are given by Equation 2.13 and (2.14, respectively.

$$SN_{SR} = 63.07 - 1.20\,Y + 5.32\,DW + 2.69\,FNF - 0.18\,S - 0.24\,T \quad \textbf{(2.13)}$$

$$SN_{SR} = 59.64 - 0.26\,V + 5.90\,DW + 3.69\,F_{NF} - 0.13\,S - 0.29\,T \quad \textbf{(2.14)}$$

Where SN_{RS} = skid number measured with LWT with ribbed tire at speed S, S = vehicle speed in km/h, Y = pavement age in years after an early age increase in friction, V = cumulative traffic passes in millions after an early age increase in friction, T = friction test temperature in °C, DW = dry versus wet weather code (dry weather = 1 and wet weather = 0), and F_{NF} = freeze versus no freeze weather code (no freeze = 1 and freeze =

0).

In another study, Ahammed and Tighe (2012) developed models for estimating skid resistance and macrotexture. Skid resistance was measured using a BPN and LWT. Macrotexure was measured using the sand patch method and a high-speed texture laser. The models for skid resistance included the variables MTD, speed, and aggregate quality (crushing). The model for MTD included the percentage of coarse and fine aggregates. The models for estimation of SN using MTD and speed as independent variables showed an R-square of 0.56. The regression models for predicting MPD and SN models are given by Equation 2.15 and 2.16.

$$MTD = 0.50 + 0.29\left(CA/FA\right) \quad \textbf{(2.15)}$$

$$SN_{SR} = 57.03 + 11.43\,MTD - 0.25\,S \quad \textbf{(2.16)}$$

Where MTD = mean texture depth in mm, CA/FA = coarse to fine aggregate ratio, SN_{RS} = skid number measured with LWT with ribbed tire at speed S, and S = vehicle speed in km/h.

Various researchers have developed models for predicting friction by exploring the relationship between skid resistance, macrotexture, aggregate properties, and laser scanners (Serigos *et al.*, 2014; Rajaei *et al.*, 2014). Serigos *et al.* (2014) developed a model to predict skid resistance using data collected in asphalt pavements in the state of Texas, USA. Serigos *et al.* (2014) measured skid resistance using a BPN and macrotexture with a CTM. The surface textures were also measured in 12 road sections with a laser texture scanner (LTS) before and after texturing treatments were applied. The skid resistance model exhibited an R-square of 0.67. The model specification is given by

Equation 2.17.

$$BPN = \alpha + (\beta_{Macro} \times Macro_{MPD}) + (\beta_{Treat} \times Treat) \quad \textbf{(2.17)}$$

Where BPN = British pendulum number, $Macro_{MPD}$ = macrotexture in MPD in mm, Treat = categorical variable (1 when the section receives light texture and 0 otherwise), α, β_{Macro}, and β_{Treat} = parameters estimated for each test surface using the generalized least square method.

In another study that correlated skid resistance (microtexture) and macrotexture, Rajaei *et al.* (2014) examined the correlation between microtexture and macrotexture using data collected in the field and specimens from roads in the states of Wisconsin and Minnesota, USA. In the laboratory, microtexture and macrotexture profiles were measured using a stationary laser device (SLP) and CTM. In the field, skid resistance was measured using LWT with a smooth tire at 65 km/h. Rajaei *et al.* (2014) also studied the correlation between macrotexture measured with CTM and SLP. Macrotexture was estimated from the volumetric properties of aggregates and mix design properties. The correlation between skid resistance and macrotexture measured with CTM exhibited an R-square of 0.77. The correlation is given by Equation 2.18.

$$SN_{65S} = 54.91 + 30.36\ ln\ (MPD_{CTM}) \quad \textbf{(2.18)}$$

Where MPD_{SLP} = mean profile depth in mm measured with SLP device, SN_{S65} = skid number measured with LWT with smooth tire at 65 km/h, and MPD_{CTM} = MPD macrotexture measured with CTM.

In a more recent study, Meegoda and Gao (2015) attempted to develop models to

predict skid resistance based on macrotexture measurements from asphalt pavements in New Jersey, USA. Meegoda and Gao (2015) collected skid resistance measurements using LWT with a ribbed tire at 40 mph and macrotexture measurements using a laser mounted in a vehicle travelling at a high speed (100 km/h). The models exhibited a positive correlation between SN and MPD when the MPD was lower than 0.75 mm (R-square of 0.27) and a negative correlation when the MPD was between 0.75 and 0.90 mm (R-square of 0.29) and when MPD was greater than 0.90 mm (R-square of 0.83). The correlations are given by Equations 2.19, 2.20, and 2.21.

- For MPD < 0.75 mm:

$$SN_{40} = 34.73 + 20.40\,MPD + 6.78\,MPD^2 \quad \textbf{(2.19)}$$

- For 0.75 mm ≦ MPD ≦ 0.90 mm:

$$SN_{40R} = 540.34 + 1474.9\,MPD - 914.82\,MPD^2 \quad \textbf{(2.20)}$$

- For MPD > 0.90 mm:

$$SN_{40R} = 76.97 + 18.91\,MPD - 7.16\,MPD^2 \quad \textbf{(2.21)}$$

Where SN_{R40} = skid number measured with LWT with ribbed tire at 40 mph (64 km/h), and MPD = macrotexture in mm.

In summary, a number of researchers have attempted to develop models for predicting pavement surface friction. It is noted from the abovementioned studies that models for estimating skid resistance and macrotexture vary significantly depending on the type of equipment used for collecting the pavement textures, the location where the textures were collected (field or laboratory), sample size, statistical approach, and the

variables included in the models. Despite the specificity of each model, it should be noted that the variables of loads or the polishing effect of loads, speed, and mix design parameters were found in the majority of models.

2.4 Pavement Condition and Road Safety

Maintaining road safety not only demands satisfactory pavement surface conditions and friction, but also that drivers adapt their behaviour to different situations and environments, usually by adjusting their speed (Wallman and Astrom, 2001). To further discuss these relationships, the following sections present a summary of relevant research findings related to pavement friction, pavement distress, and road safety.

2.4.1 Friction and Road Safety

A number of studies have suggested that by improving pavement friction there will be a reduction of collision rates (Flintch *et al.*, 2012; Mayora and Pina, 2009). Kamel and Gartshore (1982) compared collisions rates before and after the application of resurfacing treatments that improved friction at black spots in Ontario's highway locations that presented high rates of wet pavement accidents. Kamel and Gartshore reported a reduction of 46% in the total number of collisions at intersections and a reduction of 29% for highways. The reduction in wet collisions specifically was more noticeable: 71% reduction at intersections and 54% for highways.

In Spain, Mayora and Pina (2009) evaluated pavement surface friction and collision data collected over 10 years from two-lane rural roads on the Spanish national road system. Their results demonstrated that collision rates (collisions/10^6 x traffic volume) decreased as skid resistance increased for wet and dry pavements. They observed that accident rates on wet pavements were significantly higher along horizontal

curves than on tangents, with a difference ranging from two to three times more depending on the radius of the curves. Under dry conditions, this difference was not noticeable. Mayora and Pina (2009) also reported that by improving pavement friction from a SCRIM below 50 to a SCRIM above 60 collisions on wet pavement could be reduced by 68% in tangents and 84% in curves.

Pulugurtha *et al.* (2010) likewise assessed the role of pavement macrotexture on road safety in North Carolina, USA. The results indicated that macrotexture has a statistically significant effect on road safety. The researchers concluded that maintaining a threshold macrotexture greater than 1.524 mm contributed to reduced road collisions, while macrotexture beyond 3.048 mm compromised ride quality.

Zeng *et al.* (2014) evaluated the safety effectiveness of resurfacing rural two-lane undivided highways in Virginia, USA. The authors observed that by improving pavement friction, there was a significant reduction in the number of collisions related to sideswipe. While improving pavement conditions from a low level to a satisfactory level did not exhibit a significant effect on reducing the total number of collisions. Zeng *et al.* (2014) observed that good pavement condition reduced fatal and injury collisions by 26% when compared with poor pavement conditions.

In another study, Li *et al.* (2010) studied the impact of macrotexture depth on wet collision rates on freeways in Western China. The authors reported a significant correlation between macrotexture and collisions during wet conditions. The wet collision rate decreased with the increase in the levels of macrotexture. They also observed that collision rates on rainy days increased when macrotexture was below 0.4 mm.

Finally, in a recent study, Fernandes and Neves (2014) examined the influence of

skid resistance (SCRIM number) and macrotexture (MPD) on road safety. They also established skid resistance and macrotexture threshold values for road maintenance and safety levels when considering three road environments: (E1) rural environment with urban zones and intersections; (E2) rural environment with a predominance of intersections; and (E3) curved segments with high longitudinal gradients and speeds over 90 km/h. Fernandes and Neves (2014) observed that collision risks increased with the reduction of skid resistance and macrotexture. For E1 and E2, the risk of collision increased when MPD was below 0.4 mm and SCRIM number below 40. For E3, the risk of collision increased for MPD was below 0.5 mm and SCRIM number below 50.

2.4.2 Pavement Distress and Road Safety

Despite there being limited studies on pavement condition and road safety, there are nonetheless several studies investigating the influence of the general condition of pavement and a variety of factors (e.g., environmental, road geometry) on collision frequency and severity. Al-Masaeid (1997) investigated the effects of pavement condition, road geometry, and roadside conditions on rural road collisions in Jordan. The pavement condition was defined using the IRI and another indicator of serviceability similar to the PSI, the Present Serviceability Rating (PSR). Al-Masaeid (1997) developed two statistical models to conduct the analysis: a single-vehicle collision rate model and a multiple-vehicle collision rate model. Results indicated that the IRI and PSR had a significant impact on single and multiple-vehicle collision rates. Al-Masaeid (1997) observed that a high level of IRI contributed to an increased multiple-vehicle collision rate, while a low level of IRI contributed to an increased single-vehicle collision rate.

In Tennessee, USA, Chan *et al.* (2009) investigated the relationship between

collision frequency on urban highways and pavement condition variables. The authors developed various binomial regression models for several types of collisions including rut depth (mm), IRI, and PSI as explanatory variables. Chan *et al.* (2009) observed that rut depths were not significant on collision frequency. Chan *et al.* (2009) also observed that the IRI and PSI were significant predictors in all types of collisions. The increase of IRI and pavement in fair and poor conditions were correlated to an increase in collision frequency.

Buddhavarapu *et al.* (2013) created a collision injury severity model by integrating accident and pavement surface condition databases on two-lane horizontal curves in Texas, USA. The pavement surface condition was assessed through skid resistance (SN), DMI, and IRI. Buddhavarapu *et al.* (2013) observed that SN was not significant for predicting injury severity collision on curves, whereas the DMI and IRI exhibited a significant correlation with collision and injury severity. The probability of a fatal collision occurring was found to be greater at sites with minimal DMI and smoother pavements. The authors concluded that superior road conditions may in fact contribute to increased fatalities because drivers tend to be more aggressive on smoother pavements.

In a similar study, Li *et al.* (2013) examined the impact of pavement condition and type of collision severity in Texas, USA. For collisions involving passenger vehicles and overall pavement condition, the authors observed that pavements in poor condition were associated with more severe collisions compared to pavements in fair condition. Notably, pavements in very poor condition were not found to be associated with more severe collisions, whereas pavements in very good condition were associated with lower collision severity. The authors observed that the effects of pavement condition on

collision severities were more significant on multilane freeways and non-freeways with relatively high-speed limits, and during favourable driving conditions characterized by dry pavement surface and daylight.

Also, in Texas, USA, Li and Huang (2014) investigated the correlation between pavement condition and traffic collisions on asphalt roadways. The overall condition of the pavement was recorded as a pavement management information system score (PMIS). The PMIS was used to classify pavement condition into four groups: very poor (1 to 49), poor (50 to 69), fair or good (70 to 89), or very good (90 to 100). Li and Huang (2014) observed that the collision rate on roadways in very poor pavement condition was more than twice as high as on roadways in very good pavement condition. Similar results were found with collision rates and pavement distress, where the collision rate was found to be more than twice as high on roadways that exhibited higher distress scores. The collision rate was three to five times higher on roadways with a rougher ride score than on roadways with smooth pavements.

In another study, Lee *et al.* (2015) investigated the relationship between pavement condition and collision severity levels for low speed roads (lower than 35 mph, or 56 km/h), medium speed roads (between 40 and 45 mph, or 64 to 72 km/h), and high-speed roads (higher than 50 mph, or 80 km/h). Pavement condition was scaled from zero to five, where zero is the poorest and five is the best pavement condition. Lee *et al.* (2015) developed a series of Bayesian ordered logistic regression models to evaluate the relationship between collision severity, speed, and single and multiple collisions. The study's findings indicated that the severity of single vehicle collisions on low speed roads decreased when the pavement condition was poor but increased on high speed roads. The

severity of multiple vehicle collisions increased when the pavement condition was poor for all speed roads.

Elghriany (2016) also investigated the relationship between changes in pavement condition and collision rates for highways in Ohio, USA. In the first part of his research, Elghriany (2016) investigated the influence of changes in the collision rate over the change in IRI. Results indicated that the risk of collisions was low for an IRI of 1.5 m/km for Portland cement concrete pavements (PCC) and 0.75 m/km for asphalt pavements (AC). Further, the risk of collision increased for an IRI greater than 2.25 m/km for PCC and 1.25 m/km for AC pavements.

In a recent study, Hussein and Hassan (2016) examined the contribution of roughness (IRI), rutting (mm), and skid resistance (SCRIM) on collision frequency and rate at 57 signalized intersections in Melbourne, Australia. The authors used negative binomial regression analysis to assess the contribution of surface condition at intersections before and after they were treated with thin asphalt surfaces. Hussein and Hassan observed that collision rates increased with an increase of roughness and that collision rates were greater during the day on dry surface at all levels of roughness. Hussein and Hassan (2016) observed that there was no clear relationship between rut depth and collision rates. Collision rates also decreased with an increase in skid resistance, though the collision rate in wet surfaces was lower than in dry surfaces regardless of skid resistance levels. Hussein and Hassan (2016) concluded that collisions occurred at all levels of skid resistances, but, in general, fewer collisions were observed when there were high levels of skid resistance.

The abovementioned studies show that the relationship between pavement

condition and collision rates and collision severity are not entirely consistent. The studies generally agree that an increase in the roughness of pavement (IRI) correlates to an increase in collision rates.

The studies also suggest that the correlation between rutting and collision rates are not clear and even controversial: one study showed that rut depth is not correlated with collision rates, yet another study showed that collisions decrease with an increase in rutting (Chan *et al.,* 2008; Hussein and Hassan 2016). Likewise, studies also provide controversial results for pavements in good and poor condition. Fair and poor pavements were correlated with higher collision rates and severe collisions, but good pavements were also correlated with higher collision rates and severe and fatal collisions (Chan *et al.*, 2008; Li *et al.*, 2013; Li and Huang, 2014; Lee *et al.*, 2015; Elghriany, 2016).

2.5 Summary

This chapter defined the indicators of pavement condition and pavement friction. It also presented the equations, methods used for data collection, and reference values of skid resistance and macrotexture used by transportation agencies to investigate friction deficiencies. This information is important to define the framework of the research.

The review of studies that estimated friction from pavement texture and macrotexture showed that despite the specificity of each model, variables related to traffic or the polishing effect of loads, the speed of the test, and mix design parameters were found in the majority of models. Also notable is that few studies included variables that accounted for changes in pavement friction over time; this is a gap in the literature that requires further investigation. Understanding changes over time can make a significant contribution to pavement management and road safety, which is what the

present study proposes to do for Ontario roadways.

This chapter also showed that claims about the relationship between pavement condition and road safety is not entirely consistent. Studies show controversial results about the influence of good and poor pavements on collision frequency and severity. Therefore, the correlation between pavement condition and pavement distress and collisions requires a more comprehensive investigation to improve road safety and proper pavement management for Ontario highways.

3 Chapter: Data Sources, Attributes, and Integration

This chapter describes the sources, attributes, and integration of the data considered in this study. The data used in this research was obtained from MTO and collected at network level from road sections of 37 provincial rural highways.

The data included information about pavement surface condition, including skid resistance, macrotexture, and pavement distress; collision data; and operational condition of the roads. The network data from different sources was integrated by creating a main database using GIS. The next sections describe the data sources, the devices used for collecting pavement condition data, and approaches used for data integration.

3.1 Data Collected at the Network Level

Data collected at the network level was used for studying the factors affecting pavement friction, skid resistance modelling, and performing the road safety analysis. The data was obtained from MTO included multiple datasets with field measurement of skid resistance, macrotexture, and pavement distress. The field measurements occurred in the period from April to October in the years 2012 to 2014. Additionally, collision data and information about type of mix, pavement mix design, and the operational condition of the roads were integrated into the field measurement of pavement condition.

Multiple data sets were integrated based on the spatial location of the measurements, road section, and year of the measurement. The following subsections describe how data from different sources were collected, identified, and integrated.

3.1.1 Linear Highway Referencing System

The spatial location of field measurements and collisions was identified along the highway network using the Linear Highway Referencing System (LHRS). The LHRS is

used by MTO to record and integrate information about the Ontario road network in a consistent format. Each LHRS is labeled with a unique five-digit number.

The MTO's LHRS is based on linear measurements and offsets from a reference point (MTO, 2009). Each LHRS is unique and receives an individual identification that resets at the start of a new road section. Each LHRS is also assigned to spatial and non-spatial data referred to as road events. Road events are divided into two categories: point events and linear events (MTO, 2009). Point events occur at a specific location along the road and are identified using a single offset measurement from a reference point. An example of a point event is a collision. Meanwhile, linear events occur along a continuous section of road. They are identified using two offset measurements, the beginning and end from a reference point. Examples of linear events include measurements of skid resistance, macrotexture, pavement distress, speed zones, and road surface type (MTO, 2009).

3.1.2 Field Measurements of Skid Resistance and Pavement Condition

The field measurements of pavement condition, macrotexture, and skid resistance occurred on 37 provincial rural highways of four types: freeway, arterial, collector, and local. The highways differ in terms of function, mobility, and design (MTO, 2013).

The MTO defines a freeway as a highway designed to accommodate a large volume of traffic at high speed under free flow (MTO, 2013). Freeways have full control access, which signifies no traffic lights, intersections, property access, at-grade crossing with other roads, railways, and paths. The crossings are provided by grade-separated interchanges with overpass, underpasses, and ramps. The entrances and exits are provided by ramps and opposing traffic lanes are separated by medians (MTO, 2013). Provincial

freeways are denominated as 400-series highways.

Arterial highways, meanwhile, are typically two and four-lane divided or undivided highways with uninterrupted flow, except at-grade intersections and access connections located along a public road (MTO, 2013). Collector highways are typically two or four-lane undivided highways with interrupted flow with at-grade intersections and some degree of access control (MTO, 2013). Local highways are typically two-lane undivided highways with interrupted flow with at-grade intersections and some degree of access control. MTO outlines degrees of access control based on criteria such as connections from public roads, spacing, residential and commercial access, grade, density, frontage, and safety requirements (MTO, 2013).

Skid resistance measurements occurred on 110 road sections (1363.65 km) and macrotexture and pavement distress measurements occurred on 903 road sections (6879.46 km). Of the 903 road sections measured for pavement distress, only 75 road sections (1174.75 km) corresponded to the sections measured for skid resistance.

Table 3.1 shows the location of the road sections according to highway identification (HWY ID), type of highway (HWY Type), total number of road sections per highway (LHRS), and length of sections (in km). It is important to note that for skid resistance measurements, the number of LHRS and length of the sections represent the entire sample of the skid resistance measured for the three-year period; however, for macrotexture and pavement distress, the number of LHRS and length of sections represent the average of the number of LHRS and lengths for the three-year period. For example, HWY 1 shows the average of LHRS equal to 50 and length of 122.42 km, which represents the average of the number of road sections and average of the lengths of

sections measured from 2012 to 2014, respectively. A table with the total of road sections and lengths by highway per year is shown in Appendix C, Table C.1.

Table 3.1 Pavement Condition Information by Highway

HWY		Skid Resistance		Macrotexture and Distress	
ID*	Type**	Total		Average	
		LHRS	Length (km)	LHRS	Length(km)
1	A	10	38.56	50	122.42
3	A	2	19.20	28	150.41
6	A, C	10	198.05	48.33	329.63
7	A, C	1	10.70	68.33	406.79
9	A	3	42.80	NA	NA
10	A	4	38.15	17.67	98.06
11	A	13	253.72	135	1338.81
12	A	NA	NA	19	71.92
17	A	9	162.77	148	1328.78
21	A	3	42.67	22.67	146.79
23	A	1	9.00	8.33	82.69
24	A	NA	NA	9	44.34
26	A	1	9.70	11	71.08
28	C	1	10.00	17.67	128.36
35	A	4	22.02	33.67	146.31
40	A	1	10.80	NA	NA
41	A	2	18.39	15.67	136.71
48	A	1	10.96	NA	NA
60	A	4	39.95	22.67	195.96
62	A	1	7.99	15.33	129.67
63	C	1	21.47	4	33.49
64	L	1	10.20	11	126.89
66	L	1	40.20	7	71.09
69	F	2	20.00	NA	NA
72	C	1	14.73	6	68.48
89	A	3	36.60	NA	NA
101	C	2	41.30	23	352.83
118	C	1	31.00	11	91.41
124	A	2	10.20	NA	NA
141	C	1	0.80	6	44.38
144	A	1	17.60	12.67	232.53
400	F	3	24.42	53	217.94
401	F	12	81.36	78	711.69
403	F	2	14.80	NA	NA
404	F	1	2.12	NA	NA
409	F	2	0.72	NA	NA
417	F	3	50.70	NA	NA
Total`		110	1363.65	903	6879.46
(*) ID = Identification, (**) Type: A = Arterial, C = Collector, L = Local, F = Freeway, (NA) = Information not available					

3.1.3 Measurements of Macrotexture and Pavement Distress at the Network Level

The network pavement macrotexture and pavement distress occurred in the field using a high speed road analyzer, the automatic road analyzer (ARAN) model 9000. ARAN has been used by MTO since 2012 to collect pavement condition data at the network level. The ARAN 9000 used by MTO is shown in Figure 3.1.

Figure 3.1 ARAN Vehicle (MTO, 2016c)
(Photo reprinted with permission from the MTO, 2019)

The ARAN 9000 is a vehicle equipped with 2D and 3D laser systems (laser crack measurement systems) with the associated software and high-definition cameras. Pavement condition data collected by ARAN is recorded and processed using the Pave3D software suite (Chan *et al.*, 2016, MTO, 2016c).

The ARAN laser measurement system is based on regular contactless scanning of transverse and longitudinal sections of road. The high-resolution cameras installed in the ARAN are capable of capturing cracks up to 2 mm in width (Fugro, 2018). The lasers are

also able to simultaneously measure both wheel paths of a lane. The measurements of rutting, cracking, and macrotexture are computed as average depths for intervals of 50 m of pavement surface. The longitudinal laser profiler measures the average depth of macrotexture, reported as MPD and RMS, and pavement roughness, reported by IRI. The transverse laser profiler measures the depth of roadway rutting.

The ARAN measurements are identified by highway region (Northwestern, Northeastern, West, Central, and Eastern), type of collection (network or project level), lane, direction of measurement, and LHRS. Each measurement has a unique numerical identification (ID Segment) with its respective geographic coordinates (latitude and longitude). In addition, during pavement condition measurement, ARAN is capable to record some features of the highways, such as elevation of the points, grade, and cross fall. An example of an excel spreadsheet with the 23 initial columns of ARAN's output is shown in Appendix B. A complete excel spreadsheet of ARAN's output has 126 columns, including measurements of macrotexture, roughness, and pavement distress with their respective level of severity (slight, moderate, or severe), in addition to length, width, and area affected by the distress. The ARAN's output also gives information about cracks counts and ravelling index (RI).

The pavement distress collected by ARAN were used to calculate the DMI and PCI using Equations 2.1 and 2.3. The DMI was calculated following the Manual for Condition Rating of Flexible Pavements (MTO, 2016b) with three considerations: 1) lane widths were defined as 3.6 m, 2) severity weights were set as 1 for slight, 2 for moderate, and 3 for severe, and 3) flushing, shoving, and distortion were not included in the calculation because they were not measured by ARAN (Chan *et al.*, 2016).

The average of ARAN's measurements of MPD and IRI and the calculated indicators DMI and PCI by highway per year are shown in Table C.1 in Appendix C. Figure 3.2 to Figure 3.5 show histograms of the percentage distribution of these indicators. The percentage distribution of MPD, IRI, DMI, and PCI was calculated using the pavement condition values computed for 2,292 km where collisions occurred.

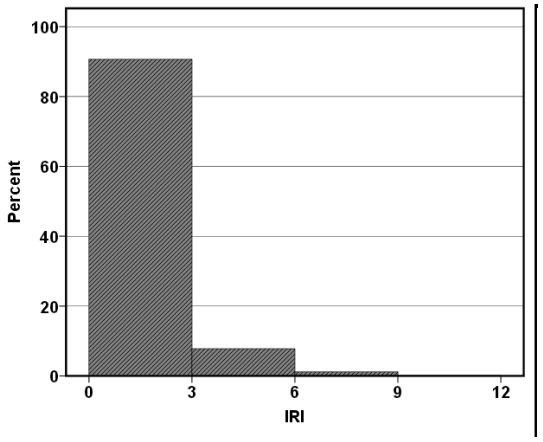

Figure 3.2 Histogram of Percent Distribution of IRI

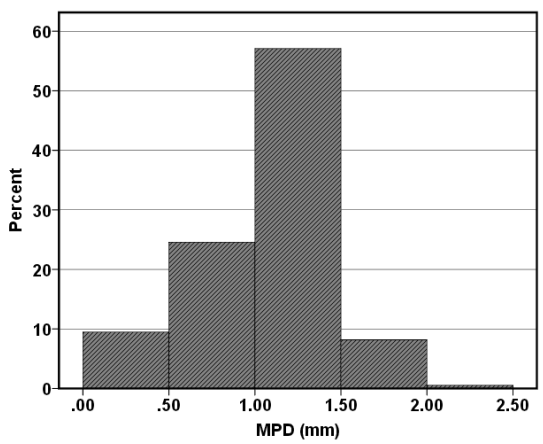

Figure 3.3 Histogram of Percent Distribution of MPD

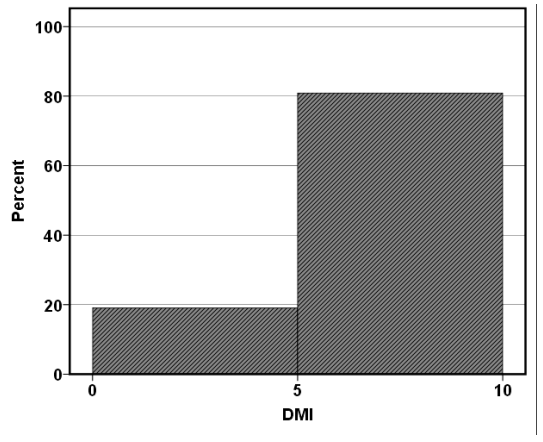

Figure 3.4 Histogram of Percent Distribution of DMI

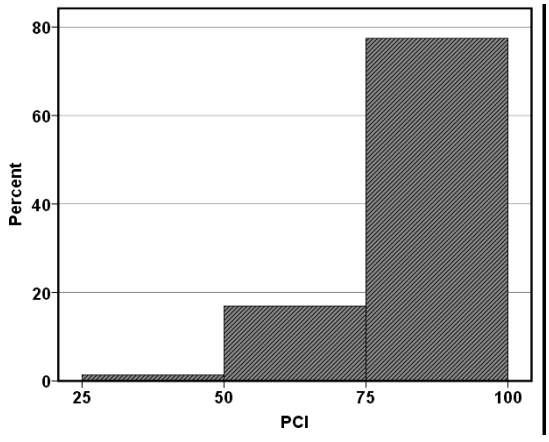

Figure 3.5 Histogram of Percent Distribution of PCI

3.1.4 Measurements of Skid Resistance at the Network Level

Network skid resistance measurements were conducted in the field using LWT equipped with a standard ribbed tire ASTM E274 (ASTM, 2015g). A weighted trailer is connected to a standard fleet truck and travelled along wetted surfaces at a constant speed of 64 km/h. An example of LWT used by MTO is shown in Figure 3.6.

The LWT provides skid resistance readings of the horizontal forces that were applied to the test tire divided by the dynamic vertical load of friction. This force, the sliding or friction, develops between the tire and the wet surface and is expressed as a skid number (SN64R). Average skid resistance numbers were generated by a sample of 20 to 30 meters of road surface. Skid resistance tests were performed on the left wheel path of the outside lane in the direction of travel. The skid test dates and pavement temperatures during the tests were not available. Only the year of the skid tests was available.

The skid resistance level for each highway section was determined as the average of SN64R measurements. Figure 3.6 illustrates the layout of the friction test performed by LWT (i.e., left wheel path) and ARAN on a six-lane divided highway. Typically, on highways with multiple lanes with more than three lanes per direction, the ARAN measurements were performed on the middle lane (lane 2). For a four-lane highway with two lanes per direction, the ARAN measurements were performed on the lane close to the median (lane 1). The ARAN measurements were performed on the same lane as the LWT only on two-lane highways with one lane per direction.

Figure 3.6 LWT trailer (MTO, 2016a)

(Photo reprinted with permission from the MTO, 2019)

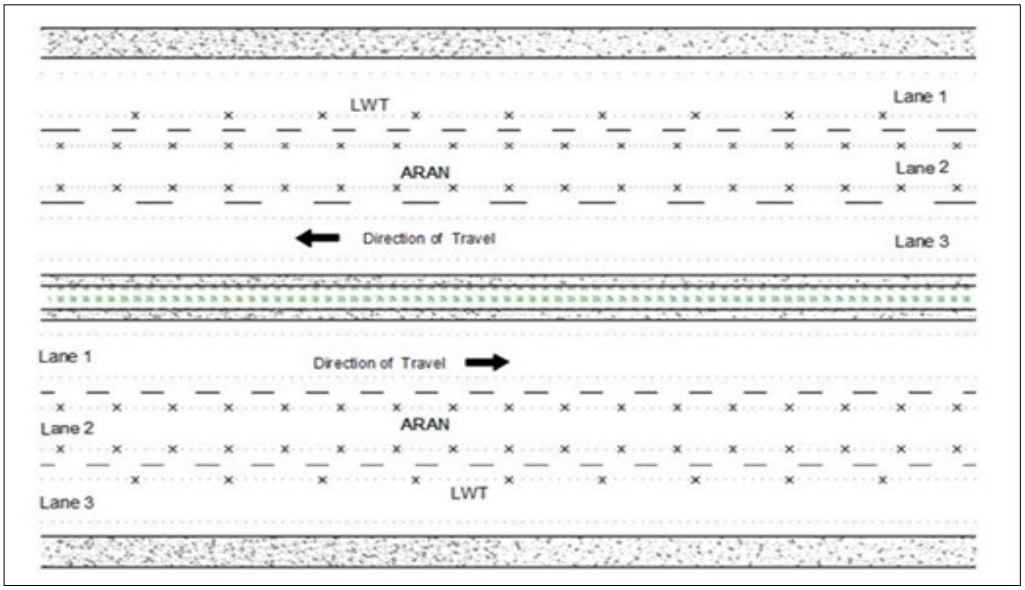

Figure 3.7 Layout of a Highway Section Surveyed with ARAN and LWT

The network skid resistance across the total 1364 km distributed within 110 road sections exhibited SN64R means of 51 with a minimum SN64R of 24 in HWY 28 and the maximum SN64R of 68 in HWY 64. In total 1346 skid tests were performed with an average of 12.24 tests per road segment. Appendix D presents a table (Table D.1) with a summary of descriptive statistics of SN64R measurements by highway, the length of the road segments, and a graphic with the ranges of the variation of SN64R by highway (Figure D1).

The frequency distribution of SN64R means show that the majority of the road sections, approximately 98% of the road sections, exhibited SN64R means between 30 and 65 and only a small portion (less than 2%) of the road sections exhibited SN64R means between 20 and 30. A histogram with the percent distribution of the SN64R average data is shown in Figure 3.8.

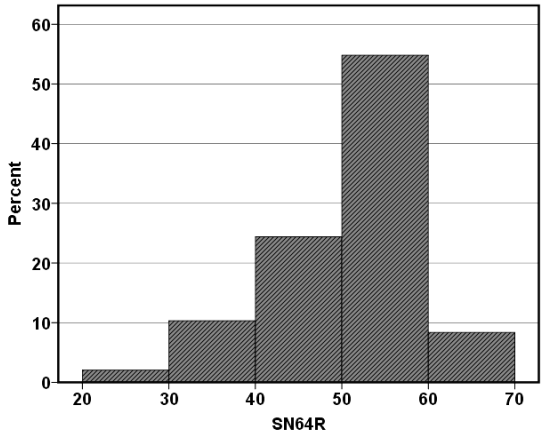

Figure 3.8 Histogram of Percent Distribution of SN64R

3.1.5 Mix Design Data

Information on the type of asphalt mix was available for 108 road sections and mix design parameters were available for 50 out of the108 road sections. Mix design parameters included: percentage of aggregates retained at sieve 4.75 mm (Coarse); percentage of aggregates passing sieve 2.36 mm (FFine); percentage of voids in the mineral aggregate (VMA); percentage of asphalt content (AC); percentage of air void content (AV); and maximum nominal aggregate size (NMAS).

The surface courses were categorized into six types of mix designs: hot mix Hot Laid 4 (HL4), Stone Mastic Asphalt (SMA), Stone Mastic Asphalt 12.5 (SMA12.5), SuperPave 12.5 (SP12.5), Superpave 12.5 Friction Course 1 (SP12.5 FC1), Superpave 12.5 Friction Course 2 (SP12.5 FC2), Table 3.2 summarizes the main mix type parameters for the 50 road sections.

Table 3.2 Summary of Mix Design Parameters

Mix Types	Coarse (%)	FFine (%)	VMA (%)	AC (%)	AV (%)	NMAS max (mm)	N*	n**
HL4	47.75	45.00	14.85	5.15	4.15	16.0	7	1
SMA	72.49	20.60	17.69	5.71	4.00	16.0	9	9
SMA 12.5	79.00	18.00	16.70	5.90	4.00	12.5	2	2
SP12.5	49.72	37.56	14.89	5.03	4.00	12.5	45	20
SP12.5 FC1	50.29	34.63	15.13	5.11	4.00	12.5	23	11
SP12.5 FC2	45.16	41.06	14.36	4.73	4.00	12.5	22	7
(*) N = Number of samples, (**) n = number of the samples with mix design parameters								

3.1.6 Operational Condition of the Roads

Information about the operational condition of the roads included the years of service of the pavement after the most recent service of maintenance, rehabilitation, or construction (pavement age), and traffic. The operational condition and traffic data were

obtained from MTO's department of maintenance and its traffic office. Traffic data included information about annual average daily traffic (AADT), annual average daily truck traffic (AADTt), and annual equivalent single-axle load traffic (AESAL). Table 3.3 summarizes the descriptive statistics of the operational condition of the roads.

Table 3.3 Descriptive Statistics of the Operational Condition of the Roads

Operational Parameters	Min.	Max.	Mean	SD*	N**
AADT	320	380000	35125.47	56241.25	22908
AADTtruck (%)	4	55	18.11	11.42	87
AESAL	4803	10866962	1522844.83	2678962.18	108
Years of Service	1	9	4.50	2.37	110
(*) SD = Standard deviation, (**) N = Number of road segments					

3.1.7 Collision Data

Collision data was obtained from the MTO's Traffic Office. The Traffic Office is responsible for collecting and maintaining a comprehensive collision database. Each collision is recorded by date (day, month, and year), time, highway identification with its LHRS and offset. The collision offset is the distance from the LHRS start point to the point where the collision occurred. Information about the lane and direction of traffic where collisions occurred was not provided.

Additionally, collisions are grouped by categories, including collision class, initial impact, and road surface condition. Some of these collision classes are similar in nature and were grouped to reduce the complexity and size of dataset. For example, the MTO's classification of road surface conditions has six sub-categories: dry, wet, ice, slush, pack snow, and loose snow. These six sub-categories were grouped into two sub-categories: dry and wet. The wet sub-category included collisions that occurred on wet, ice, slush, pack snow, and loose snow surfaces. Table 3.4 shows the MTO's collision classes and

the collision classes included in this study.

Table 3.4 Collision Classifications (MTO and the Present Study's)

Collision Categories	Collision Classes	
	MTO	**Present Study**
Severity	Property Damage Only Injury Fatal	Property Damage Only Fatal and injury
Initial impact	Single vehicle Rear-end Sideswipe Turning, approach, angle Other	Single vehicle Rear-end Sideswipe Turning, approach, and angle
Road Surface condition	Dry Wet Ice Slush Pack snow, Loose snow	Dry Wet (wet, ice, slush, pack snow, and loose snow)

In addition to the collision categories noted above, MTO uses two additional categories to describe the nature of collisions: the number of vehicles involved in the collision (e.g., 1, 2, 3) and illumination condition of the road (e.g., daylight, dark, dawn). These categories were not included in this study. This study considers collisions as a general category, regardless of the number of vehicles involved. Further, while road illumination influences drivers' visual performance and behaviour (Jackett and Frith, 2013; Fotios and Gibbons, 2018), this factor is also outside of the scope of this study.

In total, 66432 collisions occurred on the highways in the period studied, of these 40831 collisions occurred on curves and tangent segments, and 25601 collisions occurred at intersections. Table C.2 in Appendix C shows the total collisions by highway per year. Figure 3.9 to Figure 3.11 describe the frequency in percentage of collisions severity, type of impact, and surface condition.

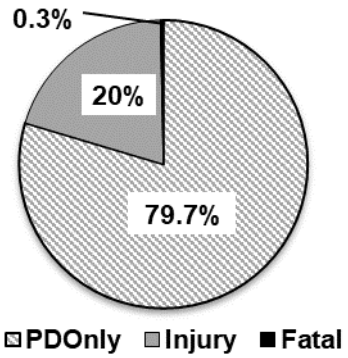

Figure 3.9 Distribution of collision by severity

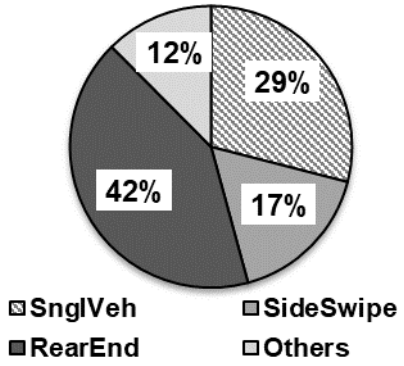

Figure 3.10 Distribution of collision by type of impact

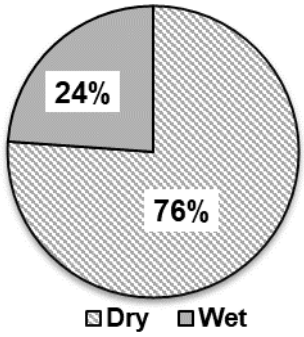

Figure 3.11 Distribution of Collision by Surface Condition

3.1.8 Highway Geometric Features

The highway geometric features included in this study are length, number of lanes, and parameters of horizontal and vertical alignments. Horizontal and vertical parameters were estimated from the geospatial data files used in ArcMap and from the ARAN measurements. More specifically, the length of segments that were not given by MTO and the location of horizontal curves and intersections were estimated from ArcMap. Grade and cross fall of highway segments were taken from the ARAN measurements.

The parameter grade (G) was used to estimate whether the road sections were at

grade or not. The threshold of 3% was used to define whether the highway segment was at-grade or not. The threshold of 3% is defined by TAC as the lowest bound of the maximum grade considered appropriate for design speeds of 100 km/h. The greatest bound of the maximum grade is 5% (TAC, 1999). For example, for a road segment to be considered at-grade, the algebraic difference between the elevation of a specific start point ($LHRS_1$ + $Offset_1$) of a road segment and the elevation of the following next point ($LHRS_2$+ $Offset_2$) has to be lower or equal to 3%. The ARAN's output gives the elevation and the grade of all points measured at each 50 m. The direction of the grade measurement, upgrade (+) and downgrade (-), was not considered because collision data did not specify the lane and traffic direction of collisions. Thus, the vertical alignments of the road sections were defined as at-grade when G is equal or lower than 3% and in-grade when G is greater than 3%.

Curved and tangent segments were identified and categorized using the cross fall information from the ARAN's output and a visual analysis of the GIS maps. The cross fall, or cross slope, of a road is the transverse slope of roads toward the shoulder, median, or gutter. In a tangent segment of a two-lane road the cross fall is normally constant and around 2% (TAC, 1999). In curved segments, the cross fall can vary due to changes of superelevation development (pavement rotation), from normal cross fall to a full superevelation for a specific curve. These changes from a normal cross fall to superelevated were used to identify and categorize road segments as tangent or curve. A two-lane road segment was defined as tangent if its cross fall fell within the interval of ±1 to ± 3.0; otherwise it was defined as curve. Figure 3.12 shows two screenshots of the ARAN measurements of pavement condition in different highways with their respective

cross fall values. It can be observed that curved segments have cross fall values above ± 3 and tangent segments have cross fall values between ±1 to ± 3.0.

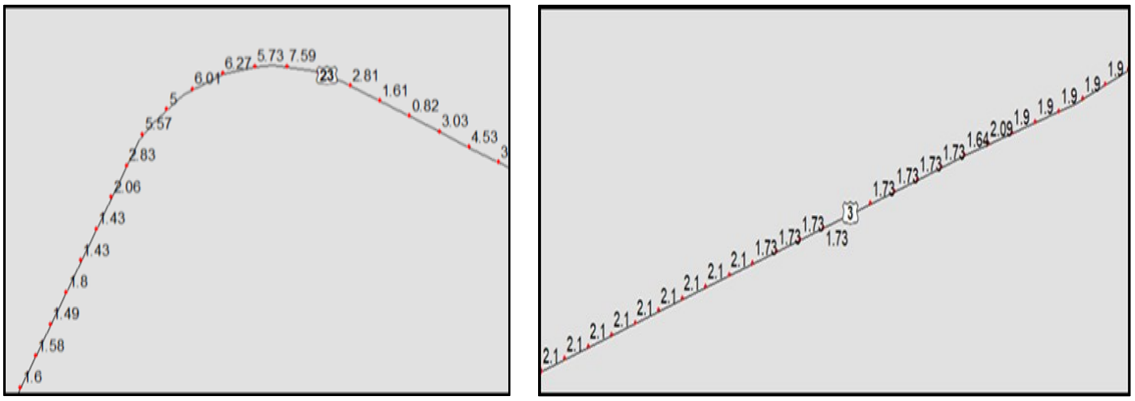

Figure 3.12 Cross fall Values from ARAN's Measurements (ArcMap 10.6, 2017)

3.2 Data Integration

Data linkage of the different datasets was done using the software ArcMap 10.6 (Environmental Systems Research Institute, 2017). The main objective of data linkage is to merge information from different datasets to create a single database that combines geometric features of the roads, collision data, and pavement condition data.

The following three steps were used to prepare and process the data from these three different sources on a GIS platform: 1) Base layers definition, 2) Pavement condition data input, and 3) Collision data input.

3.2.1 Base Layers

To start data linkage using a GIS platform, three geospatial data files (shapefiles) were obtained from MTO. These layers were used as base layers to input information about collisions, pavement condition, skid resistance, operational parameters, and geometric features. The first base layer was the Ontario map shapefile that framed the

territorial limitations of the province of Ontario. The second base layer was the road map of the provincial road network with the identification and length of the roads. The third base layer included information of the LHRSs of each road. The route number (HWY number), geographic location (longitude, latitude), road segment length, and location of the start point of each road segment identify each LHRS. The three layers were inserted into the software ArcMap 10.6 (ESRI, 2017) and used as reference for matching information from different datasets.

The base layers were given in the geographic coordinate system GCS_North American_1983 and transformed into the Universal Traverse Mercator Projection NAD_1983_UTM_Zone 16N (UTM_NAD 83) to reduce distortions due to the curved surface of the Earth. The UTM_NAD 1983_Zone 16N is the projection used by MTO to represent the road and features along the routes (MTO, 2013). Figure 3.13 shows the map of the Ontario road network and LHRSs generated by the software ArcMap 10.6 (ESRI, 2017) using three base layers in a GIS platform.

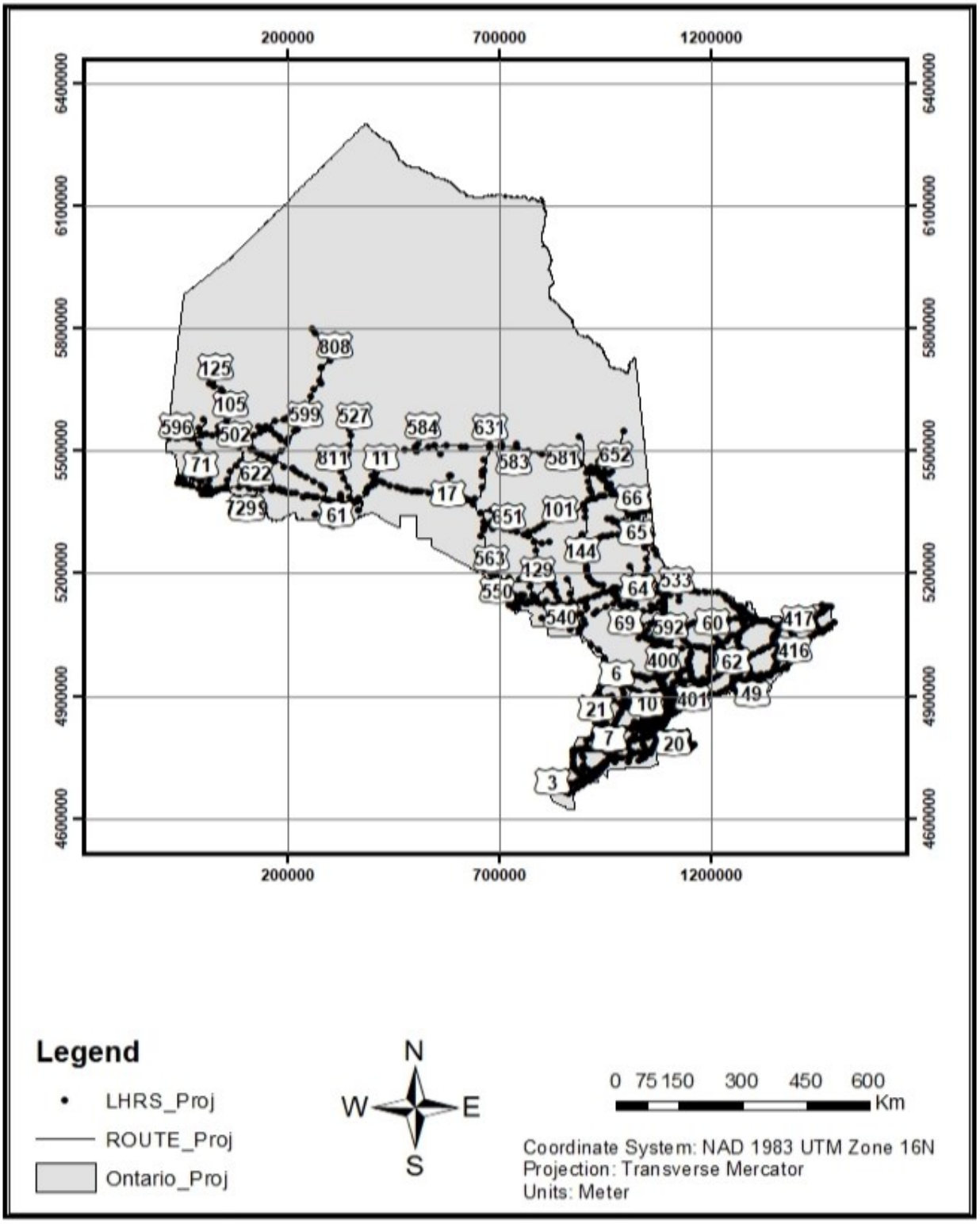

Figure 3.13 Ontario Road Network (ArcMap10.6, 2017)

3.2.2 Pavement Condition Input

The pavement condition, pavement distress, macrotexture, and skid resistance datasets were linked to the road network layer by matching the coordinates of the pavement measurements and LHRS of the road section. The pavement distress and macrotexture datasets were given by year and by HWY in excel spreadsheets that were converted into database file (dBASE tables). This was done in ArcMap 10.6 using the *ArcToolbox > Conversion Tools > Excel to Table*. The pavement condition dBASE tables (PC Tables) with the pavement condition and macrotexture measurements were added to the map as a layer using the *ArcToolbox > Data Management > Features > XY to Line*, where X is the longitude and Y is the latitude of each pavement condition measurement. The XY coordinates were transformed into UTM_NAD83 to match with the map layer.

The table with the skid resistance measurements (SN table) included mix design parameters and the operational condition of the roads. This table did not have XY coordinates; the locations of the SN64R measurements were given by their LHRSs. The SN table was added into the PC tables using the *ArcToolbox > Join > Join Field*, where the LHRS was selected as the *Input Join Field*. Figure 3.14 and Figure 3.15 show maps generated by ArcMap 10.6 with the locations of pavement condition and skid resistance measurements for the years 2012, 2013, and 2014.

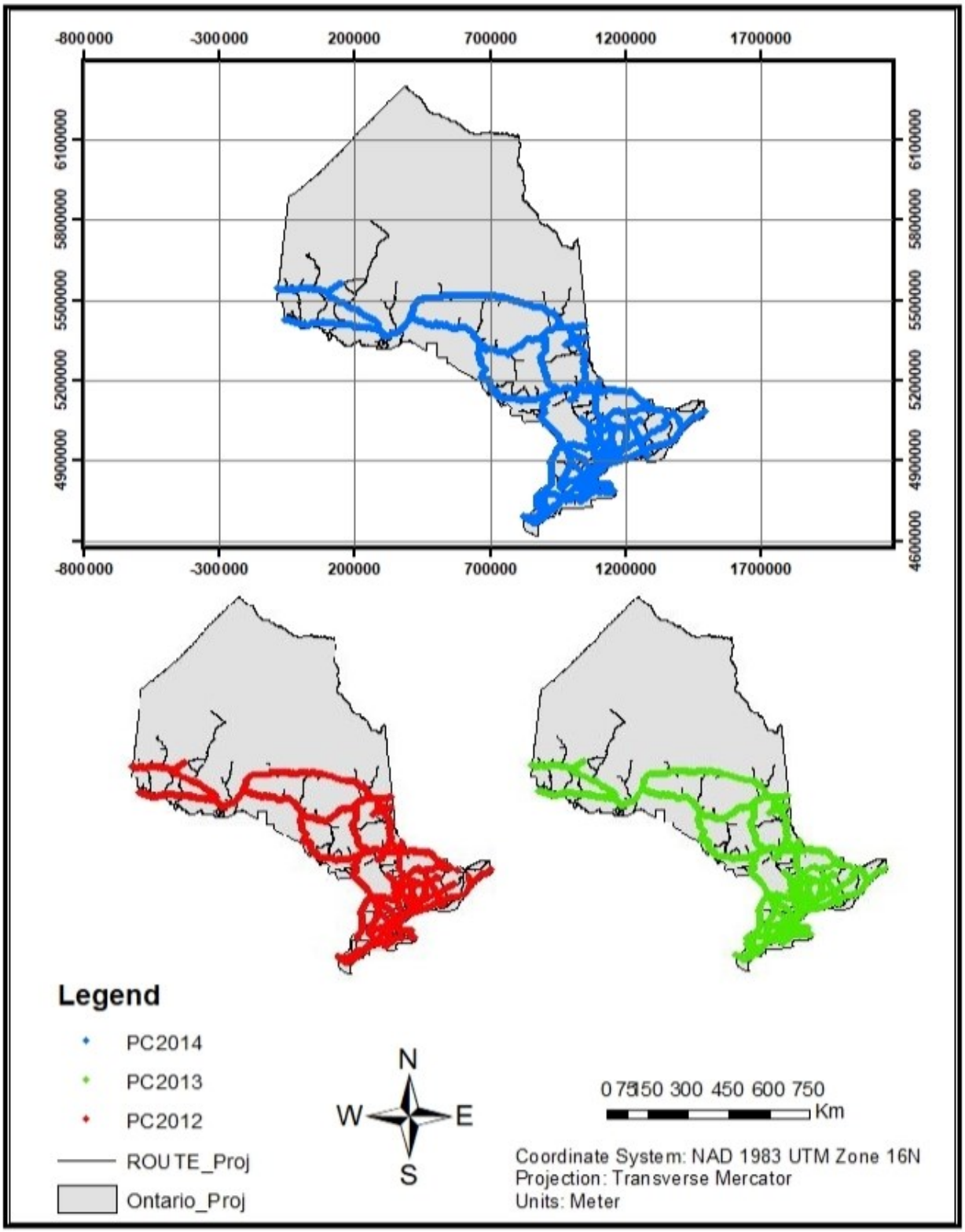

Figure 3.14 Map of Measurement of Pavement Condition (ArcMap 10.6, 2017)

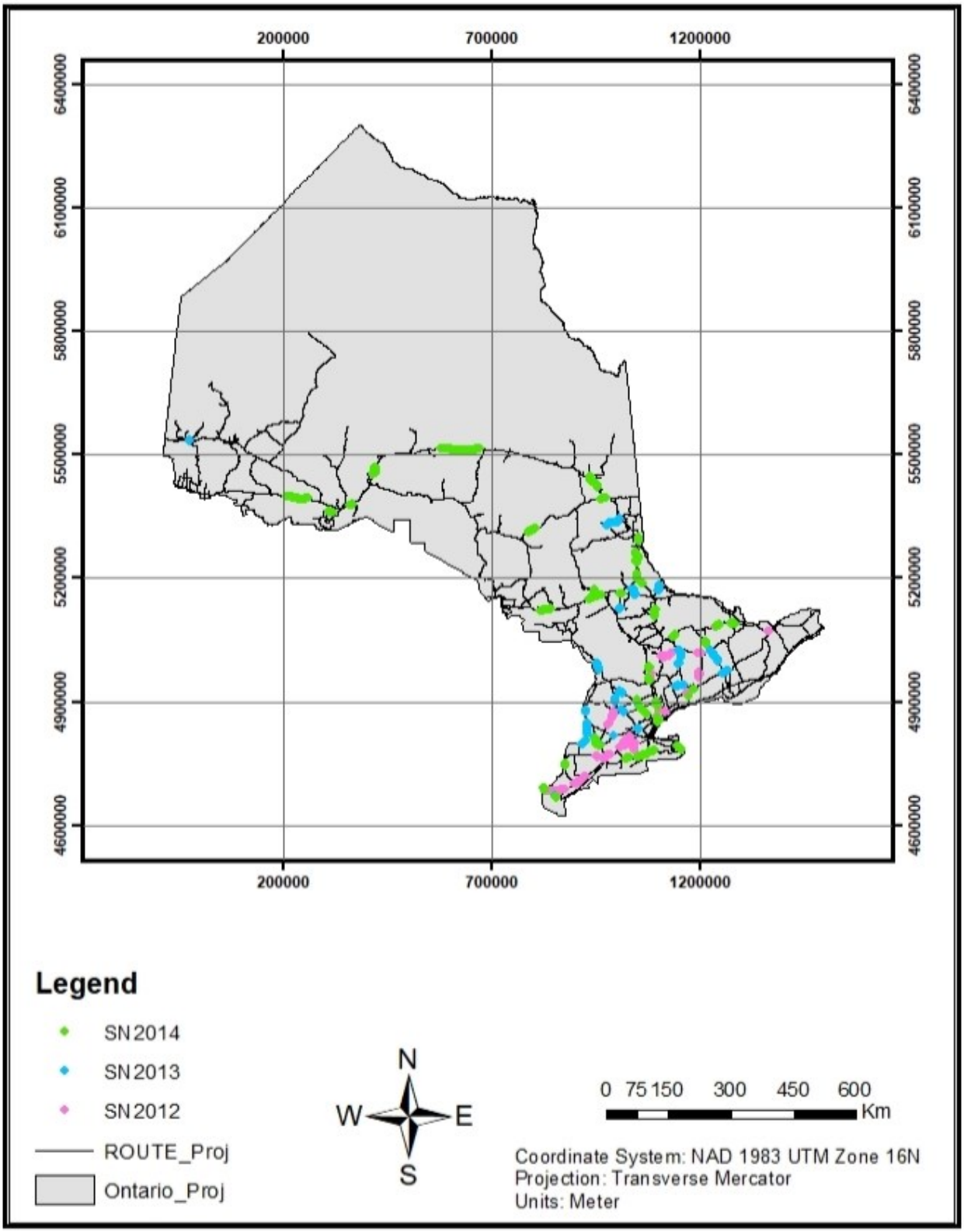

Figure 3.15 Map of Measurements of Skid Resistance (ArcMap 10.6, 2017)

3.2.3 Collision Data Input

To match the collision data with the pavement condition data, the Linear Referencing System (LRS*)* extension for ArcMap10.6.1 was used to locate collisions on the road sections. This approach was used due to lack of information about the geographic coordinates of the collisions. The collisions' locations were identified by their LHRS and offsets spaced by 100 m. The LRS extension does not require geographic coordinates as a reference to locate a point events (collisions) on a line (route); instead, the LRS extension has tools that allow to distribute point events linearly along a road section based on a reference point (i.e., LHRS) and offsets from the respective reference point.

To locate the collisions on the routes, firstly, tables with the collisions were prepared. The collision tables were categorized by year and by highway, which resulted in three tables, one for each year of pavement condition measurement. These collision tables were input into the GIS platform as dBase tables. In the GIS, each collision was treated as a point event defined by fields that contained a route identifier.

The routes were created from existing lines using the *ArcToolbox > Linear Referencing Tools > Create Routes*. To create a route from an existing line, the *Input Line Features* and the *Editor* tool were used to select *Features by Line*. Once the linear features were selected, the *Make Route* tool was selected to set the start point from where the route began, as defined by the start point of each LHRS. Once a route was created, a field with a unique *Route Identified* was created for each route.

Next, the collision tables were added into the route layers by selecting the tool

Make Route Event Layer. The route layers were selected as the *Input Route Features.* The collision tables were selected as *Input Event Table* and input as *Point Event Type.* The result was three new layers with collision events, one layer per year.

Finally, the coordinates of each collision location were calculated using the *ArcToolbox > Data Management > Features > Add XY Coordinates*. Once the coordinates of each collision were calculated, the collision layers were joined to their respective pavement condition layers. The two layers, collision and pavement condition, were joined using the tool *Join Data* and selecting the option *Join Data from another layer based on spatial location*. The results of the entire process were three tables that contained matched collision with pavement condition, skid resistance, mix design parameters, and operational condition of the roads. To export the data from the ArcMap 10.6, the layers with their respective tables were converted to excel spreadsheets using *ArcToolbox > Conversion Tools > Table to Excel*.

Figure 3.16 shows a map of the Ontario road network with the collisions layers and collisions distributed along the highways. Figure 3.17 shows a zoom-in image of collisions that occurred in a section of Highways 17 and 72 in the year 2014. This figure also shows one collision identified as 310 (highlighted in blue) and screenshots of parts of the table of attributes of this collision. This table shows part of the results of the processes of joining the collision and pavement condition datasets. The table shows the collision location (LHRS + offset), total collision in that location (All), collision attributes (classified by severity, initial impact, etc.), traffic volume (AADT), geometric elements (segment length, grade, cross fall), type of pavement (AC), ARAN's speed (52.52 km/h), and some pavement condition indicators (IRI, RUT, MPD).

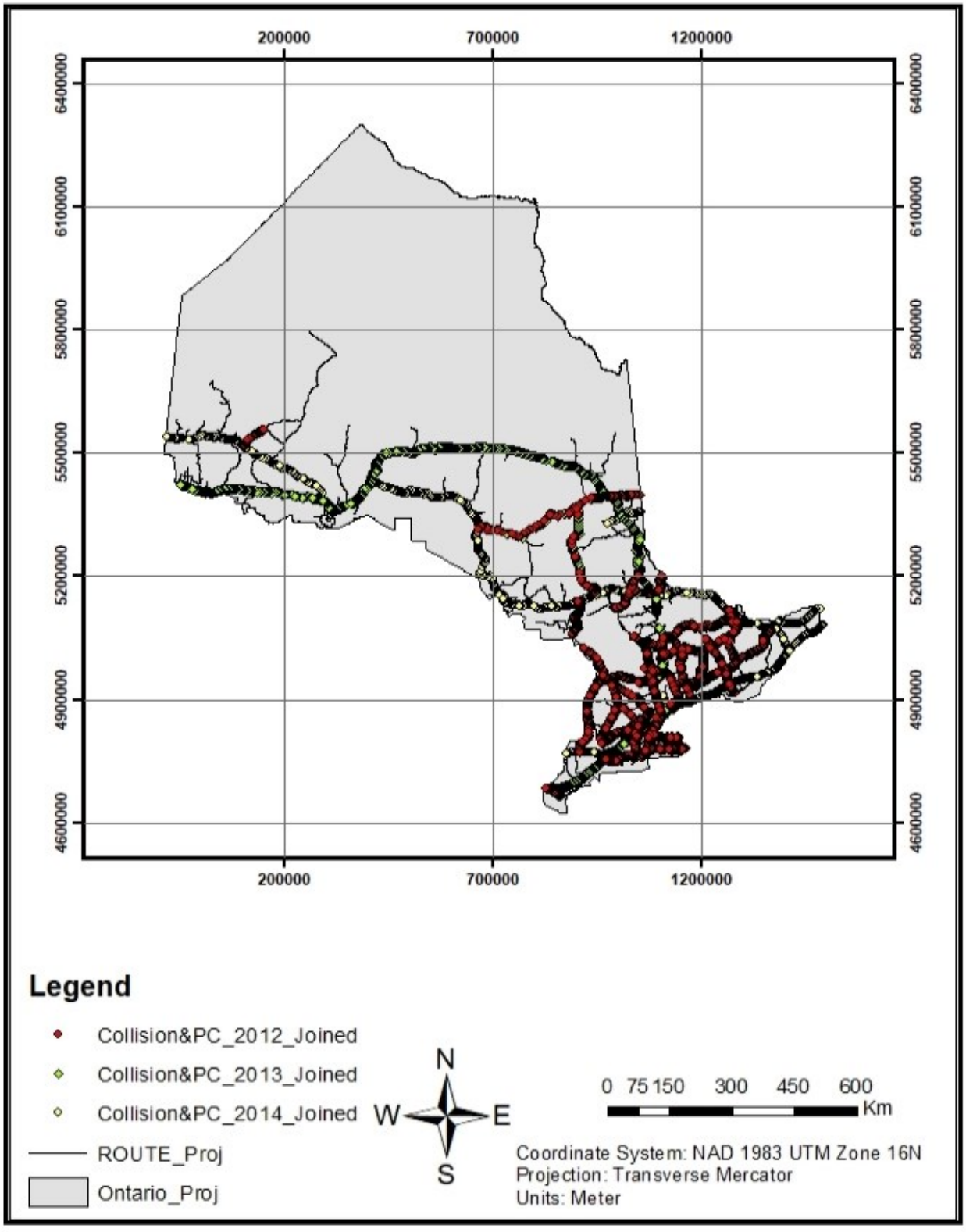

Figure 3.16 Map of Collisions (ArcMap 10.6, 2017)

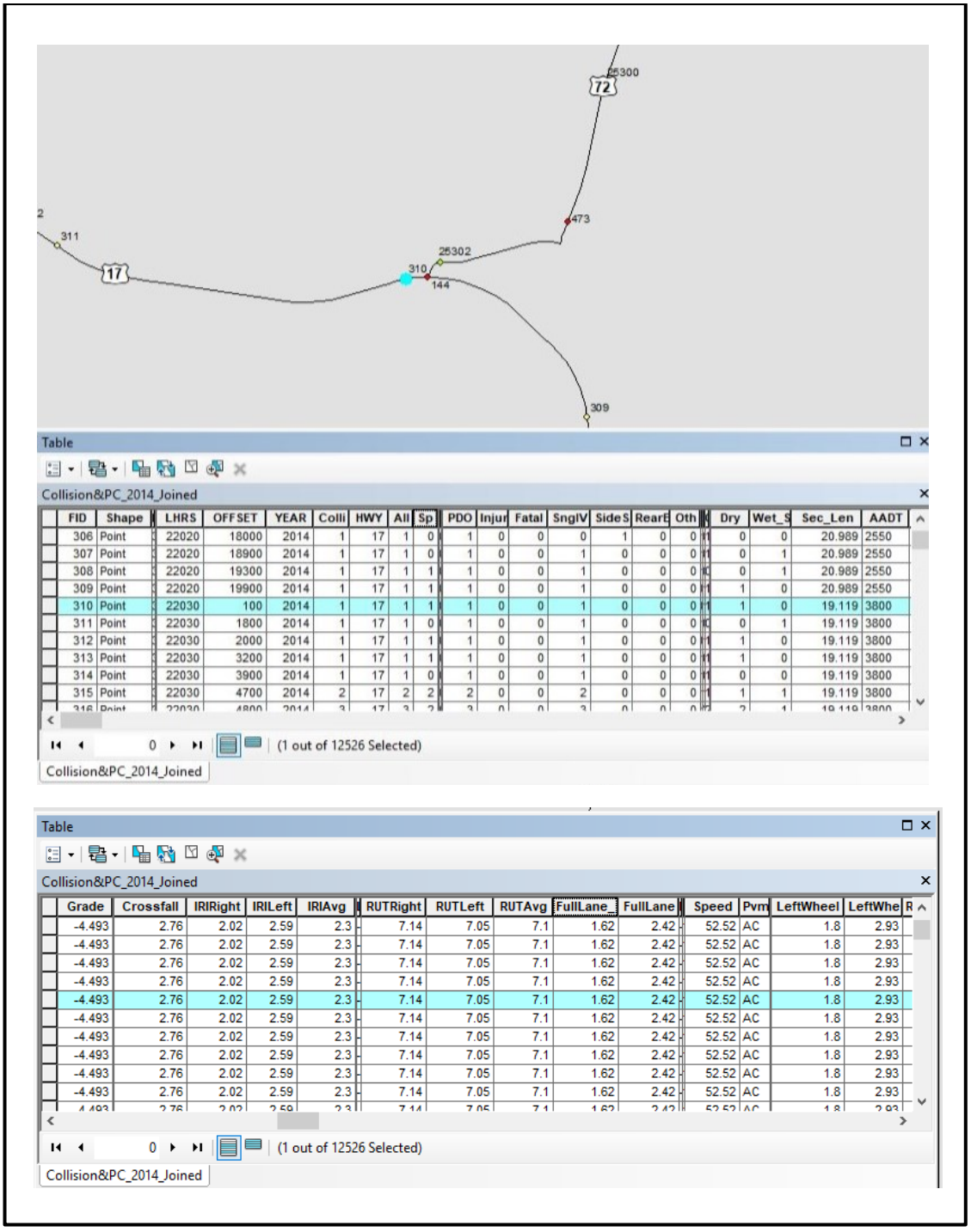

Figure 3.17 Zoom-in Image of Collisions (ArcMap 10.6, 2017)

3.2.4 Data Integration and Data Inconsistencies

During the process of matching collision excel file data with the LHRS shapefile data inconsistencies were detected. The inconsistencies included missing LHRS, mislabeled HWY identification, and missing pavement indicators. These inconsistencies can be summarized as follows:

- *Missing LHRS*. A total of 14 LHRS from the original collision excel file were not found in the LHRS shapefile. The original collision excel file had 25,962 entries (points); after removing the missing LHRS entries, the final collision shapefile had 25,786 entries with 176 fewer entries (points). These176 collision points were not included when populating the final collision shapefile since their locations were unknown.
- *Mislabeled highway identification*. A group of 50 LHRS were labelled as being present on HWY 400 in the collision excel file. However, these LHRS collisions were associated to HWY 401. This error was corrected when populating the final collision shapefile.
- *Missing pavement condition data*. Two main issues were detected in the pavement condition data collected with ARAN. First, some road segments did not have measurement of IRI. Second, some road sections were not completely surveyed for all pavement indicators with ARAN. In cases like that, where pavement data were missing, the road segment and collisions were not counted.

3.3 Summary

This chapter dealt with the data about the operational condition of the roads, pavement condition indicators, and collisions were collected from different sources and in different formats provided by MTO. The data and information were recorded by the MTO using the linear highway referencing system (LHRS). The LHRS was used as reference to create a single database using GIS which permitted the integration of spatial and non-spatial data. This single GIS data file was exported as an *xls* file extension to be used in data analysis and modelling.

4 Chapter: Investigating Factors Affecting Pavement Friction

This chapter presents the results and statistical approaches used to investigate factors that affect skid resistance and macrotexture and to develop regression models to predict skid resistance using macrotexture and pavement distress. The study was divided into two parts. The first part consisted of analysis of relationships between skid resistance and macrotexture and factors that influence pavement friction, and the second part consist of development of regression models to predict skid resistance for Ontario highways. The relationships and factors investigated included:

- The relationship between skid resistance and macrotexture,
- The influence of traffic and loads on skid resistance and macrotexture,
- The influence of mix type on skid resistance and macrotexture,
- The influence of pavement age on skid resistance and macrotexture, and
- The influence of pavement distress on skid resistance and macrotexture.

4.1 Data Attributes and Statistical Approaches

This sub-section provides a concise overview of the data attributes and statistical approaches used in the statistical analysis.

4.1.1 Data Attributes

The data obtained from MTO for 1,363.64 km of asphalt surface included 110 road segments of 36 rural highways, divided and undivided, single and multiple lanes per direction with speed limits of 80 km/h and 100 km/h. The field data was collected for the 110 road segments using LWT for skid resistance (SR64R). Among these 110 road segments only 75 road segments of 29 rural highways were measured with the ARAN for macrotexture (MPD) and pavement distress. The measurements were taken between April

and October of the year 2012 to 2014.

In addition to the SN64R and MPD data, type of mix was available for 108 road segments and mix design parameters for 50 out of the 108 road segments. Information of the operational conditions included: the years of service of the pavement (pavement age) after the most recent maintenance, rehabilitation, or construction; annual average daily traffic (AADT); percentage of trucks; annual equivalent single-axle load traffic (AESAL); and number of lanes.

Among the 15 indicators of pavement distress, only four were selected for analysis in this study: rutting (RUT), ravelling (RAV), wheel path pattern cracks (WPC), and roughness (IRI). The selection of these pavement distress was based on previous studies (see Chapter 2) that observed that rutting, ravelling, and cracks showed correlations with pavement surface textures (Li *et al.*, 2003; Ahammed and Tighe, 2008; McDaniel and Kowalski, 2012). Further, rutting and wheel path pattern cracks were selected because they were measured on the left wheel path, which matched the location of the skid resistance measurements. Roughness and ravelling were selected because they are related to pavement texture and greater levels of roughness and ravelling indicate increased pavement texture deterioration.

The other indicators of pavement distress related to pavement defects and deformation (flushing, shoving, and distortion) were not included in the analysis because they were not collected by ARAN. In addition, cracks located outside of the wheel path (centre, edge, longitudinal, and transversal) were not included in the analysis because of the difficulty of matching their location to the location of the skid resistance measurements.

Table 4.1 shows the descriptive statistics of skid resistance, macrotexture,

pavement distress, and the operational condition of the roads. The table shows that there is a wide difference between the highest and lowest values and a high standard deviation of the indicators of pavement condition and operational condition of the roads. The high standard deviation of the indicators indicates a large amount of variation in the sample, which is expected due to the nature (measurements) and source of data (locations).

Table 4.1 Descriptive Statistics of Network Level Data Sample

	Min.	Max.	Mean	SD*	N**
SN64R	25	64	51	8.22	110
MPD (mm)	0.71	1.85	1.08	0.23	75
IRI (m/km)	0.69	3.82	1.16	0.60	60
RUT (mm)	0.79	7.9	3.70	1.43	60
RAV (%)	1	60	7.2	15.53	60
WPC (%)	1	100	19.60	30.94	60
AADT	417	288678	30821	54096	110
AESAL	4803	10866962	1522845	2678962	110
LDF	0.6	1.0	0.95	0.1547	110
Percentage of truck (%)	4	55	18	11	110
N° of lanes per direction	1	4	1.70	0.92	110
Pavement age (years)	1	9	5.04	2.20	110
(*) SD = Standard deviation, (**) N = Number of road segments					

The SN64R values ranged from 25 to 64 with a mean of 51 and SD of 8.22 and MPD ranged from 0.70 mm to 1.85 mm with mean of 1.08 mm. The means of skid resistance and macrotexture were above satisfactory levels recommended by transportation agencies (TAC, 1999; DMRB, 2015). The minimum and maximum values of pavement distress indicate that pavement conditions ranged from new to aged pavements.

4.1.2 Statistical Approaches

A variety of statistical analyses were used to investigate the relationships between SN64R and MPD, as well as the influence of traffic and loads, mix design parameters,

pavement age, and pavement distress.

The relationships between SN64R and MPD and their relationships with ESAL and pavement distress were examined using simple linear regression with a single explanatory variable with one independent variable and one dependent variable. The simple regression analysis was used to investigate correlations between variables and whether they were statistically significant. The relationships were investigated using linear, quadratic, and exponential functions.

The coefficient of determination R-square was used to measure the goodness-of-fit of the relationships. The R-square multiplied by 100 indicates the percentage of the variation in the independent variable explained by the variation in the predictor. The F-test and the t-test were used to test the level of significance of the regressions. The F-test tested the overall model significance. The null hypothesis is that the independent variables have no influence on the dependent variable. The t-test tested the significance of each coefficient and the intercept. The t-test has the null hypothesis that the coefficient/intercept is zero.

The level of significance (α) adopted in this research was set at 5% and 10%. A p-value smaller than the predefined significance level α indicates that the null hypothesis is rejected and that there was a relationship between the independent and dependent variables. A p-value greater than α indicates that the null hypothesis is not rejected and there was no relationship between the variables.

A one-way ANOVA test was used to determine whether there were statistically significant differences in the means (μ) of SN64R and MPD within groups of pavement ages and types of mixes. The ANOVA tests the null hypothesis (H0), where the mean of

groups is equal (H0: $\mu 1 = \mu 2 = \ldots \mu n$). If ANOVA results were statistically significant (p-value ≤ 0.05), the null hypothesis was rejected, which indicates that there were at least two means of groups that were statistically significantly different from each other.

One-way ANOVA indicates if the difference between the means of groups was statistically significant, but it does not indicate which specific group differed. To identify differences between groups a post-hoc Tukey test was used. The Tukey test calculated the Honest Significant Difference for each pair of means.

The statistical analyses using one-way ANOVA, t-test, and Tukey post hoc test were made using the statistical software SPSS 23.0 (International Business Machines Corporation, 2015).

4.2 Data Analysis

Data analysis started with the investigation of the relationships between the variables SN64R and MPD, followed by an investigation of the relationships between SN64R and MPD with ESAL, pavement age, mix design, and pavement distress. The objective of the analysis was to identify statistically significant correlations that could be used to develop skid resistance prediction models. A flowchart of the statistical analysis is shown in Figure 4.1.

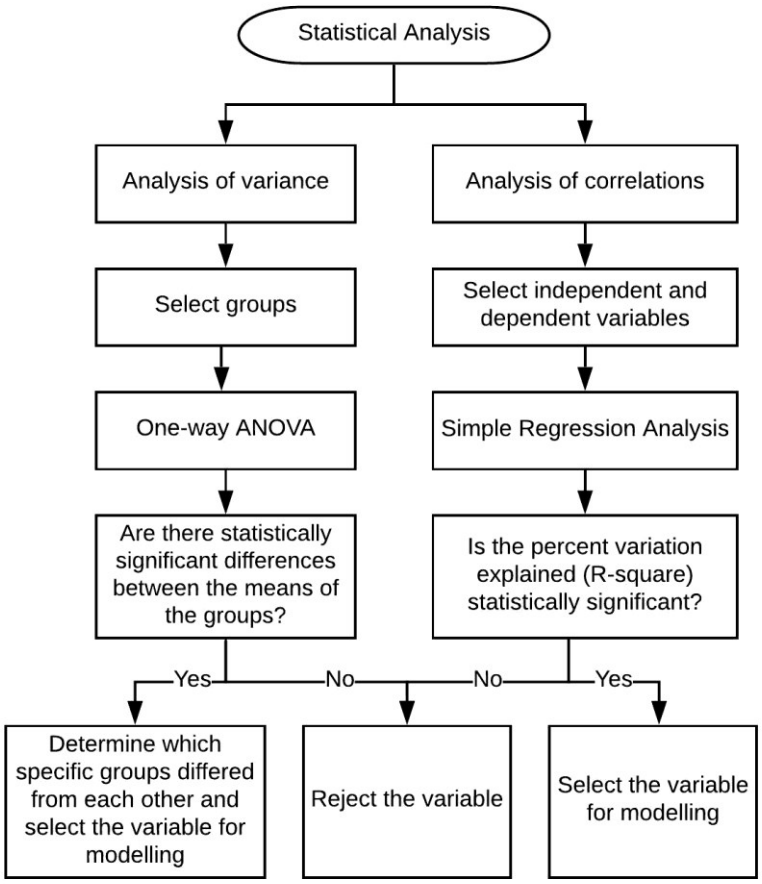

Figure 4.1 Flowchart of the Statistical Analysis

4.2.1 Relationship between Skid Resistance and Macrotexture

The relationships between SN64R and MPD for 75 road segments were examined using simple linear regression. The relationship between SN4R and MPD was not statistically significant (p-value > 0.05) with an R-square of 0.010. The poor relationship between SN64R and MPD indicates that only 1% of SN64R variation may be explained by MPD. Figure 4.2 shows the scatterplot and the linear regression line of the relationship between SN64R and MPD.

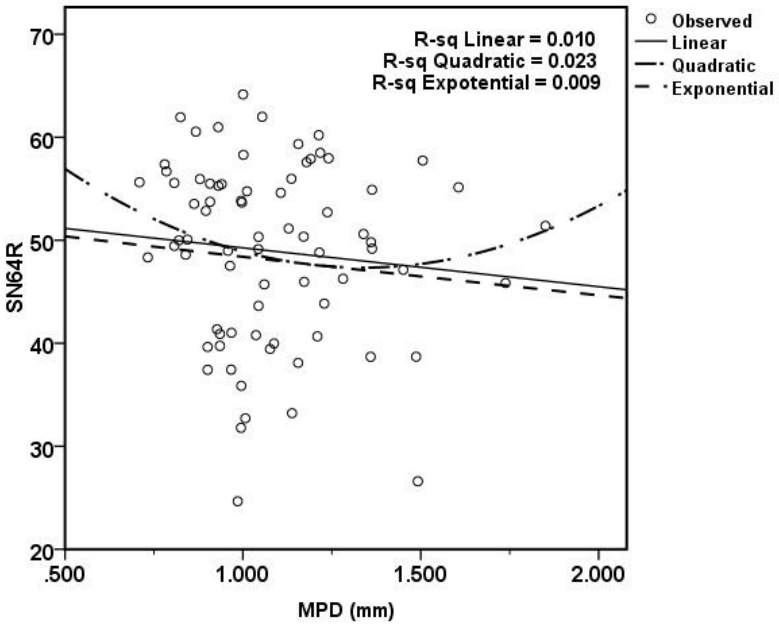

Figure 4.2 Relationship between SN64R and MPD

Nonlinear relationships between SN64R and MPD were also examined. The results showed that the R-squares of nonlinear relationships were similar to the R-square of linear function. The quadratic function exhibited an R-square of 0.023, and the exponential function exhibited an R-square of 0.009. Therefore, the R-square of the relationship between SN64R and MPD was very small and did show an improvement when nonlinear functions were used.

Previous studies have shown that skid resistance and macrotexture were correlated with R-squares that ranged from 0.29 to 0.83, depending on the type of data and devices used for data collection (Ahammed and Tighe, 2012; Rajaei *et al*., 2014; Serigos *et al*., 2014; Meegoda and Gao, 2015). It is possible the poor correlation between SN64R and MPD was influenced by several factors, including problems with data collection, device calibration, errors in the LWT tests, environmental conditions, and

contaminants on the pavement surface (e.g., dust, debris), among other things.

Of these factors, only data collection can be explained as a potential source of error because information regarding the other factors was not collected as part of this study. In particular, data collection may have caused problems due to inconsistencies in the measurement process. Firstly, SN64R and MPD were measured with different devices that used different approaches to measure pavement textures. Skid resistance measured by LWT was not a measurement of pavement microtexture, but a measurement of the frictional forces affected by pavement microtexture and macrotexture. Meanwhile, the macrotexture measured by ARAN was existing macrotexture. It is possible that SN64R measurements were affected by macrotexture due influence of speed test.

Secondly, measurements of SN64R and MPD did not occur in the same month for the majority of the road segments in the sample. This may have contributed to accentuating a seasonal influence on the measurements. Several studies reported variations in skid resistance over a short-term period (daily and weekly) due to the influence of environmental factors, such as after rainfall and temperature increases (Wallman and Astrom, 2001; Ahammed and Tighe, 2008; Mayora and Pina, 2009; DMRB, 2015).

Finally, the specific location of SN64R and MPD measurements did not match. Measurement of MPD with ARAN occurred consistently along the roads and MPD was recorded as the average of macrotextures for every 50 m. Yet, SN64R measurements occurred on only part of road segments and inconsistently spaced. Further, SN64R measurements were recorded as minimum, maximum, and mean of SN64R, but only the means of SN64R were used in the analysis. It is possible that the variance of SN64R was

a potential source of variation in the data and the results. The SN64R variation by highway is shown in Appendix D. In sum, the above described differences in data collection methods, time, and location of measurements could contribute to explaining the poor correlation between SN64R and MPD.

4.2.2 Investigating the Influence of Traffic on Skid Resistance and Macrotexture

The relationships between SN64R and MPD and traffic were examined in terms of AESAL. The AESAL corresponds to the number of repetitions of an 80 kN single axle load applied to the pavement on two sets of dual tires over a one-year period.

The AESAL was adjusted for AESAL in the design lane (i.e., the lane surveyed with LWT) according to the lane distribution factor (LDF). The LDF used by MTO is based on the number of lanes in one direction, percentage of trucks in the design lane, and AADTt. The LDF differs within the highways due to the predominant type of truck (vehicle class), operational condition of the roads (AADT), and geometric characteristics of the road (number of lanes). To estimate the AESAL on the design lane, the AESAL was adjusted according to the LDF as defined by MTO as follows (MTO, 2012):

- Two lanes in one direction: 0.8 (for AADTt < 15000) and 0.9 (for AADTt > 15000)
- Three lanes in one direction: 0.8 (for AADTt < 25000) and 0.7 (for AADTt > 25000)
- Four lanes in one direction: 0.7 (for AADTt < 40000) and 0.6 (for AADTt > 40000)

The relationships between SN64R, MPD, and AESAL were examined using simple linear regression. The simple linear regression indicated that SN64R and MPD were influenced by AESAL.

The relationship between AESAL and SN64R was statistically significant (p-

value < 0.001) with an R-square of 0.251. The relationship between AESAL and MPD was not statistically significant (p-value = 0.06) with R-square of 0.036.

Figure 4.3 shows the scatterplot and the linear regression line of the relationship between SN64R and AESAL in the design lane. The regression line shows that SN64R decreases as the AESAL in the design lane increases. The square of the correlation coefficient (R-square) indicates that 25.1% of the variation of SN64R may be explained by AESAL in the design lane.

Figure 4.4 shows the scatterplot and the linear regression line of the relationship between MPD and AESAL in the design lane. The regression line shows that MPD increases as the AESAL in design lane increases. The square of the correlation coefficient (R-square) indicates that 3.6% of MPD variation may be explained by AESAL in the design lane.

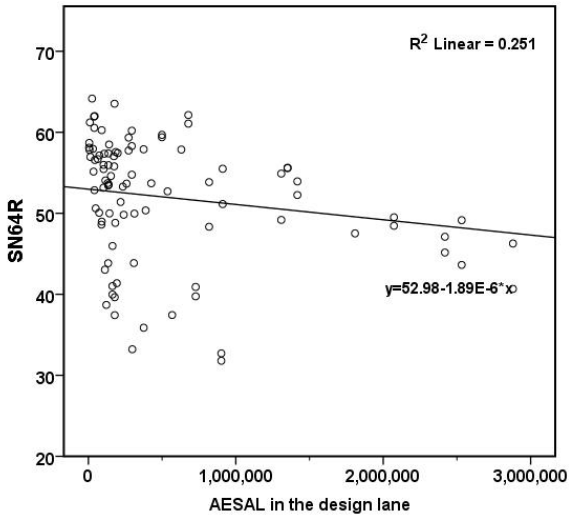

Figure 4.3 SN64R and AESAL in Design Lane

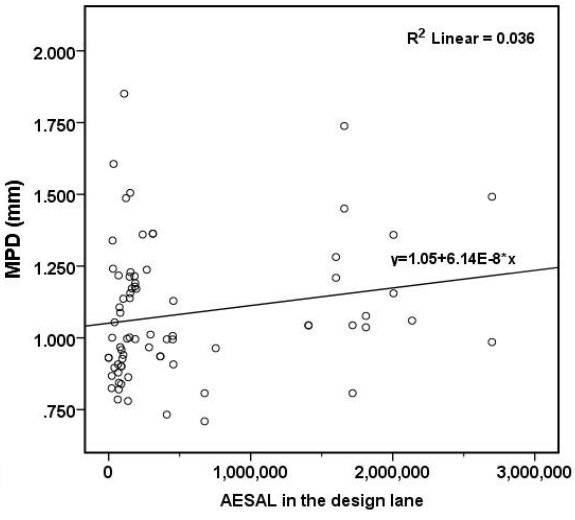

Figure 4.4 MPD and AESAL in Design Lane

Nonlinear relationships between SN64R and AESAL were also examined. The quadratic and exponential relationships exhibited R-squares of 0.257 (p-value < 0.001) and 0.237 (p-value < 0.001), respectively. These results showed that nonlinear relationships between SN64R and AESAL did not contribute to R-squares increase.

Nonlinear relationships between MPD and AESAL were also examined. The results showed that the R-squares for nonlinear relationships were similar to the R-square for linear functions. The quadratic function between MPD and AESAL exhibited an R-square of 0.038 (p-value = 0.26) and the exponential function exhibited an R-square of 0.034 (p-value = 0.12). These results showed that nonlinear relationships between MPD and AESAL did not contribute to R-squares increase.

The results of the influence of traffic and loads on skid resistance and macrotexture showed that skid resistance decreases as AESAL increases, and macrotexture increases as AESAL increases. The relationship between AESAL and macrotexture was weaker than between traffic and loads and skid resistance. The difference in the influence of AESAL on skid resistance and macrotexture can be related to complications related to data collection. Specifically, MPD measurements on multilane highways did not always occur on the heaviest lane, which they did for SN64R. This inconsistency may have reduced the accuracy of the estimation of the influence of AESAL on macrotexture. Thus, the results of influence of traffic and loads on macrotexture may have been underestimated.

4.2.3 Investigating the Influence of Surface Course on Skid Resistance and Macrotexture

The surface courses were categorized into six types of mix designs HL4, SMA,

SMA12.5, SP12.5, SP12.5 FC1, and SP12.5 FC2. Table 4.2 displays a summary of the descriptive statistics of SN64R and MPD by type of mix. Figure 4.5 and Figure 4.6 show boxplots of the statistical distribution (minimum, median, quartiles, maximum, and outliers) of SN64R and MPD by type of mix.

Table 4.2 Descriptive Statistics of SN64R and MPD by Type of Mix

Mix Types	SN64R					MPD				
	Min.	Max.	Mean	SD *	N **	Min.	Max.	Mean	SD *	N **
HL 4	43	64	56.77	7.41	7	0.82	1.50	1.15	0.27	6
SMA	38	49	42.69	4.09	9	0.96	1.36	1.13	0.13	9
SMA12.5	49	55	52.04	4.04	2	1.36	1.36	1.36	0.00	2
SP12.5	32	64	53.00	7.27	45	0.70	1.85	1.03	0.25	30
SP12.5FC1	33	60	48.99	8.45	23	0.82	1.49	1.05	0.17	18
SP12.5FC2	25	62	48.92	8.90	22	0.81	1.74	1.22	0.29	9
Total	25	64	50.71	8.24	108	0.71	1.85	1.08	0.23	74
(*) SD = Standard Deviation, (**) N = Number of road sections										

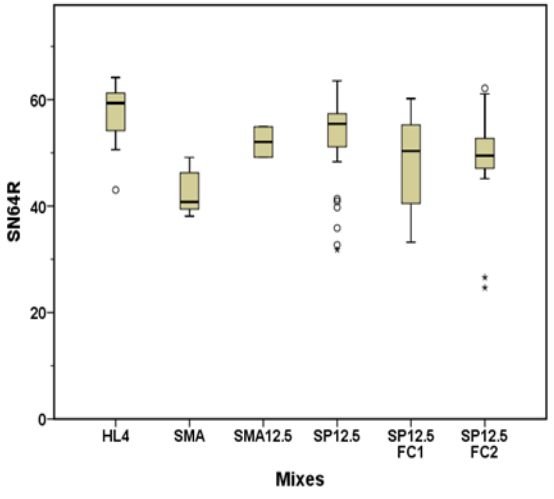

Figure 4.5 SN64R by Mix Type

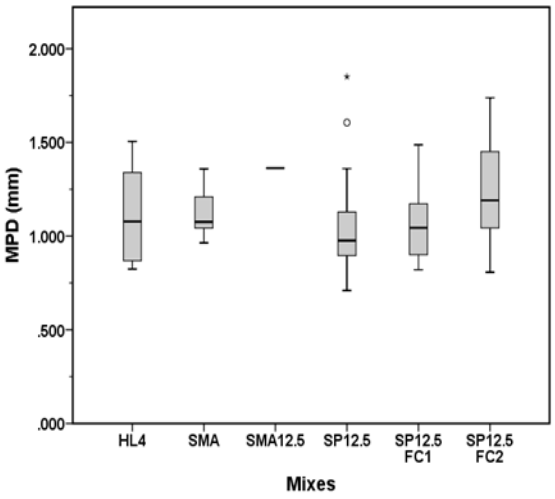

Figure 4.6 MPD by Mix Type

ANOVA and Tukey post hoc test were used to compare the difference of SN64R and MPD means between the mixes. The ANOVA results indicated that SN64R means

differed statistically significantly (p-value < 0.10) within the mixes. The Superpave mixes (SP12.5, SP12.5 FC1, SP12.5 FC2) and HL4 exhibited greater SN64R means than the SMA. The SMA12.5 mix exhibited SN64R means comparable to the SN64R mean of SP12.5.

The ANOVA results for MPD means indicated that MPD means did not differ statistically significantly (p-value > 0.10) within the six types of mixes. However, except for SP12.5 FC2, the Superpave mixes exhibited a lower MPD than other mixes. SMA12.5 exhibited the greatest MPD mean.

A possible explanation for the significant difference in SN64R and nonsignificant difference in MPD within the mixes could be related to mix gradations. However, the analysis including mix gradation differences was inconclusive. The open graded mix (SMA) exhibited lower SN64R means than dense graded mixes (Superpave mixes and HL4); on the other hand, the mix SMA 12.5, which is also an open graded mix, exhibited the greatest SN64R means. Thus, differences in the type of mixes were not sufficient to explain variations in SN64R means.

Another possible explanation for the significant difference in SN64R and nonsignificant difference in MPD within the mixes could be related to the physical properties of the coarse and fine aggregates in the mixes. The physical properties of aggregates are defined by a series of requirements and laboratory tests specified in the OPSS PROV 1003 (Ontario Provincial Standard Specification, 2013). Among the specifications, two requirements for aggregates could influence pavement friction: the requirement that provides the percentage of flat and elongated particles in the mixes; and the requirement that provides the percentage of Micro-Deval abrasion loss of aggregates,

which quantifies the resistance of aggregates to polishing. Unfortunately, no information regarding the physical properties of aggregates were available and analysis of the influence of aggregates could not be investigated.

4.2.4 Investigating the Influence of Pavement Age on Skid Resistance and Macrotexture

The relationship between SN64R and MPD and pavement age were examined in terms of years of service after the most recent maintenance, rehabilitation, or construction. Table 4.3 displays a summary of the descriptive statistics of SN64R and MPD by pavement age. Figure 4.7 and Figure 4.8 show boxplots of the statistical distribution (minimum, median, quartiles, maximum, and outliers) of the SN64R and MPD of each category of pavement age.

Table 4.3 Descriptive Statistics of SN64R and MPD by Pavement Age

Pavement Age (years)	SN64R					MPD				
	Min.	Max.	Mean	SD *	N **	Min.	Max.	Mean	SD *	N **
1	25	58	40.00	13.09	6	0.82	1.49	1.10	0.01	6
2	39	62	53.14	5.70	25	0.90	1.85	1.25	0.28	12
3	48	60	55.34	2.83	16	0.99	0.09	0.81	0.71	7
4	37	53	43.35	5.41	7	0.90	1.74	1.16	0.33	7
5	32	62	45.50	9.74	17	0.84	1.34	1.07	1.44	16
6	40	64	51.17	6.56	14	0.81	1.34	1.00	1.21	10
7	38	60	50.76	11.31	5	1.15	1.38	1.04	0.82	3
8	44	64	54.06	6.10	15	0.82	1.36	1.04	0.15	12
9	43	58	53.30	5.97	5	0.86	1.6	1.23	0.52	2
Total	25	64	50.71	8.24	110	0.71	1.85	1.08	0.23	75
(*) SD = Standard Deviation, (**) N = Number of road sections										

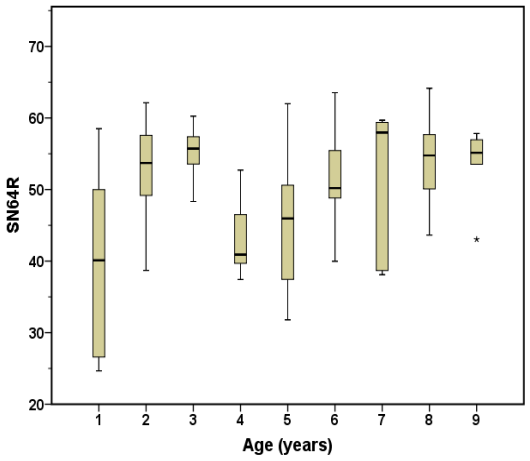

Figure 4.7 SN64R by Age

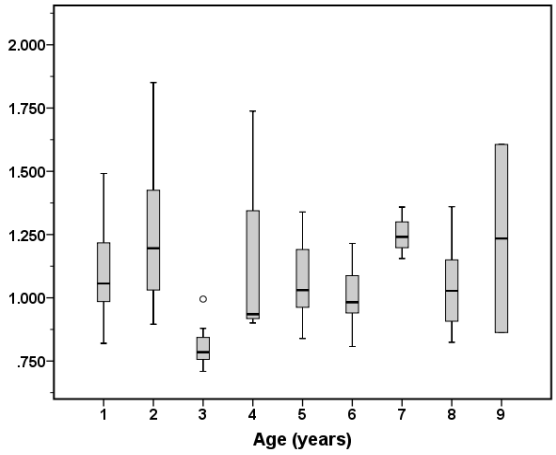

Figure 4.8 MPD by Age

The data examined did not show a trend of SN64R decreasing over time. Figure 4.7 shows an increase of SN64R in the first three years, which was expected due to surface wearing that could contribute to increased exposure of the fractured faces of aggregates covered by the asphalt binder. The following year, the fourth year, SN64R decreased, as expected. The decreasing of SN64R can be attributed to the polishing effects of the aggregates due to traffic. In the period between the fifth and seventh year, contrary to what was expected, SN64R did not decrease at a constant rate or remain constant over time; instead, SN64R gradually increased over these three years, and then exhibited a slight decrease in the eighth and ninth years. The increasing of friction in pavements over five years can be related to influence of surface distress, such as cracking and ravelling, as observed by Li *et al.* (2003) and Ahammed and Tighe (2008).

As for SN64R, the data examined did not show a trend in changes of MPD over time. Figure 4.8 shows that MPD values alternated between increasing and decreasing over periods of two and three years. It was expected that over time MPD would increase due to the polishing effects of traffic. However, this decrease was not observed in the

data analyzed, as MPD increased after the sixth year.

In conclusion, the relationships between pavement age, SN64R, and MPD were non-monotonic relationships because they were not in the same direction and not always at the same rate. A possible explanation for the variation of SN64R and MPD values over time is that the cross-sectional data organization was not adequate to capture SN64R and MPD variations. It is possible that longitudinal (historical) data of SN64R and MPD for each road segment would be more adequate to investigate SN64R and MPD performance over time. Another possible explanation is the influence of surface distress on SN64R and MPD in aged pavements. This possible influence was examined in the following sub-section.

4.2.5 Investigating the Influence of Pavement Distress on Skid Resistance and Macrotexture

In the previous analysis, the influence of pavement age on skid resistance and macrotexture was investigated. The results showed that pavement age was not sufficient to explain the performance of skid resistance and macrotexture over time, where skid resistance increased after the fourth year and macrotexture after the third year.

One possible explanation for the increase of skid resistance of aged pavements might be related to the influence of pavement distress on pavement surface textures. For instance, the loss of fine aggregates in asphalt surfaces might have influenced the increase of surface roughness by exposing the fractured faces of coarse aggregates that were not previously exposed to traffic and polishing effects. In addition, the loss of fine aggregates might have influenced the increase of macrotexture by creating new channels for water drainage, which would have influenced the increase of pavement friction.

Therefore, the occurrence of pavement distress might have affected the general configuration of the pavement texture and thus influenced pavement friction performance over time.

The objective of this analysis was to investigate the relationships between SN64R, MPD, and pavement distress using regression analysis to examine correlations between the variables and their statistical significance.

The relationships between SN64R and MPD and IRI, RUT, RAV, and WPC were examined using linear and nonlinear relationships (quadratic, power, and exponential). The results of the relationships that exhibited the greatest R-squares are shown in Table 4.4. The quadratic curves of the relationships between SN64R, MPD, IRI, RUT, and WPC are shown in Appendix E.

Table 4.4 Correlation between SN64R, MPD, and Pavement Distress

Pavement Indicators	SN64R			
	R-square	**p-value**	**SE***	**Equation**
IRI	0.02	0.49	6.91	$49.7 + 3.64\ IRI - 0.45\ IRI^2$
RUT	0.00	0.92	6.75	$53.80 - 0.76\ RUT + 0.07\ RUT^2$
RAV	0.16	0.07	5.92	$58.7 - 41.96\ RAV + 53.04\ RAV^2$
WPC	0.18	0.07	6.00	$49.9 - 34.34\ WPC + 34.58\ WPC^2$
	MPD			
IRI	0.94	< 0.001	0.27	$2.74 - 2.68\ IRI + 1.03\ IRI^2$
RUT	0.43	< 0.001	0.93	$5.42 - 1.97\ RUT + 0.21\ RUT^2$
RAV	0.32	0.05	0.17	$0.83 - 0.72\ RAV + 0.32\ RAV^2$
WPC	0.22	0.03	1.55	$2.9 - 9.292\ WPC + 7.89\ WPC^2$
(*) SE = Standard error of the estimate				

The relationship between SN64R and IRI was not statistically significant (p-value > 0.10) with an R-square of 0.024. The relationship between MPD and IRI was statistically significant (p-value < 0.001) with an R-square of 0.941. The quadratic curve showed that there was a slight increase in SN64R with the increase of IRI and there was an increase in MPD when IRI is above 1.5.

The relationship between SN64R and RUT was not statistically significant (p-value > 0.10) with an R-square of 0.003. The relationship between MPD and RUT was statistically significant (p-value < 0.001) with an R-square of 0.435. The quadratic curve of the relationship SN64R and RUT showed that there was a slight increase in SN64R with the increase of RUT. The quadratic curve of the relationship MPD and RUT showed that there was a decrease in MPD with increase of RUT and MPD started increasing when RUT is above 5 mm.

The relationship between SN64R and RAV was statistically significant (p-value < 0.10) with an R-square of 0.164. The relationship between MPD and RAV was statistically significant (p-value < 0.10) with an R-square of 0.317. The quadratic curve of the relationship between SN64R and RAV showed that SN64R decreased with the increase of RAV and then SN64R started increasing when the percentage of RAV increases above 35%. The quadratic curve of the relationship between MPD and RAV showed that MPD increased with the increase of RAV.

The relationship between SN64R and WPC was statistically significant (p-value < 0.10) with an R-square of 0.181. The relationship between MPD and WPC was statistically significant (p-value < 0.10) with an R-square of 0.224. The quadratic curve of the relationship between SN64R and WPC showed that SN64R increased with the increase of WPC and then SN64R started decreasing when the percentage of WPC increases above 50%. The quadratic curve of the relationship between MPD and WPC showed that MPD decreased with the increase of WPC and then start increasing when the percentage of WPC increased above 60%.

In summary, it was observed an increase of pavement friction due to increase of

pavement distress. The relationships between the pavement friction and pavement distress was not linear. The increase of areas affected by ravelling and wheel path cracks influenced skid resistance and macrotexture. Skid resistance increased when the percentage of ravelling increased above 50%. Macrotexture increased when the area affected by wheel path cracks increase above 60% and when rutting increased above 5 mm. Macrotexture also increased with the increase of ravelling. The results support the initial hypothesis that pavement distress affects pavement friction. Thus, variables related to pavement distress should be considered in models for pavement friction prediction.

4.3 Skid Resistance Modelling

4.3.1 Objective

One of the objectives of this study was to develop a model to predict skid resistance (SN64R) using the factors that affect pavement friction investigated in the previous analysis.

4.3.2 Skid Resistance Modelling Approach

For the purpose of developing a model of skid resistance, this study uses the OLS statistical technique to investigate the relationships between a single dependent variable (SN64R) and several independent variables. In an OLS regression analysis, each independent variable is weighted by the regression. The weights, represented by unstandardized coefficients (regression weights β, $\beta 1$, $\beta 2$…), denote the relative contribution of each independent variable to the overall prediction.

The independent variable datasets were graphically analyzed to meet three assumptions: normal distribution, homoscedasticity, and linearity. The frequencies of the data were plotted to verify whether the data distribution follows a Gaussian distribution.

The linearity was examined using standardized residual plots of residual versus the predicted dependent value. The independent variables that violated these assumptions were transformed using the logarithm function.

The modelling procedure started with a bivariate Pearson correlation matrix that displayed all of the combinations of dependent and independent variables. The variable selection procedure was maximized using a stepwise approach. This approach enabled adding and removing variables based on the contribution of each independent variable to the model. For each variable added to the model, several measures were analyzed to determine their contribution to the overall model fit regarding an increase in the R-square, a decrease in standard error (SE), the significance of the partial correlation (p-value), and the influences of collinearity. The influence of multicollinearity was assessed using the Variance Inflation Factor (VIF) with a threshold of five, which indicates a low level of collinearity (Hair *et al.*, 2015). The variables with a VIF greater than five were discarded.

The final product of the multiple regression analysis was a regression model that can be used to predict friction characterized by a skid number in response to changes in the independent variables. The goodness-of-fit was examined by employing ANOVA to determine how well the model fits the data. The model fit was explained through the statistical coefficient of determination R-square, which indicates the percentage of total variation of the dependent variable as explained by the regression model.

4.3.3 Model Development

Statistical models were developed using multivariate regression with skid resistance (SN64R) as the dependent variable and a set of potential predictors as

independent variables. The set of independent variables used in the modelling process included: macrotexture (MPD), pavement age (Age), traffic loads per lane (AESAL), nominal aggregate size (NMAS), percentage of voids in mineral aggregate (VMA), percentage of air voids (AV), percentage of asphalt content (AC), percentage of aggregates retained sieve 4.75 mm (Co), percentage of aggregates passing sieve 4.75 mm (Fi), and percentage of aggregates passing sieve 2.36 mm (FFi).

Additionally, four variables were tested to examine their relevance in the modelling. The first variable was calculated to address the cumulative influence of traffic over time by combining the Influences of traffic and load on the design lane (AESAL) and pavement age (Age). The variable AAESAL was the result of the multiplication of the variables AESAL per design lane and Age. The second variable was calculated to address the mix design characteristics using the coefficient of percentage of fine (FFi) and coarse aggregates (Co) in the mixture. The variable FFi/Co denotes the percentage of aggregates passing sieve 2.36 mm aggregates over the percentage of aggregates retained at sieve 4.75 mm. The third variable, RVPC, denotes the sum of the percentage of area of the road segment affected by ravelling and wheel pattern cracks. The fourth variable included was the percentage of roughness (IRI) per road section.

In total, 14 independent variables were tested. This procedure allowed an examination of the contribution of each independent variable to the regression model. In the multivariate procedure, the independent variables were added or deleted from the regression model based on their relative contribution to the coefficient of determination (R-square) and their statistical significance. All the predictor variables in the models were statistically significant at 10% of level of significance (p-value ≤ 0.10). The process

continued until none of the variables contributed statistically significantly to the predictive accuracy of the model (Hair *et al.*, 2015).

4.3.4 Skid Resistance Models

The skid resistance modelling was divided into two categories: one for pavement ages three years old and less ("new pavements") and the other for pavement ages greater than three years old ("aged pavements"). This categorization was necessary, as the relationship between skid resistance and pavement age is not linear and the relationship between skid resistance and pavement age is better explained as a polynomial of third order with a cubic spline function. However, a third order polynomial in the multivariate regression models has some constraints that affect the regression weights of the independent variables and increase errors in the estimated values of the dependent variable (Brauner and Schacham, 1999; Gelman and Imbens, 2018). Therefore, instead of a polynomial of third order to describe the relationship between skid resistance and pavement age, two polynomials of second order were used in two models, one for new pavements and the other for aged pavements. The developments of polynomials for new and aged pavement are shown in Appendix F.

Multiple linear regressions using stepwise estimation were used to predict skid resistance for new and aged pavements. Among the 14 variables tested, only four — AESAL, AGE, RVPC, and FFi/Co were used in the models due to their contribution of increasing the R-square and their level of statistical significance. Table 4.5 shows the descriptive statistics of the sample used to estimate skid resistance models.

Table 4.5 Descriptive Statistics of Data Used in the Models

Pavement		Min.	Max.	Mean	SD*
New	Age	1	3	2.32	0.56
	AESAL	4803	2698354	553659	722819
	RVPC (%)	1.01	18.06	2.62	4.74
	FFi/Co	0.23	1.00	0.85	0.17
Aged	Age	4	9	6.27	1.55
	AESAL	5687	2005203	467408	627490
	RVPC (%)	1.01	40.00	1.42	6.08
	FFi/Co	0.25	1.00	0.72	6.08
(*) SD = Standard deviation					

Table 4.6 displays a summary of modelling using stepwise estimation for new and aged pavements. The model regression summaries, ANOVA results, regression weights, p-values, and collinearity statistics for each variable in the models are shown in Appendix G.

Table 4.6 Summary of Stepwise Modelling for New and Aged Pavements

Pavement Age	Model	R	R-Square	Adjusted R-Square	SE*	Predictors
New	1	0.546	0.299	0.268	6.63	AESAL
	2	0.750	0.563	0.524	5.35	AESAL, Age
	3	0.789	0.623	0.569	5.09	AESAL, Age, RVPC
	4	0.797	0.635	0.562	5.13	AESAL, Age, RVPC, FFi/Co
Aged	5	0.763	0.582	0.597	4.67	AESAL, Age
	6	0.864	0.746	0.708	3.73	AESAL, Age, FFi/Co
	7	0.884	0.784	0.736	3.54	AESAL, Age, FFi/Co, RVPC
(*) SE = Standard error of the estimate						

The initial model (Model 1) for predicting skid resistance for new pavements using only one variable exhibited an R-value of 0.546 and R-square of 0.299 (p-value < 0.001). The initial model was improved with the addition of the second and third variables. The addition of these variables improved the model fit with an increase of R-value, R-square, adjusted R-square, and a decrease in the standard error of estimate. The model with three variables (Model 3) exhibited an R-square of 0.623 (p-value < 0.001)

and standard error of estimate of 5.09. The addition of a fourth variable the model (Model 4) increased the R-value and R-Square values; however, the adjusted R-square decreased and the standard error of the estimate increased, which indicates that the model fit did not improve with the addition of the fourth variable. This occurred because the variable FFi/Co was not statistically significant. The R-square increase was due to an excessive number of predictors in the model, which indicated an overestimated model. The model equation to predict skid resistance using Model 2 for new pavements is shown in Equation 4.1. The regression line of the regression model for new pavements is shown in Figure 4.9.

$$SN64R_{new} = 13.85 - 2.24\ \log AESAL + 6.97(40.08Age - 7.18Age^2) + 2.39\ \log RVPC \quad \textbf{(4.1)}$$

The initial model (Model 5) for predicting skid resistance for aged pavements using two variables exhibited R-square of 0.582 (p-value < 0.001). Model 5 was improved with the addition of the third and fourth variables. The addition of these variables improved the model fit with an increase in R-value, R-square, and adjusted R-square, and a decrease in the standard error of estimate. The model with four variables (Model 7) exhibited an R-square of 0.784 (p-value < 0.001) and standard error of estimate of 3.54. The model equation to predict skid resistance using Model 7 for aged pavements is shown in Equation 4.2. The regression line of the regression model for aged pavements is shown in Figure 4.10.

$$SN64R_{aged} = 78.61 - 4.74\ \log AESAL + 0.051(13.58Age - 0.85Age^2) + 15.65\ \log FFi/Co + 1.23\ \log RVPC \quad \textbf{(4.2)}$$

Where SN64R = Skid number measured with LWT with ribbed tire at 64 km/h, AESAL

= annual ESAL in the design lane, Age = pavement age, FFi/Co = coefficient of the percentage of aggregates passing sieve 2.36 mm over the percentage of aggregates retained at sieve 4.75 mm, and RVPC = sum of the percentage of area affected by ravelling and wheel path cracks.

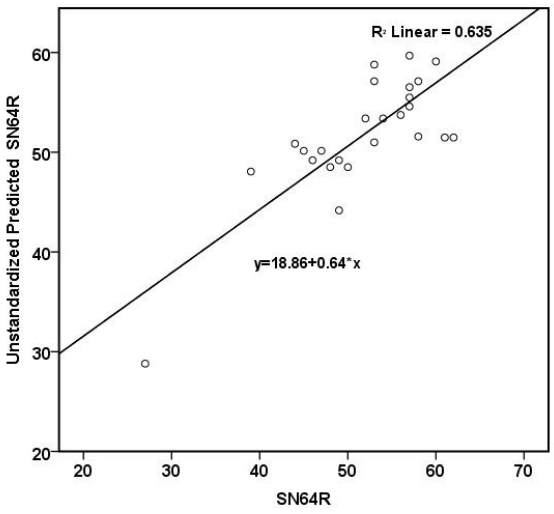

Figure 4.9 Model 2 Regression Line

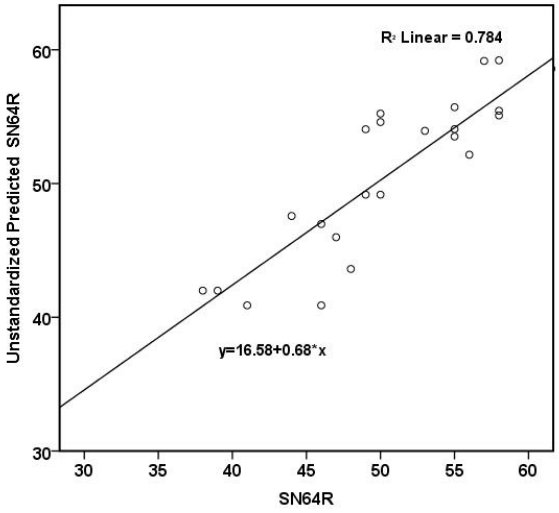

Figure 4.10 Model 7 Regression Line

The variables related to traffic, age, mix design, and distress showed different influences on predicting skid resistance for new and aged pavements. The main differences between the influences of the variables in the models can be summarized as follows:

- The influence of the AESAL was negative in the models, which indicates that skid resistance decreases with the increase of AESAL. The regression coefficient was lower in the model for new pavements than in the models for aged pavements, which indicates that AESAL had greater influence in aged pavements.

- The influence of pavement age was positive in the models, which indicates that skid resistance increases with the increase of pavement age. The regression coefficient was lower in aged pavements, which indicates that age had greater influence in new pavements.
- The variable related to mix design properties, FFi/Co, did not show an influence on skid resistance for new pavements, but it did for aged pavements. This result suggests that the mix gradation may not have influenced new pavements, but it makes a difference in aged pavements. Since the data sample analyzed included mostly dense mixes with a greater percentage of fine aggregates (e.g., SuperPave mixes) and few samples of open graded mixes (e.g., SMA), it can be inferred that dense mixes had a positive influence on skid resistance in aged pavements. This influence could be related to the quality of the coarse aggregates in the Superpave mixes that resulted in better final texture. However, the quality of the aggregates in the mixes could not be verified.
- The influence of ravelling and wheel path cracks was positive in the models, which indicates that skid resistance increases with the increase of ravelling. The regression coefficient was lower in aged pavements, which indicates that ravelling and cracks had greater influence in new pavements than in aged pavements. This indicates that ravelling in the early ages of pavements may have contributed to an increase in skid resistance.

4.3.5 Skid Resistance Model Evaluation

The primary concern in developing a regression model is the model adequacy, which is given by the coefficient of determination R-square. A great R-square indicates good model fit. However, R-square is not the only indicator of a good model because regression models are tied to certain assumptions regarding the distribution of error terms (Hair *et al.*, 2015; Matson *et al.*, 2017). When seriously violated, these error terms indicate that the models cannot be used for making inferences. Thus, the statistical assumptions to examine the regression models include linearity, homoscedasticity, independent errors, and normality (Hair *et al.*, 2015; Matson *et al.*, 2017).

The linearity assumption means that the predictor variables in the regression have a linear relationship with the independent variable. This assumption was checked by inspecting the residuals versus the estimated values of SN64R. The relationship is assumed linear if there is no pattern in the residual plots (Hair *et al*., 2015). The assumption of homoscedasticity and independent errors of the models was also checked using analysis of residuals. The data is considered homoscedastic and the error is independent if there is no pattern in the plot and the points are equally distributed above and below zero.

Figure 4.111 and Figure 4.12 show the unstandardized residuals and estimated SN64R values for new and aged pavements. The figures show a nonlinear and non clear pattern of the residuals; the points were randomly distributed with an even spread of residuals at all estimated values, which indicates that the models met the assumption of linearity, homoscedasticity, and independent errors (Hair *et al*., 2015).

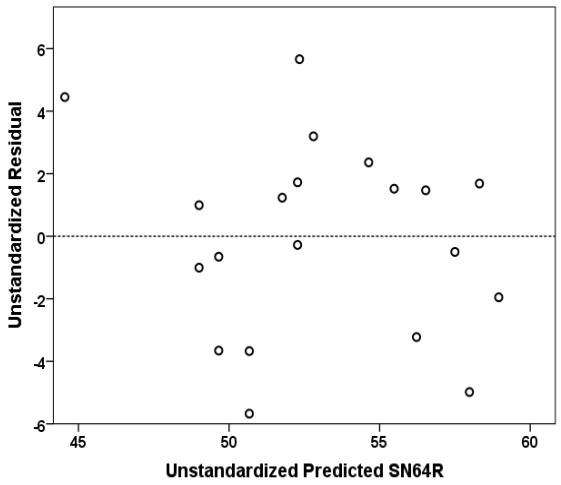

Figure 4.11 Predicted SN64R and Residuals for New Pavements

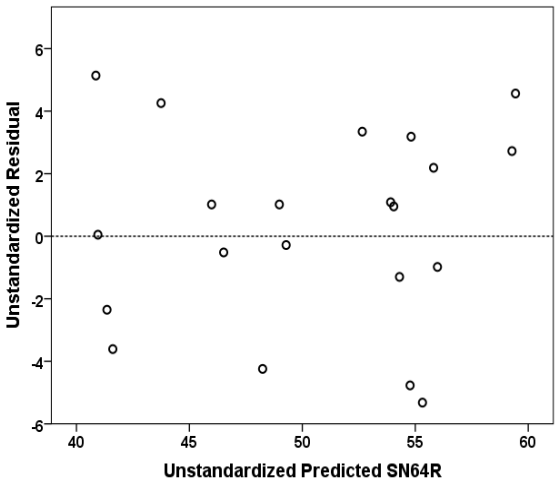

Figure 4.12 Predicted SN64R and Residuals for Aged Pavements

The normality of the errors of residuals was examined using the observed and expected cumulative proportion. Figure 4.13 and Figure 4.14 show the expected and observed cumulative probabilities fairly match, which indicates that the regressions met the assumption of normality.

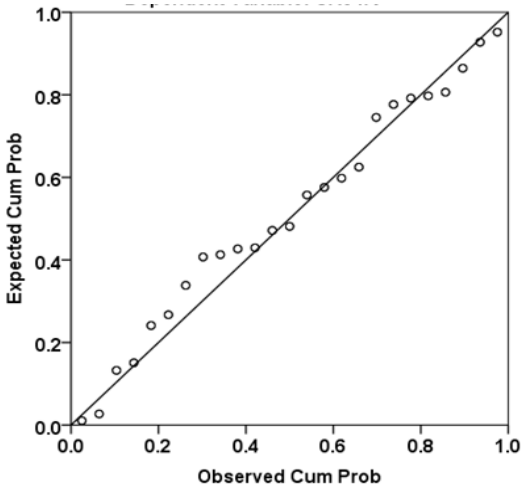

Figure 4.13 Observed and Expected Cumulative Proportion for New Pavements

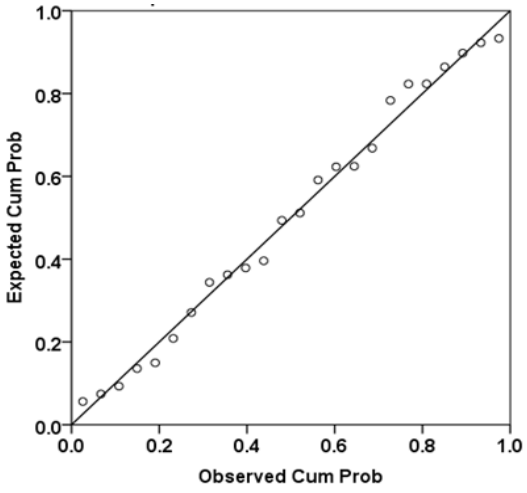

Figure 4.14 Observed and Expected Cumulative Proportion for Aged Pavements

Another important factor assessed in the regression models was the influence of

multicollinearity of the variables in the models because highly correlated variables create combined variances between variables that affect model prediction and violate the assumption of independence of variables in the models (Hair *et al.*, 2015). The influence of multicollinearity was assessed by the variance inflation factor (VIF) that indicated small degree of multicollinearity.

The VIF values are shown in Appendix G (Table G.3 and Table G.6). The variables in the models exhibited VIF between 1.07 and 1.98, which are lower than the pre-defined threshold of five. Thus, all the variables in the models met the assumption of independence.

4.3.6 Model testing

The accuracy of the regression models was tested using the bootstrapping statistical technique. Bootstrapping allowed testing of the models by resampling the same data sample using the percentile method with a confidence interval of 95%. The bootstrap sample with 95% percentile confidence interval was calculated using the range of the bootstrap values corresponding to the 2.5th and 97.5th percentiles. The bootstrap values were generated with 1000 bootstrap replications using the statistical software SPSS 23.0 (IBM, 2015). The models obtained using the bootstrap resampling exhibited R-squares and regression coefficients, level of significance, and standard errors analogous to the original model. The bootstrapped model to predict skid resistance for new pavements exhibited an R-square of 0.631 (p-value < 0.01) and the model to predict skid resistance exhibited an R-square of 0.781 (p-value < 0.01).

4.4 Results and Study Limitations

The objective of this chapter was to examine the relationship between pavement

friction and the influence of traffic and loads, pavement age, type of mix, and pavement distress on skid resistance and macrotexture. The results can be summarized as follows:

- The regression analysis showed that there was a poor relationship between skid resistance and macrotexture. Skid resistance (SN64R) cannot be predicted from macrotexture (MPD).
- The regression analysis showed that skid resistance and macrotexture were affected by traffic and loads. This suggests that skid resistance decreases as traffic and loads increase, and macrotexture increases as traffic and loads increases. The relationship between traffic and loads and macrotexture was weaker than between traffic and loads and skid resistance.
- The comparison of the means tests showed that skid resistance differed noticeably across various types of mixes. The HL4 and Superpave mixes exhibited skid resistance means greater than SMA mixes. Macrotexture did not differ to the same magnitude within the mixes; however, SMA exhibited the highest levels of macrotexture and Superpave mixes exhibited the lowest levels of macrotexture.
- The comparison of the means tests showed that the decrease of skid resistance and macrotexture cannot be explained by pavement age. Skid resistance showed an increase over time in the first three years, which was expected due to wearing of the surface; yet, after three years, skid resistance alternated between increasing and slightly decreasing until the end of the ninth year. Macrotexture was expected to increase over time due to the polishing influences of the traffic; however, this trend was not confirmed. Similar to skid resistance, macrotexture alternated between increasing and decreasing over periods of two and three years.

- The regression analysis showed that pavement textures were influenced by pavement distress. The results showed that the influence of pavement distress was greater on macrotexture more than on skid resistance.

A series of models using multivariate regression were developed using a stepwise approach. In total, 14 independent variables were tested, but only four remained statistically significant. The specification of the regression models for skid resistance prediction incorporated variables related to traffic and loads, pavement age, mix gradation, and pavement distress. In the models, the variable related to traffic and loads exhibited a negative correlation with skid resistance, while the variables related to pavement age, mix design characteristic, and pavement distress exhibited a positive correlation with skid resistance. These correlations indicate that skid resistance decreases with the increase of traffic and loads and increases as pavements age and surfaces become rougher due to the influence of ravelling and wheel pattern cracks. In addition, the mix design with a greater percentage of fine aggregates influenced the increase of skid resistance.

Pavement friction is a complex subject due to various variables that can affect the correlations between a tire and pavement. It was expected to find low R-squares values for single regressions, as pavement friction cannot be determined by one single variable. Furthermore, the R-square is a statistical measure that represents the proportion of the variance for a dependent variable, and relationships with low R-squares with statistically significant p-values should not be ignored.

The R-squares of the multivariate models ranged from 0.63 and 0.78 with all variables statistically significant. These R-squares can be considered satisfactory due the

enormous variance in the dependent and independent variables.

It is important to note that this study has potential limitations that may have influenced the model estimates. The first limitation pertains to the limited data sample size, which was restricted to a small sample of 50 road segments. It is possible that significant relationships from the data were not identified due to this data sample size.

The second limitation pertains to the consistency of data collection, where different devices and approaches were used to collect skid resistance and macrotexture. It is possible that these factors influenced the results of the analysis of the relationships between skid resistance and macrotexture, and the influence of AESAL on macrotexture.

The third limitation refers to uneven distribution of the mixes and lack of information about the quality of aggregates in the mixes. It is possible that the models showed a bias toward Superpave mixes, as they represented the majority of the mixes in the sample. Further, the relationship between coarse and fine aggregates should consider aggregate properties as aggregates with superior quality may influence the ratio between fine and coarse aggregates.

The fourth limitation refers to the contribution of pavement distress to the increase of skid resistance. This should not be interpreted as an indication that pavement with more distress would give safer conditions due to the increase of pavement friction. Pavement distress are indicators of pavement deterioration that should be treated before requiring costly major repairs. The increase of pavement distress may also increase the risk of collisions, generate congestion problems, increase noise, and reduce road serviceability.

Finally, this study was conducted using cross-sectional data analysis to investigate

correlations between pavement friction and variables related to traffic, age, mix design, and pavement distress in a single point in time. This approach was used to measure the prevalence of these factors with no intention to define causal relationships between them. Thus, due to the numerous limitations revealed, one must be circumspect when interpreting the model results.

4.5 Summary

This study investigated the influence of traffic and loads, type of mix, pavement age, and pavement distress on pavement friction. The results showed that skid resistance decreased with the increase of traffic and increased with the increase of roughness, ravelling, and wheel path pattern cracks. Macrotexture increased with traffic, roughness, ravelling, and wheel path pattern cracks.

Predictive models for skid resistance were developed for new and aged pavements. The model for new pavements included pavements aged three years or less, while the model for aged pavements included pavements four to nine years old. In the models, the variable related to traffic showed a negative influence on skid resistance. Pavement age, mix design gradation, and pavement distress characterized by ravelling and wheel path pattern cracks showed positive influence on skid resistance. This result can be related to the increase in pavement deterioration that affects pavement texture by modifying pavement textures and changing the spatial arrangement of aggregates, thus contributing to skid resistance variation. The variable related to mix design gradation did not show an influence on skid resistance for new pavements, but it did for aged pavements. This result suggests that the type of mix did not influence younger pavements but made a difference in aged pavements.

5 Chapter: Investigation of the Influence of Pavement Condition on Road Safety

This chapter presents the data attributes, statistical approaches, and results of the investigation of the influence of pavement condition on road safety. Pavement condition was defined by the pavement condition indicator (PCI), which is a combination of indicators of pavement distress and roughness, by the macrotexture indicator (MPD), and by the International Friction Indicator (IFI). These indicators were collected at network level by ARAN and LWT.

In this study, road safety was defined by collision rate and collision frequency. Collision rate included the number of collisions and traffic for each location (LHRS and Offset) for the period of study. The collision rate for a spot location (100-meter road segment) was calculated using Equation 5.1.

$$CR = \frac{Collision \times 1{,}000{,}000}{AADT \times 365 \times T} \quad \textbf{(5.1)}$$

Where CR = collision rate; Collision = number of collisions for the study period, AADT = Average Annual Daily Traffic during the study period, and T = period of study.

In the CR equation, the period of study (T) was equal to one because collisions that occurred in a specific year were related to traffic and pavement condition indicators of the same year. For instance, locations with three years of data had three collision rates calculated, one per year of available data. This approach was selected to address changes in traffic volume and pavement condition over time.

The collision rates examined in this study included the classes of collisions most likely influenced by pavement condition. The selection of the classes was based on

previous studies (see Chapter 2) that observed that pavement condition and pavement friction influenced collision severity, type of impact, and surface condition (Chan *et al.*, 2008; Li *et al.*, 2013; Li and Huang, 2014; Lee *et al.*, 2015; Elghriany, 2015). The following collision classes were examined:

- *Severity of collisions* included the classifications property damage only (PDO), fatal and injury,
- *Impact of collisions* included the classifications single vehicle, sideswipe, and rear-end,
- *Surface condition of collisions* included the classifications wet and dry. Wet condition included collisions that occurred on iced, snowed, and slushed surfaces, and
- *Total number of collisions* included all collision classifications, regardless of the type of impact, severity, or surface condition.

Collisions involving turning and breaking maneuvers, such as turning, approaches, and angle, were not included because intersections at-grade were excluded.

5.1 Overview of Study Organization

This study was divided into two parts. The first part included statistical analysis of the correlation between collision rates and pavement condition indicators, PCI and MPD. The data used in the analysis included data of collisions, AADT, and pavement condition data for rural freeways and arterial highways.

For rural arterial highways, collisions that occurred 200 m before and after intersections were excluded. The threshold of 200 m was defined based on the stopping sight distance recommended by TAC for vehicles travelling at 100 km/h (TAC, 1999).

For rural freeways, collisions that occurred at intersections were not excluded because freeways have controlled intersections with crossing roads in different levels. Intersections were excluded from analysis because collisions involving intersections can be affected by driver's behavior, road signs, obstructions, lane width, geometric design of the intersections, and other elements that are beyond of the scope of this study.

The second part included the development of general linear models (GLM) that can be used for estimating the mean and standard deviation of collisions due to safety-related variables (explanatory variables), such as traffic and pavement condition (Srinivasan and Bauer, 2013; Hauer, 2015). First, several GLM models were developed using combined data of freeways and arterial highways. The results showed that pavement condition did not show to be statistically significant when freeways and arterial highways were combined. A summary of the results is presented in Appendix H.

To increase model accuracy and improve the goodness of fit of the models, data was reexamined, and the study was restricted to analysis of collisions that occurred on two-lane undivided arterial highways. The study was divided into two parts: the first part considered collisions that occurred on tangent segments, the second part considered collisions that occurred on curves. The reason for dividing the road segments by segment type was to increase model accuracy by selecting homogenous road segments and avoid combining influence of geometric elements such as curve radius and superelevation in the models for tangent segments. In addition, the international friction indicator, IFI, could not be calculated for curves because skid resistance was not surveyed on curves.

A further reason for selecting two-lane undivided arterial highways was to reduce the pavement condition variation that can occur across lanes of multilane roads. In

multilane highways, for example, variation in pavement condition between lanes (in the same direction) can be greater than in two-lane undivided roads due to the influence of traffic distribution, which is not uniform across all lanes. For example, pavement deterioration and wear due to traffic is expected to be greater on lanes that carry the heaviest loads and the slowest traffic. Figure 5.1 shows the analysis decision diagram.

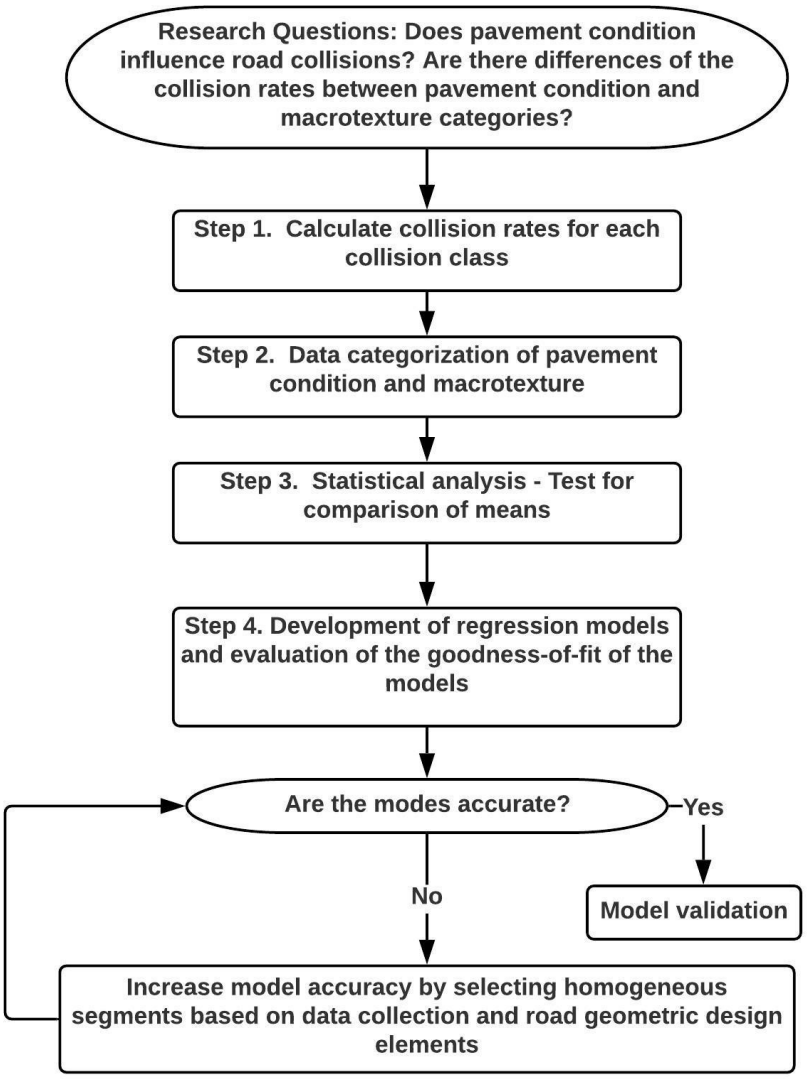

Figure 5.1 Analysis Decision Diagram

The following sub-sections describe the data manipulation, statistical approaches, statistical analysis, and development of the models, and the results and discussion of the influence of pavement condition on road safety.

5.1.1 Data Manipulation

This section outlines the data manipulation process used to investigate the influence of pavement condition on road safety. Figure 5.2 describes the data manipulation process.

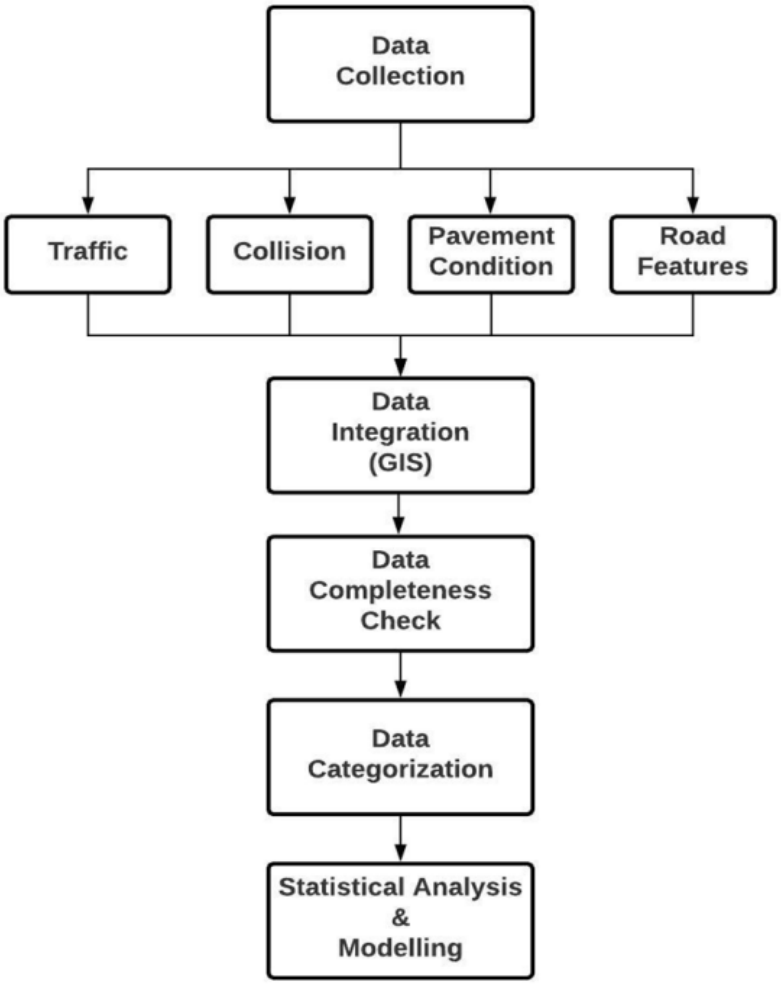

Figure 5.2 Data Manipulation Process

As described in Chapter 3, all datasets were obtained from MTO. The datasets included traffic, collisions, and pavement condition data. All data were collected at the network level and provided in *xls* format. Information about road features, which included segment length, location (LHRS), and horizontal elements of the road alignments, were obtained in shapefile format. The datasets were integrated in a GIS platform and exported as a single dataset in *xls* format to create one main dataset. This dataset was examined to detect inconsistencies and incompleteness.

The elements of the main dataset were categorized and some of them were eliminated to reduce the complexity and size in preparation for statistical analysis and modelling. For example, pavements in "excellent" and "good" condition were combined into a single category, "good". The threshold values used for categorization were based on values defined by MTO and Austroads (Chan *et al.,* 2016; Austroads, 2003). The PCI was categorized into three groups poor, fair, and high, as follows:

- Group 1, pavements in poor condition with $0 < PCI \leq 55$,
- Group 2, pavements in fair condition with $55 < PCI \leq 70$, and
- Group 3, pavements in good condition with $70 < PCI < 100$.

Pavement macrotexture (MPD) was similarly categorized into three groups, low, medium, and high, as follows:

- Group 1, pavements with low level of macrotexture with $MPD \leq 0.5$ mm,
- Group 2, pavement with medium level of macrotexture with $0.5 \text{ mm} < MPD \leq 0.8$ mm, and
- Group 3, pavement with high level of macrotexture with $MPD > 0.8$ mm.

5.1.2 Statistical Approaches

The relationship between collision rates and pavement condition was examined using parametric and non-parametric methods. Initially, the data was examined for normal distribution using 1) visual inspection of histograms of frequency distribution and 2) Levene's test for homogeneity of variance. For data that met the requirements for normal distribution, ANOVA (analysis of variance) was used to determine whether there were statistically significant differences between the means of groups. For data that did not meet the assumptions of normality and homogeneity, non-parametric tests were used (described below). The statistical computations were performed using the statistical software SPSS 23.0 and the R 3.1.0 extension for SPSS (IBM, 2015; R, 2014).

The non-parametric hypothesis test of medians used in this study was the Kruskal-Wallis test. The non-parametric Kruskal-Wallis test is also called a one-way ANOVA on ranks and is comparable to the parametric ANOVA One-Way test (Gibbons, 1993; Salkind, 2010). The Kruskal-Wallis test determined whether the means of two or more groups were different. The hypotheses for the Kruskal-Wallis test were that the population means are equal (null hypothesis) and the population means are not equal. The test statistic for the Kruskal-Wallis test is denoted by H, defined in Equation 5.2.

$$H = \left(\frac{12}{N(N+1)}\sum_{j}^{k}\frac{R_j^2}{n_j}\right) - 3\,(N+1) \qquad \textbf{(5.2)}$$

Where k = the number of comparison groups, N= the total sample size, n_j is the sample size in the j_{th} group, and R_j = is the sum of the ranks in the j_{th} group.

The H value is compared to the critical chi-square with *k - 1* degrees of freedom

and a significance level (alpha level) of 5%, or 0.05. If the critical chi-square value is less than the H statistic, the null hypothesis (equal medians) is rejected. If the chi-square value is greater than the H statistic, there is not enough evidence to suggest that the medians are unequal (Gibbons, 1993; Salkind, 2010).

When the Kruskal-Wallis test showed a statistically significant difference between groups, the non-parametric Dunn-Bonferroni's pairwise post hoc test was performed to identify groups that differed statistically (p-value ≤ 0.05) within the groups (Dinno, 2015).

Outliers were detected and removed from the data using different criteria. For parametric analysis, values greater than three standard deviations away from the mean were considered outliers. For non-parametric analysis, values outside of the first (25th) and third quartile (75th) were considered as outliers. In the non-parametric approach, the median was used as the central tendency (Kalina *et al.*, 2014). These tests and their results are described in detail in the sections that follow.

5.2 Statistical Analysis

The following sections present the results of the analysis of the relationship between collision rates and the indicators of pavement condition, PCI and MPD, for arterial highways. The data included 11,564 cases with 27,900 collisions for arterial highways, and 2,878 cases with 12,719 collisions for freeways. The collision and pavement condition indicators were collected for the period of 2012 to 2014. The cases were defined per location of collision (HWY and LHRS + Offset).

Table 5.1 shows a summary of the descriptive statistics of the data for arterial and freeways for the period of three years (2012-2014). The descriptive statistics included

mean, standard deviation (SD), minimum (Min), maximum (Max), sum of collisions (Sum), and number of road segments (N).

Table 5.1 Descriptive Statistics of Data for Arterial Highways and Freeways

Arterial Highways						
Collision Class	**Min.**	**Max.**	**Mean**	**SD***	**Sum**	**N****
Total	1	137	2.41	4.94	27900	11564
PDO	0	115	1.91	4.16	22120	11564
Fatal and injury	0	34	0.51	1.31	5859	11564
Single vehicle	0	31	0.29	1.17	3357	11564
Sideswipe	0	38	0.99	1.25	11500	11564
Rear-end	0	103	0.83	3.38	9584	11564
Dry	0	119	1.55	4.03	17963	11564
Wet	0	27	0.58	1.21	6668	11564
Pavement Indicators						
AADT	320	206000	24447	44	-	11564
MPD	***0	3.52	1.17	0.26	-	10281
PCI	25	100	87.03	11.79	-	11564
Freeways						
Collision Class	**Min.**	**Max.**	**Mean**	**SD***	**Sum**	**N****
Total	1	99	4.49	8.79	12931	2878
PDO	0	79	3.51	7.10	10090	2878
Fatal and injury	0	42	0.99	2.37	2837	2878
Single vehicle	0	31	0.98	2.34	2828	2878
Sideswipe	0	40	1.67	2.51	4795	2878
Rear-end	0	57	1.74	4.94	5010	2878
Dry	0	73	2.62	5.98	7540	2878
Wet	0	24	1.16	2.22	3327	2878
Pavement Indicators						
AADT	16900	378700	903710	80610	-	2878
MPD	***0	2.82	1.12	0.26	-	2813
PCI	17	100	78.95	18	-	2878
(*) SD = Standard deviation, (**) N = Number of road segments, (***) ARAN reports MPD < 0.5 mm as zero						

5.2.1 Relationship between Pavement Condition and Collision Rates

The objective of this study was to examine the relationship between pavement condition and road safety using the pavement condition indicator (PCI) and collision rates. This part of study included statistical analysis using comparison tests to determine

if there were differences in the mean (or medians) of collision rates between the three groups of pavement condition (poor, fair, good).

Firstly, the relationship between pavement condition and collision rate for total collisions was checked for normality. This approach was used to determine which statistical approach, parametric or non-parametric, would be appropriate for analysis.

Analysis of the total collisions showed a non-normal distribution with skewness of 3.70 and kurtosis of 22.15. A log transformation was applied to reduce data skewness. The log transformation reduced data skewness to 1.89 and kurtosis to 4.22. However, the log transformation was not sufficient to reduce data asymmetry. Data distribution exhibited highly skewed and not normally distributed.

After the data was checked for normality, the Levene's test for homogeneity of variances was performed for the total collisions and groups of PCIs. The Levene's test results showed that the p-value was lower than the alpha level of 0.05 (p-value $\leq$ 0.05), which means that the null hypothesis was rejected (i.e., the variances are not equal). Therefore, the assumption of homogeneity of variance required for parametric tests was not met, and the non-parametric Kruskal-Wallis test was applied.

The same approach was applied to the other categories of collisions. The results showed that the data did not meet the requirement for parametric analysis, and therefore non-parametric tests were performed for all collision classes for comparison of medians. Outliers were identified and removed using a non-parametric approach.

5.2.2 Results for Arterial Highways

The Kruskal-Wallis test showed that there was a statistically significant difference in collision rates within the three groups of pavement condition for arterial highways. The

results of the Kruskal-Wallis tests (H) with their significance level (p-value), Dunn-Bonferroni's pairwise comparison, and the collision rate medians by group of pavement condition are shown in Table 5.2 Comparison of Collision Rates.

Table 5.2 Comparison of Collision Rates and PCI for Arterial Highways

Collision Class		Kruskal-Wallis		Dunn-Bonferroni		Collision Rates	
		H	Sig	Pairs	p-value	Group	Median
Total		122.9	Yes*	1-2	Yes*	1	0.60
				2-3	Yes**	2	0.30
				3-1	No***	3	0.50
Severity	PDO	61.1	Yes**	1-2	No***	1	0.32
				2-3	Yes**	2	0.28
				3-1	No***	3	0.36
	Fatal and injury	98.1	Yes**	1-2	Yes**	1	0.44
				2-3	Yes**	2	0.19
				3-1	Yes**	3	0.33
Impact	Single vehicle	250.7	Yes**	1-2	Yes**	1	0.51
				2-3	Yes**	2	0.30
				3-1	No***	3	0.52
	Sideswipe	34.7	Yes**	1-2	Yes**	1	0.30
				2-3	Yes**	2	0.10
				3-1	Yes**	3	0.13
	Rear-end	73.2	Yes**	1-2	Yes**	1	0.42
				2-3	Yes**	2	0.19
				3-1	Yes**	3	0.24
Surface	Wet	189.1	Yes**	1-2	Yes**	1	0.47
				2-3	Yes**	2	0.23
				3-1	No***	3	0.42
	Dry	38.8	Yes**	1-2	Yes*	1	0.47
				2-3	Yes**	2	0.29
				3-1	Yes*	3	0.38
(*) p-value ≤ 0.05, (**) p-value ≤ 0.001, (***) p-value > 0.05							

- **Total Collisions**

The Kruskal-Wallis test showed a statistically significant difference (p-value < 0.001) in the rate of total collisions between the groups of poor, fair, and good pavement condition. The Dunn-Bonferroni's pairwise post hoc test showed statistically significant

differences (p-value < 0.001) in the collision rate medians between the groups of poor and fair pavements, and between the groups of fair and good pavements.

There was no statistically significant difference (p-value > 0.05) in the collision rate medians between the groups of poor and good pavements. Fair pavements exhibited the lowest collision rate median of 0.30, while good and poor pavements exhibited collision rate medians of 0.50 and 0.60, respectively. The collision rate median in poor pavements was 50.0% greater than in fair pavements and 16.7% greater than in good pavements.

- **Level of Severity**

The Kruskal-Wallis test showed that there was a statistically significant difference (p-value < 0.001) in the level of collision severity within the groups of poor, fair, and good pavement condition. The Dunn-Bonferroni's pairwise post hoc test for PDO collision rate showed that there was a statistically significant difference (p-value ≤ 0.05) in the collision rate medians between the groups of fair and good pavements. There was no statistically significant difference (p-value > 0.05) in the collision rate medians between the groups of poor and fair pavements and the groups of poor and good pavements. Fair pavements exhibited the lowest collision rate median of 0.28, while poor and good pavements exhibited collision rate medians of 0.32 and 0.36, respectively. The collision rate median in poor pavements was 12.5% greater than in fair pavements and 12.5% lower than in good pavements.

The Dunn-Bonferroni's pairwise post hoc test for fatal and injury collision rates showed that there was a statistically significant difference (p-value < 0.001) in the collision rate medians between the groups of poor, fair, and good pavements. Fair

pavements exhibited the lowest collision rate median of 0.19, while poor and good pavements exhibited collision rate medians of 0.44 and 0.33, respectively. The collision rate median in poor pavements was 58.8% greater than in fair pavements and 25.0% greater than in good pavements.

- **Type of Impact**

The Kruskal-Wallis test showed that there was a statistically significant difference (p-value < 0.001) in the type of impact of collisions within the groups of poor, fair, and good pavement condition. The Dunn-Bonferroni's pairwise post hoc test for single vehicle collisions showed that there was a statistically significant difference (p-value ≤ 0.05) in the collision rate medians between the groups of poor and fair pavements, and fair and good pavements. There was no statistically significant difference (p-value > 0.05) in the collision rate medians between the groups of poor and good pavements. Fair pavements exhibited the lowest collision rate median of 0.30, while poor and good pavements exhibited similar collision rate medians of 0.51 and 0.52, respectively. The collision rate median in poor pavements was 41.2% greater than in fair pavements and 1.96% lower than in good pavements.

The Dunn-Bonferroni's pairwise post hoc test for sideswipe collision rates showed that there was a statistically significant difference (p-value < 0.001) between the groups of poor, fair, and good pavements. Fair pavements exhibited the lowest collision rate median of 0.10, while poor and good pavements exhibited collision rate medians of 0.30 and 0.13, respectively. The collision rate median in poor pavements was 66.7% greater than in fair pavements and 56.7% greater than in good pavements.

The Dunn-Bonferroni's pairwise post hoc test for rear-end collision rates showed

that there was a statistically significant difference (p-value < 0.001) in the collision rate medians within the groups of poor, fair, and good pavement condition. Fair pavements exhibited the lowest collision rate median of 0.19, while poor and good pavements exhibited collision rate medians of 0.42 and 0.24, respectively. The collision rate median in poor pavements was 54.8% greater than in fair pavements and 42.9% greater than in good pavements.

- **Surface Condition**

A Kruskal-Wallis test showed that there was a statistically significant difference (p-value < 0.001) in the rate of collisions due to surface conditions within the groups of poor, fair, and good pavement condition. The Dunn-Bonferroni's pairwise post hoc test for wet surfaces showed that there was a statistically significant difference (p-value < 0.001) in the collision rate medians between the groups of poor and fair pavements, and between the groups of fair and good pavements. There was no statistically significant difference (p-value > 0.05) in the collision rates between the groups of poor and good pavements. Fair pavements exhibited the lowest of collision rate median of 0.23, while poor and good pavements exhibited collision rate medians of 0.47 and 0.42, respectively. The collision rate median in poor pavements was 38.3% greater than in fair pavements and 19.1% greater than in good pavements.

The Dunn-Bonferroni's pairwise post hoc test for dry surfaces showed that there was a statistically significant difference (p-value < 0.001) in the collision rate medians between the groups of poor, fair, and good pavement condition. Fair pavements exhibited the lowest collision rate median of 0.29, while poor and good pavements exhibited collision rate medians of 0.47 and 0.38, respectively. The collision rate median in poor

pavements was 38.3% greater than in fair pavements and 19.1% greater than in good pavements.

5.2.3 Relationship between Macrotexture and Collision Rates

The results of the Kruskal-Wallis tests (H), Dunn-Bonferroni's pairwise post hoc tests, and the collision rate medians per group of macrotextures are shown in Table 5.3.

Table 5.3 Comparison of Collision Rates and Macrotexture for Arterial Highways

Collision Class		Kruskal-Wallis		Dunn-Bonferroni		Collision Rates	
		H	Sig.	Pairs	p-value	Group	Median
Total		11.6	Yes**	1-2	Yes*	1	0.71
				2-3	Yes**	2	0.29
				3-1	Yes*	3	0.50
Severity	PDO	37.4	Yes*	1-2	Yes*	1	0.43
				2-3	No	2	0.33
				3-1	Yes*	3	0.35
	Fatal and injury	19.3	Yes*	1-2	Yes*	1	0.68
				2-3	Yes*	2	0.11
				3-1	Yes*	3	0.38
Impact	Single vehicle	22.8	Yes*	1-2	No	1	0.55
				2-3	No	2	0.53
				3-1	Yes*	3	0.51
	Sideswipe	27.7	Yes*	1-2	Yes**	1	0.23
				2-3	Yes*	2	0.09
				3-1	Yes**	3	0.13
	Rear-end	34.6	Yes*	1-2	Yes*	1	0.35
				2-3	Yes**	2	0.21
				3-1	Yes*	3	0.24
Surface	Wet	17.2	Yes*	1-2	Yes**	1	0.45
				2-3	No	2	0.36
				3-1	Yes*	3	0.39
	Dry	76.6	Yes*	1-2	Yes*	1	0.45
				2-3	Yes*	2	0.25
				3-1	Yes*	3	0.37
(*) p-value ≤ 0.05, (**) p-value ≤ 0.001, (***) p-value > 0.05							

- **Total Collision**

The Kruskal-Wallis test showed that there was a statistically significant difference (p-value ≤ 0.001) in the total collision rates between the groups of low, medium, and high levels of macrotexture. The Dunn-Bonferroni's pairwise post hoc tests showed that there were statistically significant differences between the groups of macrotextures. The group of medium level of macrotexture exhibited the lowest collision rate median of 0.29, while the groups of low and high levels of macrotexture exhibited collision rate medians of 0.71 and 0.50, respectively. The collision rate median for pavements with a low level of macrotexture was 59.1% greater than for those with a medium level of macrotexture and 29.6% greater than for pavements with a high level of macrotexture.

- **Level of Severity**

The Kruskal-Wallis test showed that there was a statistically significant difference (p-value < 0.001) in the level of severity of collisions within the groups of low, medium, and high levels of macrotexture. The Dunn-Bonferroni's pairwise post hoc test for PDO collision rates showed that there was a statistically significant difference (p-value ≤ 0.05) in the collision rate medians between the groups of low and medium levels of macrotexture and between low and high levels of macrotextures. There was no statistically significant difference (p-value > 0.05) in the median collision rates between the groups of medium and high levels of macrotexture. The group of medium level of macrotexture exhibited the lowest collision rate median of 0.33, while the groups of low and high levels of macrotexture exhibited collision rate medians of 0.43 and 0.35, respectively. The collision rate median for pavements with a low level of macrotexture was 23.26% greater than for those with a medium level of macrotexture and 18.60%

greater than for pavements with a high level of macrotexture.

The Dunn-Bonferroni's pairwise post hoc test for fatal and injury collision rates showed that there was a statistically significant difference (p-value < 0.001) in collision rate medians between the groups of low, medium, and high levels of macrotexture. The group of medium level of macrotexture exhibited the lowest collision rate median of 0.11, while the group of low level of macrotexture exhibited the greatest collision rate median of 0.68. The group of high level of macrotexture exhibited a collision rate median of 0.38. The collision rate median for pavements with a low level of macrotexture was 83.8% greater than for those with a medium level of macrotexture and 44.1% greater than for pavements with a high level of macrotexture.

- **Type of Impact**

The Kruskal-Wallis test showed that there was a statistically significant difference (p-value < 0.001) in the type of collision impact between the groups of low, medium, and high levels of macrotexture. The Dunn-Bonferroni's pairwise post hoc test for single vehicle collisions showed that there was a statistically significant difference (p-value ≤ 0.05) in the collision rate medians between the group of low and high levels of macrotexture. There was no statistically significant difference (p-value > 0.05) in the collision rate medians between the groups of low and medium levels of macrotexture, and medium and high levels of macrotexture. The group of high level of macrotexture exhibited the lowest collision rate with median of 0.51, while the groups of low and medium macrotexture exhibited collision rate medians of 0.55 and 0.53, respectively. The collision rate median for pavements with a low level of macrotexture was 3.6% greater than for those with a medium level of macrotexture and 7.3% greater than for pavements

with a high level of macrotexture.

The Dunn-Bonferroni's pairwise post hoc test for sideswipe collision rates showed that there was a statistically significant difference (p-value < 0.001) between within the groups of low, medium, and high levels of macrotexture. The group of medium level of macrotexture exhibited the lowest collision rate median of 0.09, while the groups of low and high levels of macrotexture exhibited collision rate medians of 0.23 and 0.13, respectively. The collision rate median for pavements with a low level of macrotexture was 60.9% greater than for those with a medium level of macrotexture and 43.5% greater than for pavements with a high level of macrotexture.

The Dunn-Bonferroni's pairwise post hoc test for rear-end collision rates showed that there was a statistically significant difference (p-value < 0.001) in the collision rates between the groups of low, medium, and high levels of macrotexture. The group of medium level of macrotexture exhibited the lowest collision rate median of 0.21, while the groups of low and high levels of macrotexture exhibited collision rate medians of 0.35 and 0.24, respectively. The collision rate for pavements with a low level of macrotexture was 40.0% greater than for those with a medium level of macrotexture and 31.4% greater than for pavements with a high level of macrotexture.

- **Surface Condition**

A Kruskal-Wallis test showed that there was a statistically significant difference (p-value < 0.001) in the median rates of collisions due to surface conditions between within the groups of low, medium, and high levels of macrotexture. The Dunn-Bonferroni's pairwise post hoc test for wet surfaces showed that there was a statistically significant difference (p-value < 0.001) in the collision rate medians between the groups

of low and medium levels of macrotexture, and between the groups of low and high levels of macrotexture. There was no statistically significant difference (p-value > 0.05) in the collision rates between the groups of medium and high levels of macrotexture. The group of medium level of macrotexture exhibited the lowest collision rate median of 0.36, while low and high levels of macrotexture exhibited collision rate medians of 0.45 and 0.39, respectively. The collision rate for pavements with a low level of macrotexture was 20.0% greater than for those with a medium level of macrotexture and 13.3% greater than for pavements with a high level of macrotexture.

The Dunn-Bonferroni's pairwise post hoc test for dry surfaces showed that there was a statistically significant difference (p-value < 0.001) in the collision rate medians between the groups of low, medium, and high levels of macrotextures. The group of medium level of macrotexture exhibited the lowest collision rate median of 0.25, while low and high levels of macrotextures exhibited collision rate medians of 0.45 and 0.37, respectively. The collision rate for pavements with a low level of macrotexture was 44.4% greater than for those with a medium level of macrotexture and 17.8% greater than for pavements with a high level of macrotexture.

5.2.4 Results of Statistical Analysis for Freeways

The Kruskal-Wallis test showed that there was a statistically significant difference in the majority of collision rates within the three groups of pavement condition for freeways. The results of the Kruskal-Wallis tests, Dunn-Bonferroni's pairwise post hoc, and the collision rate medians by group of pavement condition are shown in Table 5.4.

Table 5.4 Comparison of Collision Rates and PCI for Freeways

Collision Class		Kruskal-Wallis		Dunn-Bonferroni		Collision Rate	
		H	Sig	Pairs	p-value	Group	Median
Total		6.7	Yes**	1-2	No	1	0.09
				2-3	Yes**	2	0.07
				3-1	No	3	0.09
Severity	PDO	12.1	Yes**	1-2	Yes**	1	0.11
				2-3	Yes**	2	0.11
				3-1	No	3	0.13
	Fatal and injury	6.7	Yes*	1-2	Yes**	1	0.05
				2-3	No	2	0.04
				3-1	Yes**	3	0.04
Impact	Single vehicle	2.9	No	1-2	No	1	0.08
				2-3	No	2	0.08
				3-1	No	3	0.08
	Sideswipe	33.8	Yes*	1-2	Yes*	1	0.07
				2-3	Yes*	2	0.05
				3-1	Yes**	3	0.06
	Rear-end	24.8	Yes*	1-2	Yes*	1	0.06
				2-3	Yes*	2	0.04
				3-1	No	3	0.05
Surface Condition	Wet	40.9	Yes*	1-2	Yes*	1	0.06
				2-3	Yes*	2	0.04
				3-1	No*	3	0.05
	Dry	6.4	Yes**	1-2	Yes	1	0.17
				2-3	Yes*	2	0.15
				3-1	Yes	3	0.17
(*) p-value ≤ 0.05, (**) p-value ≤ 0.001, (***) p-value > 0.05							

- **Total Collisions**

The Kruskal-Wallis test showed that there was a statistically significant difference (p-value < 0.05) in the total collisions in the groups of poor, fair, and good pavement condition. The Dunn-Bonferroni's pairwise post hoc test showed that there was a statistically significant difference (p-value ≤ 0.05) in the collision rate medians between the groups of fair and good pavements. There was not a statistically significant difference (p-value > 0.05) in the collision rates between the groups of poor and fair pavements, nor

between the groups of poor and good pavements. Fair and good pavements exhibited the lowest collision rate medians, while poor and good pavements exhibited similar medians of 0.09. The collision rate median in poor pavements was 22.2% greater than in fair pavements.

- **Level of Severity**

A Kruskal-Wallis test showed that there was a statistically significant difference (p-value < 0.05) in the level of collision severity within the groups of poor, fair, and good pavement condition. The Dunn-Bonferroni's pairwise post hoc test for PDO collision rates showed that there was a statistically significant difference (p-value < 0.05) in the collision rate medians between the groups of poor and fair pavements, and between the groups of fair and good pavements. There was no statistically significant difference (p-value > 0.05) in the collision rate medians between the groups of poor and good pavements. Poor and fair pavements exhibited similar collision rate medians of 0.11, while good pavements exhibited the greatest median of 0.13. The collision rate median in poor pavements was 18.2% lower than in good pavements.

The Dunn-Bonferroni's pairwise post hoc test for fatal and injury collision rate medians showed that there was a statistically significant difference (p-value < 0.05) between the groups of poor and fair pavements, and between the groups of poor and good pavements. There was no statistically significant difference (p-value > 0.05) in the collision rate medians between the groups of fair and good pavements. Fair and good pavements exhibited the lowest collision rate median of 0.04, while poor pavements exhibited a median of 0.05. The collision rate median in poor pavements was 20.0% greater than in fair and good pavements.

- **Type of Impact**

The Kruskal-Wallis test showed that there was a statistically significant difference (p-value < 0.001) in the type of impact of collisions within the groups of poor, fair, and good pavement condition. The Dunn-Bonferroni's pairwise post hoc test for single vehicle collisions showed that there was no statistically significant difference (p-value > 0.05) in the collision rate medians between the groups of poor, fair, and good pavements. The pavements exhibited similar collision rate medians of 0.08.

The Dunn-Bonferroni's pairwise post hoc test for sideswipe collisions showed that there was a statistically significant difference (p-value < 0.001) between the groups of poor, fair, and good pavements. Fair pavements exhibited the lowest median collision rates of 0.05, while poor and good pavements exhibited collision rate medians of 0.07 and 0.06, respectively. The collision rate median in poor pavements was 28.6% greater than in fair pavements and 14.3% greater than in good pavements.

The Dunn-Bonferroni's pairwise post hoc test for rear-end collisions showed that there was a statistically significant difference (p-value < 0.001) between the groups of poor and fair pavements, and between the groups of fair and good pavements. Fair pavements exhibited the lowest collision rate median of 0.04, while poor and good pavements exhibited collision rate medians of 0.06 and 0.05, respectively. The collision rate median in poor pavements was 33.3% greater than in fair pavements and 16.7% greater than in good pavements.

- **Surface Condition**

A Kruskal-Wallis test showed that there was a statistically significant difference (p-value ≤ 0.05) in the rates of collisions due to surface conditions within the groups of

poor, fair, and good pavement condition. The Dunn-Bonferroni's pairwise post hoc test for wet surfaces showed that there was a statistically significant difference (p-value < 0.001) in collision rate medians between the groups of poor and fair pavements, and between the groups of fair and good pavements. There was no statistically significant difference (p-value > 0.05) in the collision rates between the groups of poor and good pavements. Fair pavements exhibited the lowest collision rate median of 0.04, while poor and good pavements exhibited collision rate medians of 0.06 and 0.05, respectively. The collision rate median in poor pavements was 33.3% greater than in fair pavements and 16.7% greater than in good pavements.

The Dunn-Bonferroni's pairwise post hoc test for dry surfaces showed that there was a statistically significant difference (p-value < 0.001) in collision rate medians between the groups of poor and fair, and the groups of good pavements. Fair pavements exhibited the lowest collision rate median of 0.15, while poor and good pavements exhibited similar collision rate medians of 0.17. The collision rate median in poor pavements was 11.8% greater than in fair and good pavements.

5.2.5 Results of the Statistical Analysis

The results of the statistical analysis using the Kruskal-Wallis test to compare the collision rate medians between the groups of the pavement condition and macrotexture for rural arterial highways and freeways can be summarized as follows:

- **For Arterial Highways**

Figure 5.3 shows the collision rate medians and pavement condition for arterial highways. The figure shows that pavement with poor condition exhibited the greatest collision rates for total, fatal and injury, sideswipe, rear-end, wet, and dry collisions.

Pavement with fair condition exhibited the lowest collision rates for all classes of collisions. Pavement with good condition exhibited the greatest collision rate for PDO and single vehicle collisions.

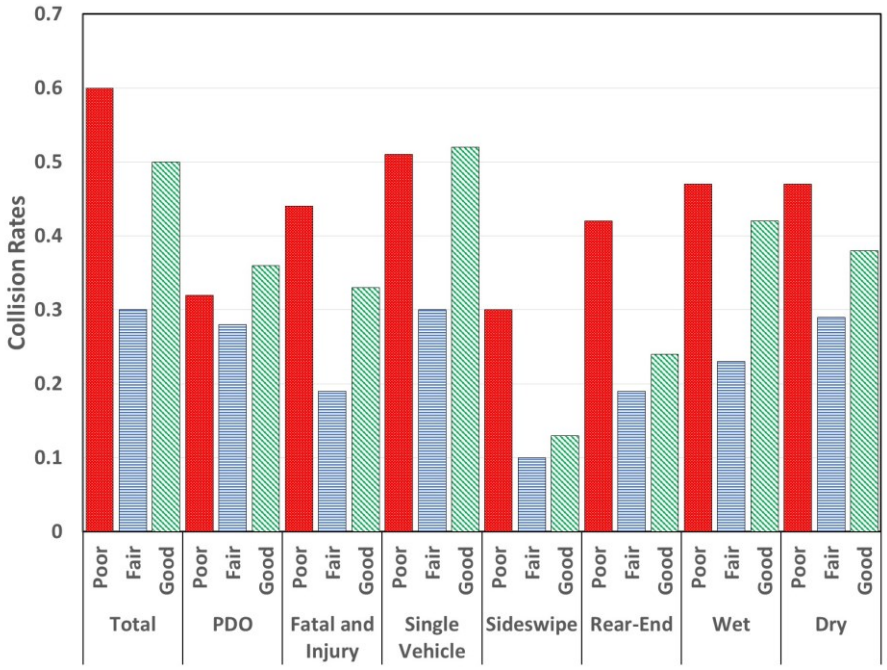

Figure 5.3 Collision Rates and Pavement Condition for Arterial Highways

Figure 5.4 shows the collision rate medians and macrotexture for arterial highways. The figure shows that pavement with low level of macrotexture exhibited the greatest collision rate for all classes of collisions. Pavement with medium level of macrotexture exhibited the lowest collision rate for all classes of collisions. Pavement with high level of macrotexture exhibited the collision rate lower than pavement with low level of macrotexture and greater than pavement with medium level of macrotexture for all classes of collisions.

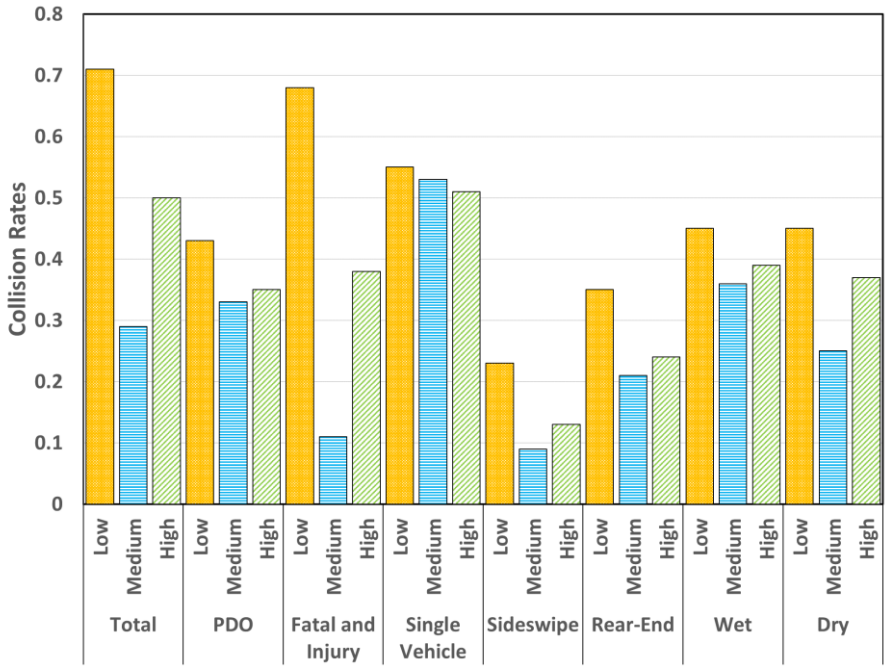

Figure 5.4 Collision Rates and Macrotextures for Arterial Highways

- **For Freeways**

Figure 5.5 shows the collision rate medians and pavement condition for freeways. The figure shows that pavement with poor condition exhibited the greatest collision rates for fatal and injury, sideswipe, rear-end, and wet collisions. Pavement with fair condition exhibited the lowest collision rates for the majority of the collision classes, except for the single vehicle collision that showed similar collision rates for good and poor pavements. Pavement with good condition exhibited the greatest collision rate for PDO collisions. Pavement with poor and good condition exhibited similar collision rates for total, single vehicle, and dry collisions.

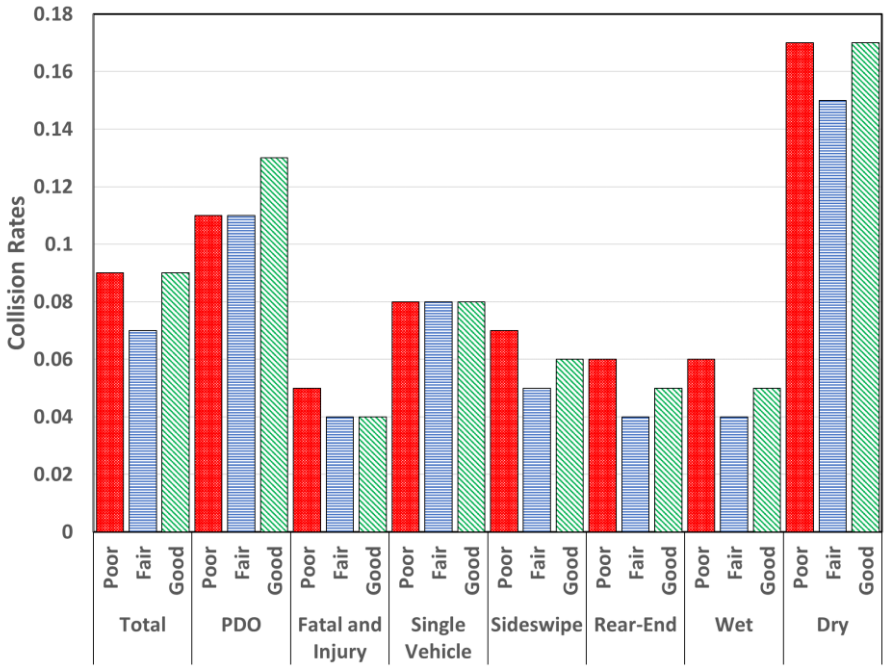

Figure 5.5 Collision Rates and Pavement Condition for Freeways

In summary, the results of the analysis of collision rate for arterial highways and freeways indicated that collision rates were greater for pavements with poor condition and with a low level of macrotexture. For arterial highways, the influence of pavement condition and macrotexture level was more noticeable in the sideswipe and fatal and injury collisions for arterial highways. In these two classes of collisions, the collision rates were expressively greater for pavements with poor condition and a low level of macrotexture than for pavements with fair and good condition and a medium or high level of macrotexture.

5.3 Development of Prediction Models for Number of Collisions

5.3.1 Objective

One of the objectives of this thesis was to develop general linear models (GLM) that can be used to estimate the number of collisions for two-lane undivided rural

highways using traffic, grade of the roads, and the three indicators of pavement condition, PCI, MPD, and IFI as explanatory variables.

5.3.2 Data for the Models

The data used for the development of the models included collision and pavement condition data of 13 undivided two-lane highways with AADT lower than 33,000. This AADT is a typical traffic volume for two-lane highways (GTA, 2009). The road segments were located at highway 6, 7, 10, 11, 24, 26, 28, 35, 41, 60, 118, 141, 144. The tangent road segments were 100 m length. The collision count was the sum of collision for the three-year period (2012 to 2014).

The PCI was calculated using Equation 2.3 and the international indicator of pavement friction (IFI) that was calculated using SN and MPD measurements. The IFI was calculated using Equation 2.7 and 2.8 with the constant values taken from the PIARC publication (PIARC, 1995). The constant values used in the IFI calculations were: A = -0.02283, B = 0.60628, C = 0.097589, a = 11.5, b = 69.13.

Table 5.5 shows descriptive statistics of the data used to develop the regression models for the period of three years (2012-2014). The table shows the mean, standard deviation (SD), minimum (Min), maximum (Max), and sum (Sum) for collisions by collision class, traffic volume (AADT), and for two indicators of pavement condition, MPD and IFI. Table 5.5 also presents the number of road segments by group of PCI and grade. The column "N" indicates the total number of road segments per collision class. The number of road segments varied from 4697 to 798 because information about skid resistance was not available for all sites.

Table 5.5 Descriptive Statistics of Data for Two-Lane Undivided Arterial Highways

Collision Class		Min.	Max.	Mean	SD*	Sum	N**
Total		1	32	2	3	8745	4697
PDO		0	22	1	2	6791	4697
Fatal and injury		0	18	0	1	1980	4697
Single vehicle		0	12	1	1	4362	4697
Sideswipe		0	8	0	1	656	4697
Rear-end		0	19	0	1	1941	4697
Dry		0	22	1	2	5028	4697
Wet		0	16	1	1	2392	4697
Pavement Indicator		**Min.**	**Max.**	**Mean**	**SD***		**N****
AADT		610	29800	10183	8040		4697
MPD		0.56	2.64	1.18	0.25		4697
IFI		18.57	38.91	32.24	4.21		798
PCI	Poor						194
	Fair						523
	Good						3980
Grade	At-grade						4340
	In-grade						357
(*) SD = Standard deviation, (**) N= Number of road segments							

5.3.3 Methodology

This study used parametric approaches to develop multivariate statistical models to investigate the influence of pavement condition on road safety. The parametric approach employed to develop the statistical models was the negative binomial (NB) regression and the zero-inflated negative binomial regression (ZINB). The NB is a generalization of Poisson regression that loosens the restrictive assumption that the variance is equal to the mean (Rodriguez, 2013). The NB is indicated for over-dispersed count data and has a similar structure as Poisson regression with an extra parameter to model, the over-dispersion parameter (θ), which represents unobserved heterogeneity (Rodriguez, 2013). The NB distribution of the outcome (Y) given an unobserved variable (θ) is Poisson with mean (μ) and variance (σ^2) equal to $\mu\theta$.

For an NB regression, the response variable is a count variable and the

explanatory variables can be continuous and categorical variables. The framework of an NB model with logarithmic link function is shown in Equation 5.3.

$$ln\,(\mu) = \beta_0 + \beta_1 X_1 + \beta_2 X_2 + \cdots + \beta_n X_n \quad \textbf{(5.3)}$$

Where μ = the predicted value of Y, X_i (i = 1. 2, …, n) = the explanatory variables, β_1. β_2. .... β_n = coefficients estimated from a set of data using the maximum likelihood estimator.

The ZINB Poisson regression was used to address the excessive number of zero counts that occurred in collision classes such as fatal and injury collisions and for collisions classified by type of impact. The ZINB model assumes that the sample has two parts: one group whose counts are generated by the NB regression model, and another group whose counts are generated by the logit model for predicting an excess of zeros (Rodriguez, 2013; SAS Institute Inc., 2015).

The goodness of fit and comparison of the parametric models were analyzed using the Akaike information criteria (AIC). The AIC is a measure of goodness of model fit that balances model fit against model simplicity (parsimonious model). When comparing models, the model with smaller AIC has better fit. The AIC has the form is given by Equation 5.4.

$$AIC = -2\,LL + 2p \quad \textbf{(5.4)}$$

Where LL = the log likelihood evaluated at the value of the estimated parameters, and p = the number of parameters estimated in the model.

The models were built to examine the main effects of each explanatory variable

on the dependent variable. The dependent variable was defined as the mean of collisions by location. The explanatory variables included variables related to traffic, road geometry, and pavement condition. The variable related to traffic was defined by the annual average daily traffic (AADT). The variable related to road geometry was defined by the grade of road segment. The variable related to pavement condition included the indicator of PCI, MPD, and IFI.

For each collision class, models with two to five explanatory variables were tested and compared. In the models, the dependent variable (y) was the collision counts for a specific collision class and AADT, PCI, MPD, and IFI were the explanatory variables. In addition, the variable grade was included as an explanatory variable to examine whether grade influenced the collision.

The variables AADT, MPD, and IFI entered in the models as continuous variables and the variable PCI and grade entered in the models as categorical variables. The variable PCI was categorized into three categories of PCI (poor, fair, and good). The variable grade was categorized into two groups, one group for road segments with grades between ± 3% ($Grade_1$) and another group for grades greater and lower ± 3% ($Grade_2$).

The models were built with IFI and without IFI because skid resistance data was not available for all the sites where macrotextures were measured. Four road segments from four different highways (highways 26, 28, 41 and 60) had their levels of skid resistance updated using the models for new pavements developed in Chapter 4. These road segments were measured by LWT in 2013, when the pavements were two years old. The road segments located at highways 26 and 60 showed an increase in skid resistance of 2.3% and 0.4%, respectively. The road segments located at highways 41 and 28

showed a decrease in skid resistance of 23.4% and 1.6%, respectively.

The other skid resistance values for new pavements were not updated because information about pavement distress and operational conditions were missing, or measurement of skid resistance occurred in 2014. The skid resistance values for old pavements were not updated because information about maintenance of those segments was not available.

The models were built by adding and testing variables and their statistical significance. If a variable was not found to be statistically significant, this variable was removed from the model; otherwise, this variable was carried out in the other models. The main framework of four regression models is described in Table 5.6.

Table 5.6. Model Framework

Model	Model Equation
1	$\ln(yi) = \beta_0 + \beta_1 \ln AADT + \beta_2 PCI_{poor} + \beta_3 PCI_{fair} + \beta_4 PCI_{good}$
2	$\ln(yi) = \beta_0 + \beta_1 \ln AADT + \beta_2 PCI_{poor} + \beta_3 PCI_{fair} + \beta_4 PCI_{good} + \beta_5 Grade_1 + \beta_6 Grade_2$
3	$\ln(yi) = \beta_0 + \beta_1 \ln AADT + \beta_2 PCI_{poor} + \beta_3 PCI_{fair} + \beta_4 PCI_{good} + \beta_7 \ln MPD$
4	$\ln(yi) = \beta_0 + \beta_1 \ln AADT + \beta_2 PCI_{poor} + \beta_3 PCI_{fair} + \beta_4 PCI_{good} + \beta_8 \ln IFI$

In the models, the categorical variable PCI_{good} was defined as the reference group for comparison of PCI groups. In SPSS, the reference group is excluded from analysis and assigned with the parameter estimated, $\beta_{PCIgood}$, equal to zero. The other two parameter estimates, $\beta_{PCIfair}$ and $\beta_{PCIpoor}$, represent the difference in the estimated parameters from the respective category to the reference category ($\beta_{PCIgood}$). For example, using the framework of Model 1and PCI_{good} as the reference group, the collision mean for each category of PCI was calculated as follows:

- $Y_{PCIgood} = \exp(\beta_0 + \beta_1 \ln AADT)$
- $Y_{PCIfair} = \exp(\beta_0 + \beta_1 \ln AADT + \beta 3\ PCI_{fair})$
- $Y_{PCIpoor} = \exp((\beta_0 + \beta_1 \ln AADT + \beta 2\ PCI_{poor})$

Likewise, in the PCI categories where one of the categories is set as the reference, one of the grade categories was also selected as the reference. The category of reference selected by SPSS was the $Grade_2$ category. The parameter estimated for the variable $Grade_2$ was defined as equal to zero and the parameter estimated of $Grade_1$ was calculated as the difference in the estimated parameters between the two groups. The model equations show the parameter estimated for $Grade_1$ only.

The ZINB models were developed using the software *R* (R Development Core Team, 2014). *R* selects automatically the lowest category as reference group, in contrast to SPSS that selects the greatest category as reference. Thus, for ZINB models, the reference group for PCI categories was defined as PCI_{poor} and the parameter estimates (βs) for PCI_{fair} and PCI_{good} were the difference in the estimated parameters using PCI_{poor} as the reference group.

To improve the goodness of fit of the models and mitigate data over-dispersion, the standardized Pearson residual was calculated for each class of collision that showed residuals that exceeded the threshold of 2.5 absolute values (Hair *et al.*, 2015). The models were compared using the AIC criteria. The models that showed the lowest AIC with all the explanatory variables statistically significant (p-value ≤ 0.05) were selected for analysis. The models were validated using the bootstrap statistical technique with *n* sample of 1000 samples.

5.3.4 Results of Development of Models for Tangent Segments

In the following sections, the results of regression of the models for tangent segments are presented in two tables for each class of collision. The first table presents the regression results of the four models for each class of collision. This table included the parameter estimates (βs) and their statistical significance (p-value), the AIC, and the observed and estimated means of collisions. The model that showed all variables statistically significant with smaller AIC was selected for fitting analysis.

The results of the fitting analysis are presented in a second table. This table included comparison of the mean and sum of observed and estimated collisions per category of pavement condition (poor, fair, good). Additionally, for the collision classes with an excessive number of zero counts, such as fatal and injury, sideswipe, single vehicle, and rear-end, ZINB regressions were performed and the results were compared with the NB regression.

The second table also shows the sum and the means with standard deviation (SD) in parentheses of the total observed collisions by category of pavement and the sum and means with standard error (SE) in parentheses of the estimated total collisions using the estimated, bootstrapped, and ZINB models. The results of the bootstrapped and ZINB models and the parameter estimates are shown at the bottom of table. The ratio of the sum of observed and estimated collisions were calculated, and ratios close to one indicates good degree of agreement (Hauer, 2015).

5.3.4.1 Regression Models for Total Collisions

Table 5.7 shows the parameter estimates for the four models. Model 1 showed the lowest AIC value with all variables statistically significant (p-value < 0.05). The variable

AADT was statistically significant in the model and the variables grade, MPD, and IFI were not statistically significant. The parameter estimates showed a positive sign for AADT and a negative sign for PCI. The positive sign for AADT indicated that collision means increased with the increase of traffic. The parameter estimates for PCI indicated that collision means were lower for pavements in fair and poor condition in comparison with the reference group (PCI_{good}).

Table 5.7 Regression Parameters for Total Collisions

Parameters		Model 1	Model 2	Model 3	Model 4
p-value		< 0.001	< 0.001	< 0.001	< 0.005
Number of road segments		4632	4632	4632	789
Intercept	β_0	-1.33	-1.37	-1.36	0.78
	p-value	< 0.001	< 0.001	< 0.001	0.57
lnAADT	β_1	0.21	0.21	0.21	0.18
	p-value	< 0.001	< 0.001	< 0.001	< 0.001
PCISa	β_{2poor}	-0.12	-0.12	-0.12	-0.07
	β_{3fair}	-0.22	-0.23	-0.21	-0.28
	p-value	< 0.001	< 0.001	< 0.001	0.33
$Grade_1$	β_5	–	0.06	–	–
	p-value	–	0.41	–	–
lnMPD	β_7	–	–	0.16	–
	p-value	–	–	0.08	–
lnIFI	β_8		–	–	-0.55
	p-value		–	–	0.11
AIC		16359	16361	16358	2674

Model 1 was validated using the bootstrapping approach. Table 5.8 shows that the estimated means and sum of total collisions calculated using the estimated and bootstrapped models were comparable and similar to the total observed collisions. The results also showed that pavement in good condition exhibited the greatest collision mean, while pavement in fair condition exhibited the lowest collision mean. The collision means for pavements in poor and fair condition were 11.6% and 13.9% lower than for

pavement in good condition, respectively.

Table 5.8 Observed and Estimated Mean of Total Collisions

Collisions	Observed	Estimated	
		Estimated Model*	Bootstrapped Model **
$y_{overall}$	1.69 (1.25)	1.70 (0.03)	1.55 (0.03)
y_{poor}	1.54	1.53	1.55
y_{fair}	1.48	1.49	1.36
y_{good}	1.73	1.73	1.75
Sum	7855	7859	7838
Observed/Estimated		0.99	1.00
(*) Estimated Model: β_0 = -1.34, β_1= 0.21, β_2 = -0.12, β_3 = -0.22 (**) Bootstrapped Model: β_0 = -1.30, β_1= 0.34, β_2 = -0.19, β_3 = -0.38			

5.3.4.2 Regression Models for PDO Collisions

Table 5.9 shows the parameter estimates for the four models. Model 3 showed the lowest AIC value and all the variables statistically significant (p-value < 0.05). The variables AADT, PCI, and MPD were statistically significant in the model and the variables grade and IFI were not statistically significant. The parameter estimates showed a positive sign for AADT and MPD and a negative sign for PCI. The positive signs for AADT and MPD indicated that PDO collision means increased with the increase of traffic and macrotexture. The parameter estimates for PCI indicated that collision means were lower for pavements in fair and poor condition in comparison with the reference group (PCI_{good}).

Table 5.9 Regression Parameters for PDO Collisions

Parameters		Model 1	Model 2	Model 3	Model 4
p-value		< 0.001	< 0.001	< 0.001	0.015
Number of Segments		4433	4433	4433	757
Intercept	β_0	-1.30	-1.37	-1.35	1.55
	p-value	< 0.001	< 0.001	< 0.001	0.293
lnAADT	β_1	0.18	0.18	0.18	0.12
	p-value	< 0.001	< 0.001	< 0.001	0.018
PCI	β_{2poor}	-0.07	-0.07	-0.07	0.09
	β_{3fair}	-0.18	-0.18	-0.16	-0.15
	p-value	0.019	0.02	0.04	0.71
$Grade_1$	β_5	–	0.10	–	–
	p-value	–	0.21	–	–
lnMPD	β_7	–	–	0.22	–
	p-value	–	–	0.02	–
lnIFI	β_8	–	–	–	-0.71
	p-value	–	–	–	0.06
AIC		13985	13985	13981	2263

Model 3 was validated using the bootstrapping approach. Table 5.10 shows that the estimated means and sum of PDO collisions calculated using the estimated model and bootstrapped models were comparable and similar to the observed PDO collisions. The results showed that pavement in good condition exhibited the greatest PDO collision mean, while pavements in fair condition exhibited the lowest collision mean. For the estimated model, the PDO collision means for pavements in poor and fair condition were 6.8 % and 10.5% lower than for pavement in good condition, respectively.

Table 5.10 Observed and Estimated Mean of PDO Collisions

Collisions	Observed	Estimated	
		Estimated Model*	**Bootstrapped Model****
$y_{overall}$	1.32 (1.04)	1.32 (0.23)	1.32 (0.22)
y_{poor}	1.26	1.24	1.26
y_{fair}	1.19	1.19	1.19
y_{good}	1.34	1.33	1.34
Sum	5836	5838	5843
Observed/Estimated		0.99	0.99
(*) Estimated Model: β_0 = -1.35, β_1= 0.18, β_2 = -0.07, β_3 = -0.16, β_7 = 0.22 (**) Bootstrapped Model: β_0 = -0.74, β_1= 0.23, β_2 = -0.07, β_3 = -0.21, β_7 = 0.29			

5.3.4.3 Regression Models for Fatal and Injury Collisions

Table 5.11shows the parameter estimates for the four models. Model 4 showed the lowest AIC value and all the variables statistically significant (p-value < 0.05). The variables AADT and IFI were statistically significant in the model and the variables PCI, MPD, and grade, were not statistically significant. The parameter estimates showed positive **s**ign**s** for AADT and for IFI, which indicated that fatal and injury collision means increased with the increase of traffic and IFI.

Table 5.11 Regression Parameters for Fatal and Injury Collisions

Parameters		Model 1	Model 2	Model 3	Model 4
p-value		< 0.001	< 0.001	< 0.001	< 0.001
Number of road segments		4433	4433	4433	757
Intercept	β_0	-3.80	-3.75	-3.75	-9.55
	p-value	< 0.001	< 0.001	< 0.001	< 0.001
lnAADT	β_1	0.27	0.27	0.27	0.34
	p-value	< 0.001	< 0.001	< 0.001	< 0.001
PCI	β_{2poor}	-0.28	-0.27	-0.29	-0.22
	β_{3fair}	-0.06	-0.06	-0.09	-0.13
	p-value	0.57	0.32	0.24	0.89
$Grade_1$	β_5	–	-0.08	–	–
	p-value	–	0.54	–	–
lnMPD	β_7	–	–	-0.29	–
	p-value	–	–	0.08	–
lnIFI	β_8	–	–	–	1.52
	p-value	–	–	–	0.03
AIC		5,543	5,544	5,542	974

Despite the fact that PCI was not found to be statistically significant, it was kept in the model for comparisons of fatal and injury collision means between the three categories of PCI. The parameter estimates of the PCI categories indicated that fatal and injury collision means decreased for pavements in fair and poor condition in comparison with the reference group (PCI_{good}).

Model 4 was validated using the bootstrapping approach. Table 5.12 shows that the estimated means and sum of collisions calculated using the estimated, bootstrapped, and ZINB models were comparable and similar to the observed fatal and injury collisions. The three models showed that pavements in good condition exhibited the greatest collision mean, while pavements in poor condition exhibited the lowest collision mean. For the estimated model, the collision means for pavements in poor and fair condition were 42.7% and 28.6% lower than for pavement in good condition,

respectively.

Table 5.12 Observed and Estimated Means of Fatal and Injury Collisions

Collisions	Observed	Estimated Models		
		Estimated*	Bootstrapped**	ZINB***
$y_{overall}$	0.27 (0.57)	0.27 (0.11)	0.27 (0.02)	0.27 (0.10)
y_{poor}	0.16	0.16	0.23	0.16
y_{fair}	0.20	0.20	0.24	0.27
y_{good}	0.28	0.28	0.27	0.28
Sum	206	206	206	205
Observed/Estimated		1.00	1.00	1.00
(*) Estimated Model: β_0 = -9.55, β_1= 0.34, β_2 = -0.23, β_3 = -0.13, β_8 = 1.52 (**) Bootstrapped Model: β_0 = -2.05, β_1= 0.11, β_2 = -0.05, β_3 = -0.03, β_8 = 0.41 (***) ZINB Model: AIC = 988 $ZINB_{zero}$=β_0 = 2.62, β_1= 0.51, β_2 = 0.36, β_3 = 1.20, β_8 = 2.50 $ZINB_{Count}$ = β_0 = -8.15, β_1= 0.53, β_2 = 0.21, β_3 = 0.65, β_8 = 0.61				

5.3.4.4 Regression Models for Single Vehicle Collisions

Table 5.13 shows the parameter estimates for the four models. Model 1 showed the lowest AIC value and all the variables statistically significant (p-value < 0.05). The variables AADT and PCI were statistically significant in the models and the variables grade, MPD, and IFI were not statistically significant. The parameter estimate showed a positive sign for AADT, which indicates that single vehicle collision means increased with the increase of traffic. The parameter estimates for PCI indicated that collision means were lower for pavements in fair and poor condition in comparison with the reference group (PCI_{good}).

Table 5.13 Regression Parameters for Single Vehicle Collisions

Parameters		Model 1	Model 2	Model 3	Model 4
p-value		< 0.001	< 0.001	< 0.001	0.08
Number of road segments		4697	4697	4697	793
Intercept	β_0	-0.00	-0.05	-0.04	0.41
	p-value	0.98	0.39	0.85	0.80
lnAADT	β_1	-0.00	-0.00	-0.003	-0.08
	p-value	0.87	0.78	0.90	0.15
PCI	β_{2poor}	-0.23	-0.24	-0.23	-0.40
	β_{3fair}	-0.27	-0.27	-0.25	-0.48
	p-value	< 0.001	< 0.001	0.00	0.10
$Grade_1$	β_5	–	0.08	–	–
	p-value	–	0.33	–	–
lnMPD	β_7	–	–	0.17	–
	p-value	–	–	0.08	–
lnIFI	β_8	–	–	–	0.04
	p-value	–	–	–	0.92
AIC		12535	12537	12535	2049

Model 1 was validated using the bootstrapping approach. Table 5.14 shows that the estimated means and sum of single vehicle collisions calculated using the estimated, bootstrapped, and ZINB models were comparable and similar to the observed single vehicle collisions. The results showed that pavements in good condition exhibited the greatest sideswipe collision mean, while pavements in poor and fair condition exhibited similar collision mean. For the estimated model, the single vehicle collision means for pavements in poor and fair condition were approximately 20.8% and 22.9% lower than for pavement in good condition, respectively.

Table 5.14 Observed and Estimated Mean of Single Vehicle Collisions

Collisions	Observed	Estimated Models		
		Estimated *	Bootstrapped **	ZINB ***
$y_{overall}$	0.93(0.84)	0.93 (0.08)	0.95 (0.08)	0.93(0.08)
y_{poor}	0.76	0.76	0.79	0.76
y_{fair}	0.73	0.74	0.76	0.73
y_{good}	0.96	0.96	0.98	0.93
Sum	4362	4363	4463	4363
Observed/Estimated		1.00	1.00	0.99
(*) Estimated Model: β_0 = -0.00, β_1= 0.00, β_2 = -0.23, β_3 = -0.27 (**) Bootstrapped Model: β_0 = 0.98, β_1= -0.00, β_2 = -0.20, β_3 = -0.23 (***) ZINB Model: AIC = 11108 $ZINB_{zero}$=β_0 = -26.22, β_1= -0.08, β_3 = 3.09, β_4 = 2.40 $ZINB_{Count}$ = β_0 = -0.25, β_1= -0.00, β_3 = -0.04, β_4 = 0.23				

5.3.4.5 Regression Models for Sideswipe Collisions

Table 5.15 shows the parameter estimates for the four models. Model 1 showed the lowest AIC value and all the variables statistically significant (p-value < 0.05). The variables AADT and PCI were statistically significant in the models and the variables grade, MPD, and IFI were not statistically significant. The parameter estimate showed a positive sign for AADT, which indicates that sideswipe collision means increased with the increase of traffic. The parameter estimates for PCI indicated that collision means were lower for pavements in fair condition and slightly greater for pavements in poor condition in comparison with the reference group (PCI_{good}).

Table 5.15 Regression Parameters for Sideswipe Collisions

Parameters		Model 1	Model 2	Model 3	Model 4
p-value		< 0.001	< 0.001	< 0.001	< 0.001
Number of road segments		4697	4697	4697	793
Intercept	β_0	-7.63	-7.84	-7.68	-4.45
	p-value	< 0.001	< 0.001	< 0.001	0.16
lnAADT	β_1	0.63	0.62	0.63	0.50
	p-value	< 0.001	< 0.001	< 0.001	< 0.001
PCI	β_{2poor}	0.01	-0.00	0.00	0.42
	β_{3fair}	-0.48	-0.49	-0.46	-0.55
	p-value	< 0.05	< 0.05	0.01	0.37
$Grade_1$	β_5	–	0.27	–	–
	p-value	–	0.15	–	–
lnMPD	β_7	–	–	0.26	–
	p-value	–	–	0.19	–
lnIFI	β_8	–	–	–	-0.62
	p-value	–	–	–	0.45
AIC		3825	3825	3825	541

Model 1 was validated using the bootstrapping approach. Table 5.16 shows that the estimated means and sum of sideswipe collisions calculated using the estimated model and bootstrapped models were comparable and similar to the observed sideswipe collisions. The ZINB model exhibited a sum of collisions similar to the estimated model and observed collisions. The results showed that pavements in poor and good condition exhibited the greatest sideswipe collision means, while pavements in fair condition exhibited the lowest collision mean. For the estimated model, the sideswipe collision means for pavements in poor and good condition were equal. Sideswipe collision mean of pavements in fair condition was 24.0% lower than for pavement in good condition.

Table 5.16 Observed and Estimated Means of Sideswipe Collisions

Collisions	Observed	Estimated Models		
		Estimated*	Bootstrapped**	ZINB ***
$y_{overall}$	0.14 (0.55)	0.14 (0.075)	0.14 (0.462)	0.14 (0.08)
y_{poor}	0.14	0.14	0.14	0.14
y_{fair}	0.11	0.11	0.08	0.11
y_{good}	0.14	0.14	0.15	0.14
Sum	656	654	657	656
Observed/Estimated		1.00	0.99	1.00
(*) Estimated Model: β_0 = -7.63, β_1= 0.63, β_2 = -0.01, β_3 = -0.49 (**) Bootstrapped Model: β_0 = -0.57, β_1= 0.08, β_2 = -0.00, β_3 = -0.07 (***) ZINB Model: AIC = 3378 $ZINB_{zero}$= β_0 = 6.16, β_1 = -0.58, β_3 = -0.47, β_4 = 1.21 $ZINB_{Count}$ = β_0 = -1.79, β_1 = 0.12, β_3 = -0.75, β_4 = 0.96				

5.3.4.6 Regression Models for Rear-End Collisions

Table 5.17 shows the parameter estimates for the four models. Model 4 showed the lowest AIC value and all the variables statistically significant (p-value < 0.05). The variables AADT and PCI were statistically significant in the models and the variables grade, MPD, and IFI were not statistically significant. The parameter estimate showed a positive sign for AADT, which indicates that rear-end collision means increased with the increase of traffic. The parameter estimated for grade was also positive, which indicates that collision means increased on flat surfaces. The parameter estimate for IFI was negative, which indicates that rear-end collisions decreased with the increase of pavement friction. The parameter estimates for PCI indicated a positive sign for poor pavements and a negative sign for fair pavements, which indicates that collision means were lower for pavements in fair condition and greater for pavements in poor condition in comparison with the reference group (PCI_{good}).

Table 5.17 Regression Parameters for Rear-End Collisions

Parameters		Model 1	Model 2	Model 3	Model 4
p-value		< 0.001	< 0.001	< 0.001	< 0.001
Number of road segments		4697	4697	4697	798
Intercept	β_0	-8.92	-9.12	-8.91	-7.89
	p-value	< 0.001	< 0.001	< 0.001	< 0.001
lnAADT	β_1	0.88	0.87	0.88	1.09
	p-value	< 0.001	< 0.001	< 0.001	< 0.001
PCI	β_{2poor}	0.06	0.04	0.06	0.16
	β_{3fair}	-0.46	-0.46	-0.46	-1.00
	p-value	< 0.001	< 0.001	< 0.001	0.04
$Grade_1$	β_5	–	0.27	–	1.04
	p-value	–	0.03	–	< 0.001
lnMPD	β_7	–	–	-0.04	–
	p-value	–	–	0.77	–
lnIFI	β_8	–	–	–	-1.14
	p-value	–	–	–	< 0.001
AIC		7367	7364	7368	994

Model 1 was validated using the bootstrapping approach. Table 5.18 shows that the estimated means and sum of rear-end collisions calculated using the estimated, bootstrapped, and ZINB models were comparable and similar to the observed rear-end collisions. The results showed that pavement in poor condition exhibited the greatest rear-end collision mean. For the estimated model, the rear-end collision means for pavements in poor and fair condition were 85.3% greater and 55.9% lower than for pavement in good condition, respectively.

Table 5.18 Observed and Estimated Mean of Rear-End Collisions

Collisions	Observed	Estimated Models		
		Estimated*	Bootstrapped**	ZINB***
$y_{overall}$	0.34 (1.19)	0.33 (0.39)	0.34(1.18)	0.34 (0.38)
y_{poor}	0.74	0.63	0. 74	0.39
y_{fair}	0.14	0.15	0.14	0.05
y_{good}	0.34	0.34	0.34	0.36
Sum	271	266	270	268
Observed/Estimated		1.02	1.00	1.01
(*) Estimated Model: β_0 = -7.89, β_1= 1.09, β_2 = 0.16, β_3 = -1.00, β_5 = 1.04, β_8 = 1.14				
(**) Bootstrapped Model: β_0 = -2.63, β_1= 0.34, β_2 = -0.23, β_3 = -0.28, β_5 = 0.21, β_8 = -0.02				
(***) ZINB Model: AIC = 902				
$ZINB_{zero}$=β_0 = 6.26, β_1= -1.07, β_3 = -0.42, β_4 = 0.39, β_6 = 0.55, β_8 = 1.14				
$ZINB_{Count}$ = β_0 = -1.78, β_1= 0.32, β_3 = -1.53, β_4 = -0.05, β_6 = -0.60, β_8 = -0.19				

5.3.4.7 Regression Models for Dry Surface Collisions

Table 5.19 shows the parameter estimates for the four models. Model 2 showed the lowest AIC value and all the variables statistically significant (p-value < 0.05). The variables AADT, PCI, and grade were statistically significant in the models and the variables MPD and IFI were not statistically significant. The parameter estimate showed a positive sign for AADT, which indicates that dry collision means increased with the increase of traffic. The parameter estimate for grade was also positive, which indicates that dry collision means increased in road segments at-grade. The parameter estimates for PCI indicated negative signs for poor and fair pavements, which indicate that dry surface collision means decreased in poor and fair pavements in comparison with the reference group (PCI_{good}).

Table 5.19 Regression Parameters for Dry Collisions

Parameters		Model 1	Model 2	Model 3	Model 4
p-value		< 0.001	< 0.001	< 0.001	< 0.001
Number of road segments		4697	4697	4697	798
Intercept	β_0	-2.80	-2.95	-2.98	-1.80
	p-value	< 0.001	< 0.001	< 0.001	0.18
lnAADT	β_1	0.32	0.31	0.32	0.36
	p-value	< 0.001	< 0.001	< 0.001	< 0.001
PCI	β_{2poor}	-0.29	-0.30	-0.31	0.03
	β_{3fair}	-0.27	-0.27	-0.27	-0.602
	p-value	< 0.001	< 0.001	< 0.001	0.037
$Grade_1$	β_5	–	0.22	0.23	0.11
	p-value	–	< 0.05	< 0.05	0.49
lnMPD	β_7	–	–	0.10	–
	p-value	–	–	0.27	–
lnIFI	β_8	–	–	–	-0.40
	p-value	–	–	–	0.29
AIC		13,275	13,270	13,270	2,119

Model 2 was validated using the bootstrapping approach. Table 5.20 shows that the estimated means and sum of dry surface collisions calculated using the estimated and bootstrapped models were comparable and similar to the observed dry surface collisions. The results showed that pavements in good condition exhibited the greatest collision mean. For the estimated model, the dry collision means for pavements in poor and fair condition were 26.4% and 15.4% lower than for pavement in good condition, respectively.

Table 5.20 Observed and Estimated Means of Dry Collisions

Collisions	Observed	Estimated Models	
		Estimated*	Bootstrapped**
$y_{overall}$	1.07 (1.63)	1.07 (0.32)	1.07 (1.15)
y_{poor}	0.82	0.81	0.82
y_{fair}	0.92	0.93	0.92
y_{good}	1.10	1.10	1.10
Sum	5028	5030	5030
Observed/Estimated		1.00	1.00
(*) Estimated Model: β_0 = -2.95, β_1= 0.31, β_2 = -0.30, β_3 = -0.27, β_5 = 0.23 (**) Bootstrapped Model: β_0 = -1.94, β_1= 0.32, β_2 = -0.30, β_3 = -0.30, β_5 = 0.23			

5.3.4.8 Regression Models or Wet Surface Collisions

Table 5.21 shows the parameter estimates for the four models. Model 3 showed the lowest AIC value and all the variables statistically significant (p-value < 0.05). The variables AADT, PCI, and MPD were statistically significant in the models and the variables grade and IFI were not statistically significant. The parameter estimate showed a positive sign for AADT, which indicates that wet surface collision means increased with the increase of traffic. The parameter estimate for MPD was negative, which indicates that wet collision means decreased with the increase of pavement macrotexture. The parameter estimates for PCI indicated a positive sign for poor pavements and a negative sign for fair pavements, which indicates that collision means decreased for pavements in fair condition and increased for pavements in poor condition in comparison with the reference group (PCI_{good}).

Table 5.21 Regression Parameters for Wet Collisions

Parameters		Model 1	Model 2	Model 3	Model 4
p-value		< 0.001	<0.001	< 0.001	< 0.001
Number of road segments		4697	4697	4697	798
Intercept	β_0	-2.95	-2.92	-2.93	-5.27
	p-value	< 0.001	< 0.001	< 0.001	0.004
lnAADT	β_1	0.25	0.26	0.26	0.26
	p-value	< 0.001	< 0.001	< 0.001	< 0.001
PCI	β_{2poor}	0.10	0.11	0.10	0.28
	β_{3fair}	-0.40	-0.39	-0.43	-0.48
	p-value	< 0.05	< 0.05	0.001	0.19
$Grade_1$	β_5	–	-0.06	–	–
	p-value	–	0.56	–	–
lnMPD	β_7	–	–	-0.13	–
	p-value	–	–	0.03	–
lnIFI	β_8	–	–	–	0.67
	p-value	–	–	–	0.18
AIC		8975	8977	8975	1467

Model 3 was validated using the bootstrapping approach. Table 5.22 shows that the estimated means and sum of wet surface collisions calculated using the estimated and bootstrapped models were comparable and similar to the observed collisions. The results showed that pavements in poor condition exhibited the greatest wet collision mean. For the estimated model, the wet collision means for pavements in poor and fair condition were 16.3% greater and 42.9% lower, than for pavement in good condition, respectively.

Table 5.22 Observed and Estimated Means of Wet Collisions

Collisions	Observed	Estimated Models	
		Estimated*	Bootstrapped**
$y_{overall}$	0.47 (0.93)	0.47 (0.95)	0.47 (0.93)
y_{poor}	0.58	0.57	0.58
y_{fair}	0.28	0.28	0.28
y_{good}	0.49	0.49	0.49
Sum	379	352	378
Observed/Estimated		1.07	1.00
(*) Estimated Model: β_0 = -2.93, β_1= 0.26, β_2 = 0.10, β_3 = -0.43, β_7 = -0.13 (**) Bootstrapped Model: β_0 = -0.55, β_1= 0.13, β_2 = -0.08, β_3 = -0.21, β_7 = -0.25			

5.3.5 Results of Development of Models for Curves

The results of the regression model (Model 3) with the parameter estimates for curves are shown in Table 5.23. The results showed that pavement condition was not statistically significant. The variables macrotexture showed to be statistically significant for sideswipe and wet surface collisions.

For sideswipe collisions on curves, the variables AADT, grade, and MPD were statistically significant in the models and the variable grade PCI was not statistically significant. The parameter estimates showed a positive sign for AADT and grade, which indicates that sideswipe collision means increased with the increase of traffic and grade. The parameter estimate for MPD was negative, which indicates that sideswipe collision means decreased with the increase of pavement macrotexture.

For wet surface collisions on curves, the variables AADT and MPD were statistically significant in the models and the variables grade and PCI were not statistically significant. The parameter estimates showed a positive sign for AADT, which indicates that wet collision means increased with the increase of traffic. The parameter estimate for MPD was negative, which indicates that wet collision means decreased with the increase of pavement macrotexture.

The models for sideswipe and wet surface collisions were validated using the bootstrapping approach. The results showed that the estimated means and sum of collisions calculated using the estimated and bootstrapped models were comparable and similar to the observed collisions.

Table 5.23 Regression Parameters for Curves

Model specification: $\ln(yi) = \beta_0 + \beta_1 lnAADT + \beta_2 PCI + \beta_3 Grade + \beta_4 MPD$									
Parameters		**Total Collision**	**Fatal and Injury**	**PDO**	**Single vehicle**	**Sideswipe**	**Rear-end**	**Dry**	**Wet**
p-value		< 0.001	< 0.001	< 0.001	< 0.001	< 0.001	< 0.001	< 0.001	< 0.001
Number of road segments		1991	1991	1991	1991	1991	1991	1991	1991
Intercept	β_0	-3.37	-5.94	-3.30	-0.56	-14.27	-10.97	-4.28	-4.09
	p-value	< 0.001	< 0.001	< 0.001	0.01	< 0.001	< 0.001	< 0.001	< 0.001
lnAADT	β_1	0.43	0.55	0.40	0.06	1.09	1.08	0.47	0.36
	p-value	< 0.001	< 0.001	< 0.001	0.05	< 0.001	< 0.001	< 0.001	< 0.001
PCI	β_{2poor}	-0.05	0.22	-0.16	-0.47	-0.10	0.26	-0.09	0.07
	β_{3fair}	-0.10	-0.334	-0.033	-0.09	-0.55	-0.22	-0.03	-0.13
	p-value	0.74	0.19	0.07	0.10	0.27	0.29	0.88	0.76
$Grade_1$	β_5	0.18	0.16	-0.310	0.01	2.15	0.32	0.29	0.02
	p-value	0.07	0.29	0.09	0.02	< 0.001	0.07	0.009	0.89
MPD	β_7	0.13	0.330	0.06	0.28	-1.32	-0.115	-0.08	-0.72
	p-value	0.38	0.13	0.68	0.10	< 0.001	0.60	0.64	< 0.001
AIC		7625	3609	6868	5527	1816	3520	6208	3792
Collisions	Observed	5143	1091	3965	2266	559	1,536	3361	1168
	Predicted	4139	1023	3410	1993	498	1521	2842	1035
Observed/Predicted		1.24	1.07	1.16	1.13	1.12	1.01	1.18	1.12

5.3.6 Summary of the Results of the Models

A summary of the regression models for tangent segments with the overall collision means (PCIo) and collision means by category of pavement condition (PCI_{poor}, PCI_{fair}, PCI_{good}) is shown in Table 5.24. The table also shows the statistically significant variables for each model.

Table 5.24 Summary of Regression Models for Tangent Segments

Collision Class	Collision Means				Variables in the Models
	PCIo	PCI_{poor}	PCI_{fair}	PCI_{good}	
Total	1.70	1.53	1.49	1.73	PCI, AADT
PDO	1.32	1.24	1.19	1.33	PCI, AADT, MPD
Fatal and injury	0.27	0.16	0.20	0.28	AADT, IFI
Single vehicle	0.93	0.76	0.74	0.96	PCI, AADT
Sideswipe	0.14	0.14	0.11	0.14	PCI, AADT
Rear-end	0.33	0.74	0.14	0.34	PCI, AADT, IFI, Grade
Dry surface	1.07	0.82	0.92	1.10	PCI, AADT, Grade
Wet surface	0.47	0.57	0.28	0.49	PCI, AADT, MPD

The variable PCI was statistically significant for the majority of collision classes, except for fatal and injury collisions. The results showed that pavements in good condition exhibited the greatest collision means, while pavements in fair condition exhibited the lowest collision means; except for the fatal and injury collision class, which showed a lower collision mean for pavements in poor condition.

The variable AADT was statistically significant and exhibited a positive sign in the models, except in the model for single vehicle collisions where it exhibited a negative sign. The results indicated that collision frequency increased with the increase of traffic volume for the majority of collision classes, except for single vehicle collisions, where traffic volume had a small positive influence on the increase of collisions.

The variable grade was not statistically significant for the majority of collision

classes, except for the rear-end and dry surface collision classes. The variable grade exhibited a positive sign for collisions that occurred at-grade, which indicates that there was an increase in rear-end and dry collisions on flat segments.

The variable MPD was statistically significant for PDO and wet surface collision classes. The variable MPD exhibited a positive sign for PDO collisions and a negative sign for wet surface collisions. The results indicate that collision frequency increased with the increase of MPD for the PDO collisions, while wet surface collision frequency decreased with the increase of MPD.

The variable IFI was statistically significant for fatal and injury collisions and rear-end collisions. The variable IFI exhibited a positive sign for fatal and injury collisions and a negative sign for rear-end collisions. The results indicate that fatal and injury collisions increased with the increase of IFI, while rear-end collisions decreased with the increase of IFI.

The regression models for curves showed that pavement condition was not statistically significant. The variable AADT was statistically significant and exhibited a positive sign in the models. The results indicated that collision frequency increased with the increase of traffic volume. The variable grade was statistically significant for the single-vehicle, sideswipe, and dry collisions. The variable grade exhibited a positive sign for collisions that occurred at-grade, which indicates that there was an increase in these types of collisions on flat segments. The variable MPD was statistically significant for sideswipe and wet surface collisions. The variable MPD exhibited a negative sign for these collisions, which indicates that there was a decrease in collision frequency in sideswipe and wet surface collisions with the increase of MPD.

5.3.7 Discussion

The results showed that pavements in poor and good condition exhibited greater collision frequency than pavements in fair condition. The influence of pavements in poor condition on road safety can be related to drivers' control of their vehicle and drivers' response to driving challenges caused by unexpected situations that include pavement condition. For example, the presence of an unexpected pavement distress such as a pothole, a pavement drop-off, or severe ruts may cause damages to the vehicle that affect a driver's control; however, the ultimate result of this encounter (between pavement distress and a vehicle) will be greatly affected by the driver's reaction to the situation. The driver's reaction will depend on various factors, including their driving skills (avoiding or successfully handling an emergency driving situation), health (mental and physical condition), and judgment which become impaired when the driver is fatigued or under influence of legal and illegal substances.

Conversely, the increase in collisions on good pavements can be related to drivers' behaviours and their perception of safety. For example, pavements in good condition may give drivers the confidence to make unsafe maneuvers and exceed speed limits. Further, if drivers perceive that the road conditions are good and the vehicle is under control, they may become engaged in other activities that distract their attention away from the road, which may result in collisions.

The distractions that may influence drivers' attention include visual, physical, and mental distractions (National Highway Traffic Safety Administration, 2019). Visual distractions include ceasing to look at the road – for example, to look at the GPS or media system or check passengers in the rearview mirror. Physical distractions include taking

their hands off the wheel – for example, to eat or search for something. Mental distractions involve brain activities and thoughts that affect a driver's focus on driving. Texting and talking on the phone, for example, combine more than one type of distraction (National Highway Traffic Safety Administration, 2017).

The lower collision means for pavement in fair condition can be related to drivers' behaviours and their perception of safety. Pavements in fair condition usually do not present dangerous road conditions but do present visible signs of deterioration and small deformations that may increase drivers' awareness that driving conditions are not excellent and attention is required to maintain control of the vehicle. Pavements with visible distress may retain the driver's attention on the road and reduce their involvement in distractive activities.

Pavement textures showed to be an important factor for collision classes that demanded satisfactory levels of macrotexture and pavement friction. Greater levels of macrotexture and pavement friction contributed to a reduction in wet surface and rear-end collisions in tangent segments, and in wet surface and sideswipe in curves. For wet surface collisions, high levels of macrotextures contribute to increased water drainage from the pavement surface, which contributes to maintaining contact between tires and the pavement. For rear-end and sideswipe collisions, greater pavement friction also contributes to maintaining contact between tires and the pavement in situations that require braking and cornering maneuvers.

The influence of grade showed that collisions increased on flat road segments on rear-end and dry surface collisions in tangent segments, and single vehicle, sideswipe, and dry collision in curves. This result can be also related to drivers' behaviors and their

perception of safety. In particular, driving in good conditions and in situations with a low level of task difficulty, such as driving on flat road segments, that requires fewer driving maneuvers than, for example, uphill or downhill driving, which requires more attention for braking and accelerating maneuvers. In a good and comfortable driving situation, drivers may reduce attention to driving and become more distracted, which affects their response to critical situations.

The influence of pavement condition on fatal and injury and PDO collisions showed that the condition of the pavement was not significant, and that pavement friction contributed to an increase in these types of collisions. This result is fairly controversial because greater levels of pavement friction are related to increase of drivers' control of vehicle which increases safety. However, the lack of correlation of pavement friction and collision severity can be also related to drivers' behaviours that can be more relevant to collision severity than the condition of pavement surface. The positive influence of pavement friction on collision severity agreed with the findings that fatal and injury and PDO collision frequencies were greater for pavement in good condition.

Another explanation for the positive influence of pavement friction on collision severity can be related to the satisfactory levels of skid resistance and macrotexture of the road segments in the data sample. In the sample, the majority of the levels of skid resistance and macrotexture were above the minimum recommended by road agencies, which are considered satisfactory values of skid resistance for investigatory and maintenance purposes. It is possible that pavement with lower levels of friction would have had a different influence if data with lower levels of friction had been considered.

Thus, it can be concluded that pavements in good condition may have a negative

influence on road safety because of how they influence drivers' behaviours and perceptions of road safety. Specifically, when road conditions are good drivers may feel a false sense of security and be more likely to get distracted by other activities that reduce their focus on the road and their driving ability. Conversely, driving on pavements in fair condition may not give the same perception of safety and ease, and so drivers may pay more attention to the road and the vehicle instead of getting distracted, which may result in collisions.

5.4 Results and Study Limitations

The analyses of pavement condition on road safety for tangent segments of rural arterial highways using statistical analysis and regression models were comparable for the majority of collision classes. The results indicated that collision frequency and collision rates were lower for pavements in fair condition and greater for pavements in poor and good condition. The results differed for the fatal and injury and dry surface collision classes.

For fatal and injury collisions using the regression models for tangent segments, pavements in poor condition exhibited the lowest collision frequency, while using statistical analysis, pavements in poor condition exhibited the greatest collision rates. In both approaches, pavements in fair condition exhibited the lowest collision rates. Similar results were found for collision on dry surface condition.

The discrepancy in the results of fatal and injury, and dry surface collisions using different approaches can be related to differences in data sample. The sample used for statistical analysis included arterial highways of multiple lanes with traffic volume (AADT) greater than 200,000, while the sample used for development of regression

models that used included two-lane highways with traffic volume lower than 33,000. Further, the models for two-lane highways were developed separately for tangent segments and curves, while the statistical analyses combined tangent segments and curves. It is possible that road geometry and traffic have affected results.

The influence of pavement texture macrotexture showed that collision rates were greater for pavements with low level of macrotexture. The regression models showed that macrotexture and pavement friction contributed to a reduction in wet surface and rear-end collisions in tangent segments, and in wet surface and sideswipe collisions in curves. Thus, it is possible to conclude that macrotexture is an important indicator of pavement condition related to road safety.

The results of the influence of pavement condition on road safety might have some limitations and the findings might not be generalized to highways outside the province because there are factors that make this study specific to Ontario provincial highways. These factors included standards, guidelines, and manuals specific to the Ontario highways, for example:

- The data collected network level by ARAN and LWT followed standards defined by MTO that may not be the same standard for data collection adopted by other transportation agencies.
- The pavement distress collected by ARAN and its configuration may not be the same used by other transportation agencies. The ARAN's configuration and settings were defined to meet the requirements for data collection of pavement distress that were defined by the manuals and practices adopted by the MTO. For example, the indicators of pavement distress collected by the

ARAN were set to agree with the indicators of pavement distress defined in the Manual for Condition Rating of Flexible Pavements: Distress Manifestations (MTO, 2016b).

- The Ontario highways were designed based on standards defined by the Canadian Transportation Agency (TAC, 1999) and the Geometric Design Standards for Ontario Highways (MTO, 1985). These standards define design parameters for highway design that may differ from the parameters used by other transportation agencies.
- The calculation of DMI and PCI used in this study were based on parameters define by MTO. However, these indicators may slightly differ from the DMI and PCI calculated by MTO due to the missing information about distress that were not collected by ARAN but are considered in the MTO's calculation of DMI and PCI.

Finally, this study did not include human factors as explanatory variables. It is possible that the inclusion of variables related to human characteristics could assist in explaining the correlation between collisions and pavements in good condition. Thus, the results of this study must be considered with an understanding of its limitations.

5.5 Summary

This chapter investigated the influence of pavement condition and macrotexture on road safety using statistical analyses for comparison of collision rate medians and development of regression models for estimating collision means. Four regression models were developed using safety-related variables that included, pavement condition, macrotexture, pavement friction, grade, and traffic.

The results of the analysis showed that collision rates and collision frequency were greater for pavements in poor and good condition than for pavements in fair condition. The influence of macrotexture showed that collision was greater in pavements with a low level of macrotexture and greater levels of macrotexture contributed to a reduction in sideswipe, rear-end and wet surface collisions. Pavement friction contributed to a reduction in rear-end collisions. Grade contributed to an increase in rear-end and dry surface collisions. Traffic contributed to an increase in collisions for all collision classes.

6 Chapter: Conclusions and Recommendations

This Chapter summarizes the main findings of this research. The highlights of the literature review, and most important conclusions are summarized and reported in Chapter 4 that investigated factors affecting pavement friction and skid resistance modelling, and Chapter 5 that investigated the influence of pavement condition on road safety. This chapter also presents the main contributions of this work to existing knowledge and makes recommendations for further research.

6.1 Summary of Key Findings

Chapter 4 investigated factors that affect skid resistance and macrotexture and developed regression models to predict skid resistance. The main findings were as follows:

- Skid resistance measured with LWT and macrotexture measured with ARAN were not correlated. Therefore, it is not possible to include pavement friction into pavement management without measuring skid resistance with LWT.
- Pavement age only was not sufficient to explain skid resistance and macrotexture performance over time. Skid resistance and macrotexture alternated between increasing and decreasing over periods of two and three years. This performance could be influenced by traffic and pavement distress
- Skid resistance decreased as traffic and loads increased, and macrotexture increased as traffic and loads increased. Skid resistance and macrotexture increased with the increase of pavement distress.
- Skid resistance and macrotexture differed noticeably across the various types of mixes. Mixes with higher percentage of fine aggregates, such as

Superpaves and HL4, exhibited greater skid resistance means than mixes with higher percentage of coarse aggregates, such as SMA mixes. SMA exhibited the highest levels of macrotexture, while Superpave mixes exhibited the lowest levels of macrotexture.

The results of the investigation of factors that affected skid resistance and macrotexture showed that traffic, pavement age, pavement distress, and type of mixes influenced skid resistance and macrotexture. Thus, these are important factors to be considered in pavement friction management.

Predictive models for skid resistance were developed for new and aged pavements. The skid resistance model for new pavements exhibited an R-square of 0.623, while the model for aged pavements exhibited an R-square of 0.782. In the models, the variable related to traffic and loads showed a negative influence on skid resistance. Pavement age, mix gradation, and pavement distress showed a positive influence on skid resistance. This result suggested that increased pavement deterioration caused by traffic loading and pavement distress affected pavement textures by changing the spatial arrangement of aggregates.

Chapter 5 investigated the influence of pavement condition and macrotexture on road safety. The main findings were as follows:

- For arterial highways, collision rates were greater in pavements in poor condition and with a low level of macrotexture. The influence of pavement condition and macrotexture was more noticeable in fatal and injury and sideswipe collisions. For these two classes of collisions, collision rates were two to six times greater for pavements in poor condition and with a low level

of macrotexture than for pavements in fair and good condition and with a medium or high level of macrotexture.

- For freeways, collision rates were lower for pavement in fair condition than for pavement in poor and good condition. Collision rates were greater for pavements in poor condition for fatal and injury, sideswipe, rear-end, and wet surface. Collision rate was greater for pavement in good condition for PDO. Collision rates were similar for single vehicle and dry surface.

The regression models for two-lane rural highways showed that pavement condition was statistically significant for tangent segments, but it was not statistically significant for curves. The regression models for tangent segments showed that collision means were greater for pavements in poor and good condition than for pavements in fair condition.

The regression models showed that high levels of macrotexture and pavement friction contributed to a reduction in wet surface and rear-end collisions in tangent segments and to a reduction in sideswipe and wet surface collisions on curves. This result suggest that high level of macrotexture and pavement friction contributed to increased water drainage from the pavement surface, which contributed to maintain contact between tires and the pavement, especially in situations that required breaking and cornering maneuvers.

The results of the regression models suggest that collisions are more likely due to drivers' behaviour and their response to situations that require control of the vehicle than to pavement condition. For example, pavements in poor condition may cause damage to the vehicle that affects the driver's control and their reaction to unexpected situation (e.g.,

swerving to avoid a pothole). Meanwhile, pavements in good condition, may give drivers the over confidence to make unsafe maneuvering decisions, exceed speed limits, and to allow themselves to become distracted while driving. However, pavements in fair condition that exhibit signs of deterioration and deformations may cause discomfort to drivers prompting them to remain more vigilant.

6.2 Contributions to Existing Knowledge

In summary, the results obtained from this research offer three main contributions to existing knowledge:

Through an investigation of factors that affect pavement friction, this research showed that pavement aging has little impact on friction variation if aging is not related to increased traffic and pavement distress. There are few studies that related pavement friction and pavement distress. Thus. this study contributes to a better understanding of pavement friction performance and its correlation with the operational condition of roads.

Through an investigation of the influence of pavement condition on road safety, this research showed that collision rates and collision frequency were greater on pavement in poor and good condition than on those in fair condition. This finding can be used to support road agencies to develop safety policies and guidelines to raise drivers' awareness of the risks of excessive speeding and distracted driving. Further, this finding can be used to encourage road agencies and automakers to increase cars' safety feature standards. Currently, there are a variety of driver assistance systems, such as lane-keeping assist, hands-off wheel detection, brake assist, and fatigue monitors, all of which may contribute to increasing driver safety, but are not a widely adopted standard for all car manufactures.

Through an investigation of the influence of macrotexture on road safety, this research showed that collision rates were greater for pavements with macrotexture lower than 0.5 mm on wet and dry surfaces. Further, macrotexture was an important factor in the reduction of rear-end, sideswipe, and wet surface collisions. This finding can be used to guide road agencies to develop policies for road construction, maintenance, and road safety.

6.3 Recommendation for Future Research

The data available for the investigation of factors affecting pavement friction and skid resistance modelling was limited to three years.

Further research is needed to examine the correlation between skid resistance, macrotexture, mix gradation, and aggregate properties, as well as the influence of mineral hardness, abrasion, and physical and geometrical characteristics (e.g., angularity, shape, and texture) of aggregates

Additional data of skid resistance, macrotexture, and pavement condition should be collected to increase model accuracy and model validation. Further, additional data should be collected to investigate skid resistance performance over time. It is recommended to use historical data measured at the same sites for a sequence of years (immediately after construction and before maintenance services), instead of cross-sectional data obtained from different sites within a few years. It is also recommended to record the environmental conditions of the roads during the measurements of skid resistance, as it would contribute to identifying seasonal variation of skid resistance.

The statistical models developed in this research were restricted to tangent segments and curves. It is recommended to investigate the influence of pavement

condition and pavement friction on situations that demand braking maneuvers, such as at intersections. It is also recommended to develop models for two-lane and multilane highways and freeways that include geometric features of the roads, such as curve radius, medians, number of lanes, and roadside elements.

It is recommended to include human factor characteristics and vehicle dynamics as explanatory variables in the development of road safety analysis. The inclusion of human factors may provide evidence that there is correlation between drivers' behaviour and collisions in good pavements. The inclusion of vehicle dynamics may also contribute to detecting driving maneuvers and drivers' behaviour.

It is also recommended to collect and record pavement skid resistance, pavement condition data, and collision data in a more consistent format to facilitate data integration. For skid resistant measurements, it is recommended to install a GPS in the LWT to collect and record skid resistance measurements with geographic coordinates. For multilane highways, it is recommended to collect skid resistance and pavement condition indicators on the same lane to increase data accuracy.

Finally, for collision data, it is recommended to record collision locations using geographic coordinates and also the lane and direction of traffic. These recommendations would increase data accuracy and facilitate the integration of collision, skid resistance, and pavement condition data.

References

Abd El Halim, A. O. (2009). *Improvement to Highway Safety through Network Level Friction Testing and Cost-Effective Pavement Maintenance* (Doctoral dissertation, University of Waterloo). Retrieved from http://hdl.handle.net/10012/5172

Ahammed, M. A., & Tighe, S. (2008). Long term and seasonal variations of pavement surface friction. In *Proceedings of the 2008 Annual Conference of the Transportation Association of Canada (TAC), Toronto, Ontario, CD-ROM*.

Ahammed, M. A. (2009). *Safe, Quiet and Durable Pavement Surface* (Doctoral dissertation, University of Waterloo). Retrieved from http://hdl.handle.net/10012/4290

Ahammed, M. A., & Tighe, S. (2012). Asphalt pavements surface texture and skid resistance – exploring the reality. *Canadian Journal of Civil Engineering, 39*, 1–9. doi:10.1139/l11-109

Al-Masaeid, H. R. (1997). Impact of pavement condition on rural road accidents. *Canadian Journal of Civil Engineering*, *24*, 523–531.

American Association of State Highway and Transportation Officials. (2008). AASHTO: Guide for Pavement Friction. Washington, DC, United States of America: American Association of State Highway and Transportation Officials.

American Association of State Highway and Transportation Officials. (2017). AASHTO M323: Standard specification for Superpave volumetric mix design. Washington, DC, United States of America: American Association of State Highway and Transportation Officials.

American Society for Testing and Materials. (2009). ASTM E1845–151: Standard Practice for Calculating Pavement Macrotexture Mean Profile Depth. West Conshohocken, PA, USA: American Society for Testing and Materials.

American Society for Testing and Materials. (2009). ASTM E1911–09: Standard Test Method for Measuring Paved Surface Frictional Properties Using the Dynamic Friction Tester. West Conshohocken, PA, USA: American Society for Testing and Materials.

American Society for Testing and Materials. (2012a). ASTM D5340–12: Standard Test Method for Airport Pavement Condition Index Surveys. West Conshohocken, PA, USA: American Society for Testing and Materials.

American Society for Testing and Materials. (2012b). ASTM E867–06: Standard Terminology Relating to Vehicle – Pavement Systems. West Conshohocken, PA, USA: American Society for Testing and Materials.

American Society for Testing and Materials. (2013). ASTM E303–93: Standard Test Method for Measuring Surface Frictional Properties Using the British Pendulum Tester. West Conshohocken, PA, USA: American Society for Testing and Materials.

American Society for Testing and Materials. (2015a). ASTM E1960–07: Standard Practice for Calculating International Friction Index of a Pavement Surface. West Conshohocken, PA, USA: American Society for Testing and Materials

American Society for Testing and Materials. (2015b). ASTM E524–08: Standard Specification for Standard Smooth Tire for Pavement Skid–Resistance Tests. West Conshohocken, PA, USA: American Society for Testing and Materials.

American Society for Testing and Materials. (2015c). ASTM E1859/E1859M–11: Standard Test Method for Friction Coefficient Measurements Between Tire and Pavement Using a Variable Slip Technique. West Conshohocken, PA, USA: American Society for Testing and Materials.

American Society for Testing and Materials. (2015d). ASTM E2101–15: Standard Test Method for Measuring the Frictional Properties of Winter Contaminated Pavement Surfaces Using an Averaging – Type Spot Measuring Decelerometer. West Conshohocken, PA, USA: American Society for Testing and Materials.

American Society for Testing and Materials. (2015e). ASTM E2157–15: Standard Test Method for Measuring Pavement Macrotexture Properties Using the Circular Track Meter. West Conshohocken, PA, USA: American Society for Testing and Materials.

American Society for Testing and Materials. (2015f). ASTM E2380/E2380M–15: Standard Test Method for Measuring Pavement Texture Drainage Using an

Outflow Meter. West Conshohocken, PA, USA: American Society for Testing and Materials.

American Society for Testing and Materials. (2015g). ASTM E274/E274M–15: Standard Test Method for Skid Resistance of Paved Surfaces Using a Full – Scale Tire. West Conshohocken, PA, USA: American Society for Testing and Materials.

American Society for Testing and Materials. (2015h). ASTM E501–08: Standard Specification for Standard Rib Tire for Pavement Skid – Resistance Tests. West Conshohocken, PA, USA: American Society for Testing and Materials.

American Society for Testing and Materials. (2015i). ASTM E670–09: Standard Test Method for Testing Side Force Friction on Paved Surfaces Using the Mu-Meter. West Conshohocken, PA, USA: American Society for Testing and Materials.

American Society for Testing and Materials. (2015j). ASTM N E965–15: Standard Test Method for Measuring Pavement Macrotexture Depth Using a Volumetric Technique. West Conshohocken, PA, USA: American Society for Testing and Materials.

American Society for Testing and Materials. (2018). ASTM E303–93: Standard Test Method for Measuring Surface Frictional Properties Using the British Pendulum Tester. West Conshohocken, PA, USA: American Society for Testing and Materials.

Anastasopoulos, P. C., Tarko, A. P., & Mannering, F. L. (2008). Tobit analysis of vehicle accident rates on interstate highways. *Accident Analysis and Prevention*, *40* (2), 768–775.

Anupam, K., Srirangam, S., Scarpas, A., & Kasbergen, C. (2013). Influence of temperature on tire – pavement friction: Analyses. *Transportation Research Record, 2369*, 114–124. doi:10.3141/2369-13

Ashraf M., & Jurgens R. (2000). *International Roughness Index (IRI) – Use & Comparison with other Jurisdictions (asphalt concrete pavements)*. Retrieved from https://open.alberta.ca/dataset/6351771/resource/7d22a447-8e0f-41e2-ba6f-b91a7afd95cc

Austroads. (2003). *Guide to the Selection of Road Surfacing, AP-G-63-03*. Retrieved from https://www.onlinepublications.austroads.com.au/

Bonneson, J. A. (2000). *Superelevation distribution methods and transition designs*, 439. Washington, DC: Transportation Research Board.

Brauner, N., & Shacham, M. (1999). Considering error propagation in stepwise polynomial regression. *Industrial & engineering chemistry research, 38*(11), 4477–4485.

British Standard. (2006). BS 7941–1: Methods for Measuring the Skid Resistance of Pavement Surfaces. Sideway-Force Coefficient Routine Investigation Machine. British Standards Institution, Bristol, UK.

Buddhavarapu, P., Banerjee, A., & Prozzi, J. A. (2013). Influence of pavement condition on horizontal curve safety. *Accident Analysis and Prevention*, *52*, 9–18. doi: http://dx.doi.org/10.1016/j.aap.2012.12.010

Burningham, S., & Stankevich, N. (2005). Why road maintenance is important and how to get it done The World Bank, Washington DC Transport Note No. *TRN-4 June*.

Canadian Strategic Highway Research Program. (1999). *Summary of Pavement Smoothness Specifications in Canada and Around the World*. Ottawa, ON: Transportation Association of Canada. Retrieved from http://www.cshrp.org/products/BR-16-E.PDF.

Cenek, P. D., Henderson, R. J., Forbes, M., Davies, R. B., & Tait, A. (2014). *The relationship between crash rates and rutting, 545*. Retrieved from http://www.nzta.govt.nz/resources/research/reports/545/

Chamorro, A., Tighe, S. L., Li, N., & Kazmierowski, T. (2010). Validation and Implementation of Ontario, Canada, Network-Level Distress Guidelines and Condition Rating.*Transportation Research Record: Journal of the Transportation Research Board*, *2153*(1), 49–57. doi:10.3141/2153-06.

Chamorro, A., Tighe, S. L., Li, N., & Kazmierowski, T. J. (2009). Development of Distress Guidelines and Condition Rating to Improve Network Management in Ontario, Canada. *Transportation Research Record: Journal of the Transportation Research Board*, *2093*(1), 128–135. doi:10.3141/2093-15.

Chan, C. Y., Huang, B., Yan, X., & Richards, S. (2009). Effects of Asphalt Pavement Conditions on Traffic Accidents in Tennessee Utilizing Pavement Management System. *Transportation Research Board 88th Annual Meeting, 09–2054*. Retrieved from https://trid.trb.org/view/881528

Chan, S., Cui, S., Lee, S. (2016). Transition from Manual to Automated Pavement Distress Data Collection and Performance Modelling in the Pavement Management System. In *Conference and Exhibition of the Transportation Association of Canada Conference of the Transportation Association of Canada*, Toronto, ON.

Chen, X., Steinauer, B., & Yang, J. (2014). Non-Contact Methods to Predict Skid Resistance of Wet Pavement. In *Design, Analysis, and Asphalt Material Characterization for Road and Airfield Pavements*, 25–31.

Chong, G. J., Phang, W. A., & Wrong, G. A. (1989). *Manual for condition rating of flexible pavements: distress manifestations*. Downsview: Ontario Ministry of Transportation.

Cordoş, N., Todoruţ, A., & Barabás, I. (2017). Evaluation of the Tire Pressure Influence on the Lateral Forces that Occur between Tire and Road. In *IOP Conference Series: Materials Science and Engineering, 252*(1), 012011. IOP Publishing.

Cummings, P. (2010). *Modeling the Locked-Wheel Skid Tester to Determine the Effect of Pavement Roughness on the International Friction Index*. (Master Dissertation, University of South Florida). Retrieved from https://scholarcommons.usf.edu/ etd/1604/

Design Manual for Roads and Bridges. (2015). DMRB: Pavement Design and Maintenance. Section 3. Pavement Maintenance Assesment. Part 1. HD 28/15 Skidding Resistance, 7. The Stationay Office. Retrived from http://www.official documents.co.uk/document/deps/ ha/dmrb/index.htm gives access to the Highways Agency's DMRB documents

Dinno, A. (2015). Nonparametric Pairwise Multiple Comparisons in Independent Groups using Dunn's test. *Stata Journal*, *15*, 292–300.

Doumiati, M., Victorino, A., Charara, A., & Lechner, D. (2010). A Method to Estimate the Lateral Tire Force and the Sideslip Angle of a Vehicle: Experimental Validation. In *proceedings of the 2010 American Control Conference*, Baltimore, 6936–6942.doi: 10.1109/ACC.2010.5531319

Ech, M., Morel, S., Yotte, S., Breysse, D., & Pouteau, B. (2009). An Original Evaluation of the Wearing Course Macrotexture evolution using Abbot Curve. *Road Materials and Pavement Design, 10*, 471–494. doi:10.3166/RMPD.10-471-494.

El Gendy, A. (2008). *Characterization of Pavement Surface Texture using Photometric Stereo Techniques*. (Doctoral Dissertation, University of Manitoba). Retrieved from https://search-proquest-com.proxy.library.carleton.ca/docview/305050179?pq-origsite=summon

Elghriany, A. (2016). *Investigating Correlations of Pavement Conditions with Crash Rates on In-Service U.S. Highway (*Doctoral Dissertation, University of Akron). Retrieved from https://etd.ohiolink.edu/

Elkin, B. L., Kercher, K. J., & Gulen, S. (1979). *Seasonal Variation of Skid Resistance of Bituminous Surfaces in Indiana*. Indiana State Highway Commission, Research and Training Center. Retrieved from http://onlinepubs.trb.org/Onlinepubs/trr/1980/777/777-008.pdf

Elvik, R., Vaa, T., Erke, A., & Sorensen, M. (2009). *The Handbook of Road Safety Measures* (2nd ed.). Bingley, UK: Emerald Group Publishing.

Environmental Systems Research Institute. (2017). ArcMap (Version 10.6) [Computer software]. Redlands, CA.

Ergun, M., Iyinam, S., & Iyinam, A. F. (2005). Prediction of Road Surface Friction Coefficient Using Only Macro- and Microtexture Measurements. *Journal of Transportation Engineering, 131*(4), 311–319. doi:10.1061/(ASCE)0733-947X (2005)131:4(311).

Federal Highway Administration. (2005). *Technical Advisory T 5040.36 Surface Texture for Asphalt and Concrete Pavements*. Retrieved from United States Department of Transportation – Federal Highway Administration: Retrieved from https://www.fhwa.dot.gov/pavement/t504036.cfm.

Federal Highway Administration. (2009). *Pavement Distress Identification Manual for the NPS Road Inventory Program*. United States Department of Transportation – Federal Highway Administration. Retrieved from http://www.wistrans.org//mrutc/files/Distress-ID-Manual.pdfn

Federal Highway Administration. (2014). *Highway Performance Monitoring System (HPMS) Field Manual*. United States Department of Transportation – Federal Highway Administration. Retrieved from https://www.fhwa.dot.gov/ohim/hpmsmanl/appe.cfm

Federal Highway Administration. (2015). *Evaluation of Pavement Safety Performance (FHWA-HRT-14-065)*. United States Department of Transportation – Federal Highway Administration. Retrieved from https://www.fhwa.dot.gov/publications/research/safety/14065/index.cfm

Fernandes, A., & Neves, J. (2014). Threshold Values of Pavement Surface Properties for Maintenance Purposes Based on Accident Modelling. *International Journal of Pavement Engineering, 15*(10), 917–924. Retrieved from http://dx.doi.org/10.1080/10298436.2014.893324.

Fernando, E. G., Musani, D., Park, D. W., & Liu, W. (2006). *Evaluation of Effects of Tire Size and Inflation Pressure on Tire Contact Stresses and Pavement Response* (No. FHWA/TX-06/0-4361-1). Austin, Texas. Retrieved from http://tti.tamu.edu/documents/0-4361-1.pdf

Flintsch, G. W., Al-Qadi, I. L., McGhee, K., and Davis, R. (2002). Effect of HMA Design Properties on Pavement Surface Friction. In *Proceedings of 3rd International Symposium*. Guimarães, Portugal.

Flintsch, G. W., McGhee, K. K., Najafi, S., & de Léon Izeppi, E. (2012). *The Little Book of Tire Pavement Friction*. Pavement Surface Properties Consortium, 1. Retrieved from https://www.apps.vtti.vt.edu/1-agers/CSTI_Flintsch/

Fotios, S., & Gibbons, R. (2018). Road lighting Research for Drivers and Pedestrians: The Basis of Luminance and Illuminance Recommendations. *Lighting Research & Technology*, *50*(1), 154–186. Retrieved from https://doi.org/10.1177/1477153517739055

Fuentes, L. G., Gunaratne, M., de Léon Izzepi, E., Flintsch, G. W., & Martinez, G. (2012). Determination of Pavement Macrotexture Limit for Use in International Friction Index Model. Transportation Research Record: *Journal of the Transportation Research Board, 2306*, 138–143.

Fugro. (2018). ARAN-Automatic Road Analyser. Retrieved from https://www.fugro.com/our-services/asset-integrity/roadware/aran-automatic-road-analyzer

Fwa, T. F., Pasindu, H. R., & Ong, G. P. (2011). Critical Rut Depth for Pavement Maintenance Based on Vehicle Skidding and Hydroplaning Consideration. *Journal of Transportation Engineering*, *138*(4), 423–429.

Garber, N. J., & Hoel, L. A. (2015). *Traffic and Highway Engineering* (5th ed.). Stamford, USA: Cengage Learning.

Gelman, A., & Imbens, G. (2018). Why High-Order Polynomials Should Not Be Used in Regression Discontinuity Designs. *Journal of Business & Economic Statistics*, 1–10. Retrieved from https://amstat.tandfonline.com/doi/abs/10.1080/07350015.2017.

Gibbons, J. D. (1993). *Nonparametric statistics: An introduction*. Newbury Park, CA: Sage.

Glennon, J. C., & Hill, P. F. (2004). *Roadway Safety and Tort Liability* (2nd ed.). Tucson, AZ: Lawyers & Judges.

Goodman, S. N. (2009). *Quantification of Pavement Textural and Frictional Characteristics Using Digital Image Analysis* (Doctoral Dissertation, Carleton University). Retrieved from https://curve.carleton.ca/4f709639-2175-4cca-95d0-d39a2baee147

Goodman, S., Hassan, Y., & El Halim, A. (2006). Preliminary estimation of asphalt pavement frictional properties from superpave gyratory specimens and mix parameters. *Transportation Research Record: Journal of the Transportation Research Board, 1949*, 173–180.

Government of Canada. (2017). *Road Transportation*. Retrieved from https://www.tc.gc.ca/eng/policy/anre-menu-3021.htm

Grivas, D. A., Schultz, B. C., & Waite, C. A. (1992). Determination of pavement distress index for pavement management. *Transportation Research Record*, *1344*, 75-80.

Guiggiani, M. (2014). The Science of Vehicle Dynamics. *Pisa, Italy: Springer Netherlands*.

Gunaratne, M., Lu, Q., Yang, J., Metz, J., Jayasooriya, W., Yassin, M., & Amarasiri, S. (2012*). Hydroplaning on multilane facilities* (No. BDK84 977-14). Federal Highway Administration, Washington, DC. Retrieve from http://trid.trb.org/view/1238517.

Hair, J. F., Black, W. C., Babin, B. J., & Anderson, R. E. (2015). *Multivariate Data Analysi*s (7th ed.). New Delhi, India: Pearson Educational Limited.

Hall, J. W., & Hanna, A. N. (2009). *Guide for pavement friction: Background and research*. Washington, DC: Transportation Research Board.

Hall, J. W., Smith, K. L., Titus-Glover, L., Wambold, J. C., Yager, T. J., & Rado, Z. (2009). Guide for pavement friction. *Final Report for NCHRP Project*, *1*, 43.

Haas, R., Hudson, W. R., & Falls, L. C. (2015). *Pavement Asset Management*. Salem, MA: Scrivener Publishing LLC.

Hauer, E. (2015). *The Art of Regression Modeling in Road Safety* (1st ed.). New York: Springer International Publishing.

Hein, D., & Croteau, J. M. (2004). The Impact of Preventive Maintenance Programs on the Condition of Roadway Networks. In *Proceedings: 2004 Annual Conference of the Transportation Association of Canada*, 19–22.

Henry, J. J. (2000). *Evaluation of Pavement Friction Characteristics*. Washington, DC: Transportation Research Board.

Highways Agency (2005). *Interim Advice Notes: Traffic speed condition surveys: Revised assessment criteria (IAN 42/05).* Retrieved from http://www.standardsforhighways.co.uk/ha/standards/dmrb/index.htm

Hoemer, T. E., & Smith, K. D. (2002). *High performance concrete pavement: pavement texturing and tire – pavement noise*. (No. FHWA-IF-02-020) Washington, DC: U. S. Department of Transportation.

Hussein, N., & Hassan, R. (2017). Surface condition and safety at signalised intersections. *International Journal of Pavement Engineering*, *18* (11), 1016–1026.

International Business Machines Corporation. (2015). SPSS Statistics for Windows (Version 23.0) [Computer Software]. Armonk, NY: IBM Corp.

International Organization for Standardization. (1984). ISO 4287–1: Surface roughness –Terminology – Part 1: Surface and its parameters. Geneva, Switzerland.

International Organization for Standardization. (1984). ISO 4287–2: Surface roughness Terminology – Part2: Measurement of surface roughness parameters. Geneva, Switzerland.

International Organization for Standardization. (2002). ISO 13473–2: Characterization of pavement texture by use of surface profiles – Part 2: terminology and basic requirements related to pavement texture profile analysis. Geneva, Switzerland.

International Transport Forum (2015). *Road Safety Annual Report 2015*. Paris: OECD Publishing. Retrieved from https://doi.org/10.1787/irtad-2015-en.

Jackett, M., & Frith, W. (2013). Quantifying the impact of road lighting on road safety—A New Zealand study. *IATSS Research*, *36*(2), 139–145.

Jannat, G.-E., & Tighe, S. L. (2015). Performance Based Evaluation of Overall Pavement Condition Indices for Ontario Highway. In *2015 Conference of the Transportation Association of Canada*. Charlottetown, PEI: TAC.

Jayawickrama, P., & Thomas, B. (1998). Correction of field skid measurements for seasonal variations in Texas. *Transportation Research Record: Journal of the Transportation Research Board, 1639*, 147–154.

Jiang, X., Huang, B., Zaretzki, R. L., Richards, S., & Yan, X. (2013). Estimating safety effects of pavement management factors utilizing Bayesian random effect models. *Traffic injury prevention*, *14*(7), 766–775.

Jo, Y., & Ryu, S. (2015). Pothole detection system using a black-box camera. *Sensors 15* (11), 29316-29331. Retrieved from http://doi.org.proxy.library.carleton.ca/10.3390/s151129316

Kalina J., Jarkovský J., Dušek L., Klánová J., Borůvková J., Šnábl. I., Šmíd. R. (2014). Time series assessment in the Era of Stockholm Convention & GMP.

Masaryk University. Retrieved from http://www.genasis.cz/time-series/index.php

Kamel, N., & Gartshore, T. (1982). Ontario's Wet Pavement Accident Reduction Program. In *Pavement Surface Characteristics and Material.* ASTM International STP763.

Kandhal, P., & Parker, F. J. (1998). *Aggregate Tests Related to Asphalt Concrete Performance in Pavements.* National Cooperative Highway Research Program Report 405. Washington: Transportation Research Board, National Research Council.

Kassem, E., Ahmed, A., Masad, E. A., & Little, D. N. (2013). Development of Predictive Model for Skid Loss of Asphalt Pavements. *Journal of the Transportation Research Board, 2372*, 83-96. doi:10.3141/2372-10

Kazmierowski, T. J., He, Z., & Kerr, B. (2001, August). A Second-Generation PMS for the Ministry of Transportation of Ontario. In *Fifth International Conference on Managing Pavements Washington State Department of Transportation Foundation for Pavement Preservation International Society for Asphalt Pavements Federal Highway Administration Transportation Research Board*. Retrieved from https://trid.trb.org/view/793792.

Kebrle, J., & Walker, R. (2007). Texture measurement and friction estimation using laser data acquisition and neural networks. In *Proceedings of the 9th WSEAS*.

Kowalski, K. J., McDaniel, R. S., Shah, A., & Olek, J. (2009). Long-term monitoring of noise and frictional properties of three pavements. *Transportation Research Record*: *Journal of the Transportation Research Board*, *2127*, 12–19.

Kummer, H. (1966). *Unified Theory of Rubber and Tire Friction* (1st ed.). College of Engineering, Pennsylvania State, University: University Park, PA.

Kummer, H., & Meyer, W. (1962). Measurement of skid resistance. In *Symposium on Skid Resistance*. ASTM International.

Lavin, P. (2003). *Asphalt Pavements: A practical guide to design production, and maintenance for engineers and architects* (1st ed.). New York: CRC Press.

Lee, J., Nam, B., Abdel-Aty, M. (2015). Effects of Pavement Surface Conditions on Traffic Crash Severity. *Journal of Transportation Engineering,* 10.1061/(ASCE)TE.1943-5436.0000785, 04015020

Leu, M. C., & Henry, J. J. (1978). Prediction of Skid Resistance as Function of Speed from Pavement Texture Measurements. *Journal of Transportation Research Board, 666*, 7–13.

Li, S., Noureldin, S., & Zhu, K. (2003). *Upgrading the INDOT pavement friction testing program.* Joint Transportation Research Program, Indiana Department of Transportation, Indianapolis, IN.

Li, S., Noureldin, S., & Zhu, K. (2010). *Macrotexture and Microtexture Testing Using Laser Sensors*. Joint Transportation Research Program, Indiana Department of Transportation and Purdue University, West Lafayette, Indianapolis, IN.

Li, Y., & Huang, J. (2014). Safety impact of pavement conditions. *Transportation Research Record*, *2455*, 77–88. doi:10.3141/2455-09

Li, Y., Liu, C., & Ding, L. (2013). Impact of pavement condition on crash severity. *Accident Analysis and Prevention, 59*, 399–405.

Lu, Q., & Steven, B. (2006). *Friction Testing of Pavement Preservation Treatments: Literature Review.* CALTRANS, California Department of Transportation.

Madli, R., Hebbar, S., Pattar, P., & Golla, V. (2015). Automatic detection and notification of potholes and humps on roads to aid drivers. *IEEE Sensors Journal*, *15*(8), 4313-4318. Retrieved from https://ieeexplore.ieee.org/abstract/document/7072547/

Masad, E., Luce, A., & Chowdhury, A. (2007). *Relationship of Aggregate Texture to Asphalt Pavement skid Resistance using Image Analysis of Aggregate Shape* (*Final Report for Highway IDEA Project*, *114)*. Retrieved from http://onlinepubs.trb.org/onlinepubs/archive/studies/idea/finalreports/highway/NCHRP114Final_Report.pdf

Matson, J. E., & Huguenard, B. R. (2017). Evaluating aptness of a regression model. *Journal of Statistics Education*, *15*(2). Retrieved from https://amstat.tandfonline.com/doi/abs/10.1080/10691898.2007

Mayora, J. M., & Pina, R. J. (2009). An assessment of the skid resistance effect on traffic safety under wet-pavement condition. *Accident Analysis and Prevention, 41*, 881–886.

McCullough, B. F., & Hankins, K. D. (1966). Skid resistance guidelines for surface improvements on Texas highways. *Highway Research Record*, *131*. Retrieved from https://trid.trb.org/view/104805

McDaniel, R. S., & Kowalski, K. J. (2012). *Investigating the Feasibility of Integrating Pavement Friction and Texture Depth Data in Modeling for INDOT PMS*. Joint Transportation Research Program, Indiana Department of Transportation and Purdue University, West Lafayette, Indianapolis, IN.

Meegoda, J. N., & Gao, S. (2015). Evaluation of pavement skid resistance using high speed texture measurement. *Journal of Traffic and Transportation Engineering, 2* (6), 382–390.

National Cooperative Highway Research Program. (1972). *Skid Resistance, NCHRP Synthesis of Practice N°14*. Washington, DC.

National Highway Traffic Safety Administration. (2019). *Policy Statement and Compiled FAQs on Distracted Driving*. Retrieved from http://www.nhtsa.gov.edgesuite-staging.net/Driving+Safety

National Highway Traffic Safety Administration. (2017, March). *Traffic Safety Notes*. Retrieved from https://www.nhtsa.gov/sites/nhtsa.dot.gov/files

Ningyuan, L., Kazmierowski, T., & Koo, A. (2011). Key Pavement Performance Indicators and Prediction Models Applied in a Canadian PMS. In *8th International Conference on Managing Pavement Assets*. Santiago, Chile (No. ICMPA064). Retrieved from https://www.worldcat.org/title/8th-international-conference-on-managing-pavement-assets-15-19-november-2011-santiago-chilie-proceedings/oclc/769647513

Ningyuan, L.(2009). *Development of a New Pavement Distress Evaluation Guide for Ontario Ministry of Transportation* [Power Point slides]. Retrieved from https://www.rpug.org/download/Session%206-4-Li%20Ningyuan.pdf

Noyce, D. A., Bahia, H., Yambo, J., Chapman, J., & Bill, A. (2007). Incorporating road safety into pavement management: Maximizing surface friction for road safety

improvements. *Work*, *005*. Retrieved from https://minds.wisconsin.edu/bitstream/handle/1793/53397/04-04_Final.pdf?sequence=1

Oliver, J. W. H. (1989). Seasonal Variation of Skid Resistance in Australia. *Special Report No. 37.*, Vermont South, VIC: Australia Road Research Board.

Ontario Ministry of Transportation. (1985). *Geometric Design Standards for Ontario Highways*. Downsview, ON: Survey and Design Office.

Ontario Ministry of Transportation. (2007). *The Formulations to Calculate Pavement Condition Indices*. Downsview, ON: Pavement and Foundation Section.

Ontario Ministry of Transportation. (2009). *Location Referencing Data Standards – Version 1.1*. Downsview, ON.

Ontario Ministry of Transportation (2012). *Ontario's Default Parameters for AASHTOWare Pavement ME Design – Interim Report*. Downsview, ON.

Ontario Ministry of Transportation (2013). *Highway Access Management Guideline*. St. Catharines, ON.

Ontario Ministry of Transportation (2016a). *Brake force trailer unit connected to a standard MTO fleet truck*. Retrieved from http://www.mto.gov.on.ca/graphics/english/publications/road-talk/

Ontario Ministry of Transportation (2016b). *Manual for Condition Rating of Flexible Pavement – SP-024*. Downsview, ON: Material Engineering and Research Office.

Ontario Ministry of Transportation (2016c). Smart Pavement Rehabilitation Decisions using Concise Pavement Condition Data. *Road talk*, 22. Retrieved from http://www.mto.gov.on.ca/english/publications/road-talk/road-talk-22-spring.shtml

Ontario Provincial Standard Specification (2013). *Material Specification for Aggregates – Hot Mix Asphalt (OPSS. PROV 1003)*. Retrieved from http://www.raqsb.mto.gov.on.ca/techpubs

Ontario Road Safety Annual Reports. (2012). *Ontario Road Safety Annual Report 201*2. Retrieved from http://www.mto.gov.on.ca/english/publications/pdfs/ontario-road-safety-annual-report-2012.pdf.

PAVER (2014). PAVER Pavement Management Software. Retrieved from http://www.paver.colostate.edu/.

Permanent International Association of Road Congresses (1987). Report of the Committee on Surface Characteristics, In *Proceedings of the 18th World Road Congress*. Brussels, Belgium.

Permanent International Association of Road Congresses. (1995). *International PIARC Experiment to Compare and Harmonize Texture and Skid Resistance Measurements*. PIARC Technical Committee on Surface Characteristics C.1. Paris, France.

Pulugurtha, S. S., Kussam, P. R., & Patel, K. J. (2010). Assessing the Role of Pavement Macrotexture in Preventing Crashes on Highways. *Traffic Injury Prevention, 11* (1), 96-103.

R. (2014). A language and environment for statistical computing. R Foundation for Statistical Computing (Version 3.1.0) [Computer software]. Vienna, Austria. Retrieved from http://www.R-project.org.

Rado, Z. (2009). *Evaluating performance of limestone prone to polishing (No. FHWA-PA-2009-022-510401-015*). University Park, PA, USA: Commonwealth of Pennsylvania, Department of Transportation.

Rajaei, M., Sefidmazgi, N., & Bahia, H. (2014). Establishment of Relationship Between Pavement Surface Friction and Mixture Design Properties. *Transportation Research Record: Journal of the Transportation Research Board, 2457*, 114–120.

Rezaei, A. (2010). *Development of a prediction model for skid resistance of asphalt pavements.* (Doctoral Dissertation, Texas A&M University). Retrieved from http://proxy.library.carleton.ca/login?url=http://search.proquest.com.proxy.library.carleton.ca/docview/856907476?accountid=989.

Rezaei, A., Masad, E., & Chowdhury, A. (2011). Development of a Model for Asphalt Pavement Skid Resistance Based on Aggregate Characteristics and Gradation. *Journal of Transportation Engineering*, *137* (12), 863–873. doi:10.1061/(ASCE)TE.1943-5436.0000280

Roberts, F. L., Kandhal, P. S., Brown, E. R., Lee, D. Y., & Kennedy, T. W. (1996). Hot mix asphalt materials, mixture design and construction. Hot Mix Asphalt Materials, Mixture Design, and Construction. National Asphalt Paving Association Education Foundation. Lanham, MD.

Rodríguez, G. (2013). Lecture Notes on Generalized Linear Models. URL: http://data.princeton.edu/wws509/notes/

Roe, P. G., Webster, D. C., & West, G. (1991). The relation between the surface texture of roads and accidents. Transport and Road Research Laboratory (TRRL). Wokingham, Berkshire, United Kingdom.

Said, D., Abd El Halim, A. O., & Pais, J. C. (2008). Study of the causes and remedies of premature surface cracking of asphalt pavements. In *EPAM3–3rd European Pavement and Asset Management Conference*, 1-15. Retrieved from https://repositorium.sdum.uminho.pt/handle/1822/16684

Sakai, H., & Araki, K. (1999). Thermal engineering analysis of rubber vulcanization and tread temperatures during severe sliding of a tire. *Tire Science and Technology*, *27*(1), 22–47.

Salkind, N. J. (2010). *Encyclopedia of Research Design*. Thousand Oaks, CA, USA: Sage.

SAS Institute Inc. (2015). SAS/STAT® 14.1 *User's Guide*. Cary, NC: SAS Institute Inc. Retrieved from https://support.sas.com/documentation/cdl/en/statug/68162/HTML/default/viewer.htm

Sayers, M. W., Gillespie, T. D., & Paterson, W. D. O. (1986). *Guidelines for Conducting and Calibrating Road Roughness Measurements*, World Bank Technical Paper Number 46, the World Bank, Washington DC.

Serigos, P., de Fortier Smit, A., & Prozzi, J. (2014). Incorporating Surface Microtexture in the Prediction of Skid Resistance of Flexible Pavements. *Transportation Research Record: Journal of the Transportation Research Board*, *2457*, 105–113.

Shaffer, S. J., Christiaen, A. C., & Rogers, M. J. (2006). *Assessment of Friction-Based Pavement Methods and Regulations (No. DTFH61-03-X-00030)*. Retrieved from http://www.ntrci.org/ntrci-24-2006-009.

Sharif Tehrani, S., Cowe Falls, L., & Mesher, D. (2017). Effects of pavement condition on roadway safety in the province of Alberta. *Journal of Transportation Safety & Security*, *9*(3), 259–272. doi. 10.1080/19439962.2016.1194352

Smith, R. H. (2008). *Analyzing friction in the design of rubber products and their paired surfaces*. Boca Raton, USA: CRC Press.

Snyder, M. B. (2006). *Pavement Surface Characteristics – A Synthesis and Guide*. American Concrete Pavement Association, Skokie, Illinois, No. EB235P. Retrieved from https://trid.trb.org/view/811732

Srinivasan, R., & Bauer, K. (2013). Safety performance function development guide: Developing jurisdiction-specific SPFs. *FHWA, Washington, DC*.

Standards Australia. (2012). Australian Standard WA 310.1: Pavement Skid Resistance: British Pendulum Method. Main Roads Western Australia, Waterloo Crescent, East Perth, http://www.wa.gov.au

Swanlund, M. (2005). Surface texture--noise and safety issues related to concrete pavements. In *PowerPoint presentation from TRB Annual Meeting*. *Federal Highway Administration*. Washington, DC. 2005.

Tighe, S., Li, N., Falls, L. C., Haas, R. (2000). Incorporating road safety into pavement management. *Transportation Research Record*. 1*699*(1), 1–10. Retrieved from https://doi.org/10.3141/1699-0

Transport Canada. (2012). *Transportation in Canada 2011, Comprehensive review. Ottawa: Minister of Public Works and Government Services*. Retrieved from https://www.tc.gc.ca/media/documents/policy/Transportation_in_Canada_2011.pdf

Transportation Association of Canada (TAC). (1999). Geometric Design Guide for Canadian Roads, TAC, Ottawa, Ontario, 1999.

Transportation Research Board. (2006). Tires and Passenger Vehicle Fuel Economy. *TR News*. Retrieved from http://onlinepubs.trb.org/onlinepubs/

Vaiana, R., Capiluppi, G. F., Gallelli, V., Iuele, T., & Minani, V. (2012). Pavement surface performances evolution: an experimental application. *Procedia-Social and Behavioral Sciences*, *53*, 1149–1160.

Voigt, A. P., Fenno, D. W., & Borchardt, D. W. (2003). *Evaluation of vehicle speeds on freeway-to-freeway connector ramps in Houston* (Vol. 4318, No. 1). Texas Transportation Institute, Texas A & M University System.

Wallman, C.-G., & Astrom, H. (2001). *Friction Measurement Methods and Correlation Between Road Friction and Traffic Safety. A Literature Review*. Linkoping: Swedish National Board and Transport Research Institute.

Wambold, J. C. (1988). Road characteristics and skid testing. *Transportation Research Record*, *1196,* 294–299. Retrieved from http://onlinepubs.trb.org/Onlinepubs/trr/1988/1196/1196.pdf

Wang, H. (2006). *Road Profiler Performance Evaluation and Accuracy Criteria Analysis*. (Master Dissertation, Virginia Polytechnic Institute and State University). Blacksburg, Virginia.

Washington State Department of Transportation. (2004). Pavement Guide. Module 9: Pavement Evaluation. Washington State Department of Transportation. Retrieved from http://training.ce.washinghton.edu/WSDOT

Xie, J. (2010). *Automated Skid Number Evaluation Using Texture Laser Measurement*. (Doctoral Dissertation, University of Houston). Retrieved from https://search.proquest.com/openview/145f9b82138c377f45f07eecaf9afcd9/1?pq-rigsite=gscholar&cbl=18750&diss=y

Zaniewski, J., & Mason, C. (2006). *Evaluation of Non-Polishing Aggregate Criteria for Various Traffic Levels and Low-Speed Road Conditions*. Morgantown, WV: West Virginia University. Retrieved from https://web.statler.wvu.edu

Zeng, H., Fontaine, M. D., & Smith, B. L. (2014). Estimation of the safety effect of pavement condition on rural, two-lane highways. *Transportation Research Record*, *2435*(1), 45–52.

Appendices

Appendix A Individual Distress Weight

Table A.1 Individual Distress Weight for Asphalt Concrete Pavements (Ningyuan, 2009; Chamorro *et al.*, 2009)

DMI		
Distress		**Weight (wi)**
Ravelling and coarse aggregate loss		3
Flushing		1.5
Rippling and Shoving		1
Wheel path rutting		3
Distortion		3
Longitudinal wheel path: single and multiple		1.5
Longitudinal wheel path: alligator		3
Longitudinal meandering and midlane		1
Traverse: half, full and multiple		1
Traverse alligator		3
Centreline: single and multiple		0.5
Centreline: alligator		2
Pavement edge: single and multiple		0.5
Pavement edge: alligator		1.5
Random/Map		0.5
Severity (si)	**Density/Extent (ei)**	Levels **(n)**
Very slight	0 to 20%	1
Slight	20% to 40%	2
Moderate	40% to 60%	3
Severe	60% to 80%	4
Very Severe	80% to 100%	5
DMI_{NT}		
Distress (%)		**Weight (βi)**
Alligator cracking (%)		-0.036
Longitudinal wheel-path crack (%)		-0.015
Non-wheel-path longitudinal crack (%)		-0.016
Transverse crack (%)		-0.021
Potholes (%)		-2.170
Rutting (%)		-0.016
Severity (si)		**Levels (n)**
Slight		0.5
Moderate		1
Severe		2

Appendix B ARAN'S output

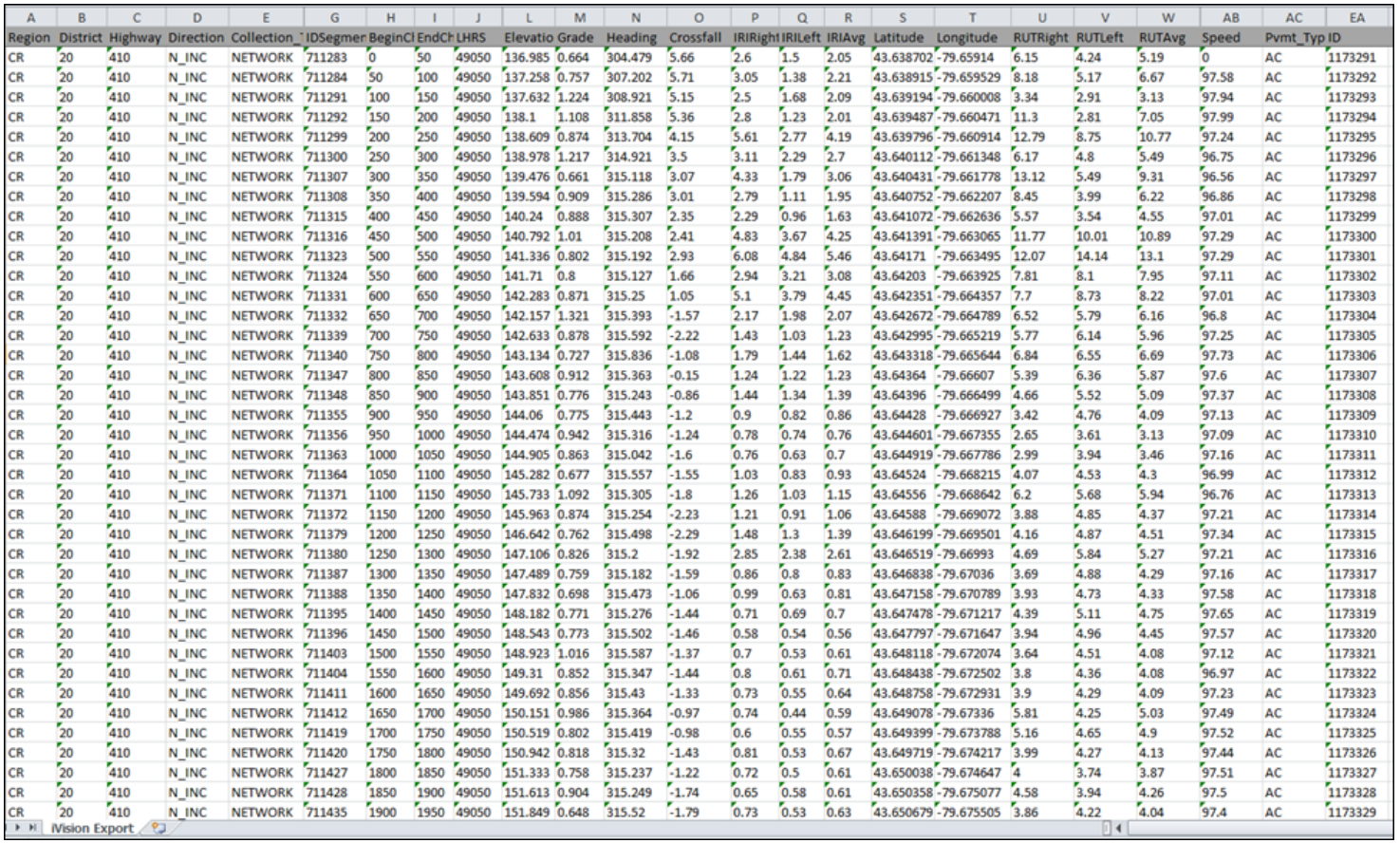

A	B	C	D	E	G	H	I	J	L	M	N	O	P	Q	R	S	T	U	V	W	AB	AC	EA
Region	District	Highway	Direction	Collection_T	IDSegmen	BeginCl	EndCl	LHRS	Elevatio	Grade	Heading	Crossfall	IRIRight	IRILeft	IRIAvg	Latitude	Longitude	RUTRight	RUTLeft	RUTAvg	Speed	Pvmt_Typ	ID
CR	20	410	N_INC	NETWORK	711283	0	50	49050	136.985	0.664	304.479	5.66	2.6	1.5	2.05	43.638702	-79.65914	6.15	4.24	5.19	0	AC	1173291
CR	20	410	N_INC	NETWORK	711284	50	100	49050	137.258	0.757	307.202	5.71	3.05	1.38	2.21	43.638915	-79.659529	8.18	5.17	6.67	97.58	AC	1173292
CR	20	410	N_INC	NETWORK	711291	100	150	49050	137.632	1.224	308.921	5.15	2.5	1.68	2.09	43.639194	-79.660008	3.34	2.91	3.13	97.94	AC	1173293
CR	20	410	N_INC	NETWORK	711292	150	200	49050	138.1	1.108	311.858	5.36	2.8	1.23	2.01	43.639487	-79.660471	11.3	2.81	7.05	97.99	AC	1173294
CR	20	410	N_INC	NETWORK	711299	200	250	49050	138.609	0.874	313.704	4.15	5.61	2.77	4.19	43.639796	-79.660914	12.79	8.75	10.77	97.24	AC	1173295
CR	20	410	N_INC	NETWORK	711300	250	300	49050	138.978	1.217	314.921	3.5	3.11	2.29	2.7	43.640112	-79.661348	6.17	4.8	5.49	96.75	AC	1173296
CR	20	410	N_INC	NETWORK	711307	300	350	49050	139.476	0.661	315.118	3.07	4.33	1.79	3.06	43.640431	-79.661778	13.12	5.49	9.31	96.56	AC	1173297
CR	20	410	N_INC	NETWORK	711308	350	400	49050	139.594	0.909	315.286	3.01	2.79	1.11	1.95	43.640752	-79.662207	8.45	3.99	6.22	96.86	AC	1173298
CR	20	410	N_INC	NETWORK	711315	400	450	49050	140.24	0.888	315.307	2.35	2.29	0.96	1.63	43.641072	-79.662636	5.57	3.54	4.55	97.01	AC	1173299
CR	20	410	N_INC	NETWORK	711316	450	500	49050	140.792	1.01	315.208	2.41	4.83	3.67	4.25	43.641391	-79.663065	11.77	10.01	10.89	97.29	AC	1173300
CR	20	410	N_INC	NETWORK	711323	500	550	49050	141.336	0.802	315.192	2.93	6.08	4.84	5.46	43.64171	-79.663495	12.07	14.14	13.1	97.29	AC	1173301
CR	20	410	N_INC	NETWORK	711324	550	600	49050	141.71	0.8	315.127	1.66	2.94	3.21	3.08	43.64203	-79.663925	7.81	8.1	7.95	97.11	AC	1173302
CR	20	410	N_INC	NETWORK	711331	600	650	49050	142.283	0.871	315.25	1.05	5.1	3.79	4.45	43.642351	-79.664357	7.7	8.73	8.22	97.01	AC	1173303
CR	20	410	N_INC	NETWORK	711332	650	700	49050	142.157	1.321	315.393	-1.57	2.17	1.98	2.07	43.642672	-79.664789	6.52	5.79	6.16	96.8	AC	1173304
CR	20	410	N_INC	NETWORK	711339	700	750	49050	142.633	0.878	315.592	-2.22	1.43	1.03	1.23	43.642995	-79.665219	5.77	6.14	5.96	97.25	AC	1173305
CR	20	410	N_INC	NETWORK	711340	750	800	49050	143.134	0.727	315.836	-1.08	1.79	1.44	1.62	43.643318	-79.665644	6.84	6.55	6.69	97.73	AC	1173306
CR	20	410	N_INC	NETWORK	711347	800	850	49050	143.608	0.912	315.363	-0.15	1.24	1.22	1.23	43.64364	-79.66607	5.39	6.36	5.87	97.6	AC	1173307
CR	20	410	N_INC	NETWORK	711348	850	900	49050	143.851	0.776	315.243	-0.86	1.44	1.34	1.39	43.64396	-79.666499	4.66	5.52	5.09	97.37	AC	1173308
CR	20	410	N_INC	NETWORK	711355	900	950	49050	144.06	0.775	315.443	-1.2	0.9	0.82	0.86	43.64428	-79.666927	3.42	4.76	4.09	97.13	AC	1173309
CR	20	410	N_INC	NETWORK	711356	950	1000	49050	144.474	0.942	315.316	-1.24	0.78	0.74	0.76	43.644601	-79.667355	2.65	3.61	3.13	97.09	AC	1173310
CR	20	410	N_INC	NETWORK	711363	1000	1050	49050	144.905	0.863	315.042	-1.6	0.76	0.63	0.7	43.644919	-79.667786	2.99	3.94	3.46	97.16	AC	1173311
CR	20	410	N_INC	NETWORK	711364	1050	1100	49050	145.282	0.677	315.557	-1.55	1.03	0.83	0.93	43.64524	-79.668215	4.07	4.53	4.3	96.99	AC	1173312
CR	20	410	N_INC	NETWORK	711371	1100	1150	49050	145.733	1.092	315.305	-1.8	1.26	1.03	1.15	43.64556	-79.668642	6.2	5.68	5.94	96.76	AC	1173313
CR	20	410	N_INC	NETWORK	711372	1150	1200	49050	145.963	0.874	315.254	-2.23	1.21	0.91	1.06	43.64588	-79.669072	3.88	4.85	4.37	97.21	AC	1173314
CR	20	410	N_INC	NETWORK	711379	1200	1250	49050	146.642	0.762	315.498	-2.29	1.48	1.3	1.39	43.646199	-79.669501	4.16	4.87	4.51	97.34	AC	1173315
CR	20	410	N_INC	NETWORK	711380	1250	1300	49050	147.106	0.826	315.2	-1.92	2.85	2.38	2.61	43.646519	-79.66993	4.69	5.84	5.27	97.21	AC	1173316
CR	20	410	N_INC	NETWORK	711387	1300	1350	49050	147.489	0.759	315.182	-1.59	0.86	0.8	0.83	43.646838	-79.67036	3.69	4.88	4.29	97.16	AC	1173317
CR	20	410	N_INC	NETWORK	711388	1350	1400	49050	147.832	0.698	315.473	-1.06	0.99	0.63	0.81	43.647158	-79.670789	3.93	4.73	4.33	97.58	AC	1173318
CR	20	410	N_INC	NETWORK	711395	1400	1450	49050	148.182	0.771	315.276	-1.44	0.71	0.69	0.7	43.647478	-79.671217	4.39	5.11	4.75	97.65	AC	1173319
CR	20	410	N_INC	NETWORK	711396	1450	1500	49050	148.543	0.773	315.502	-1.46	0.58	0.54	0.56	43.647797	-79.671647	3.94	4.96	4.45	97.57	AC	1173320
CR	20	410	N_INC	NETWORK	711403	1500	1550	49050	148.923	1.016	315.587	-1.37	0.7	0.53	0.61	43.648118	-79.672074	3.64	4.51	4.08	97.12	AC	1173321
CR	20	410	N_INC	NETWORK	711404	1550	1600	49050	149.31	0.852	315.347	-1.44	0.8	0.61	0.71	43.648438	-79.672502	3.8	4.36	4.08	96.97	AC	1173322
CR	20	410	N_INC	NETWORK	711411	1600	1650	49050	149.692	0.856	315.43	-1.33	0.73	0.55	0.64	43.648758	-79.672931	3.9	4.29	4.09	97.23	AC	1173323
CR	20	410	N_INC	NETWORK	711412	1650	1700	49050	150.151	0.986	315.364	-0.97	0.74	0.44	0.59	43.649078	-79.67336	5.81	4.25	5.03	97.49	AC	1173324
CR	20	410	N_INC	NETWORK	711419	1700	1750	49050	150.519	0.802	315.419	-0.98	0.6	0.55	0.57	43.649399	-79.673788	5.16	4.65	4.9	97.52	AC	1173325
CR	20	410	N_INC	NETWORK	711420	1750	1800	49050	150.942	0.818	315.32	-1.43	0.81	0.53	0.67	43.649719	-79.674217	3.99	4.27	4.13	97.44	AC	1173326
CR	20	410	N_INC	NETWORK	711427	1800	1850	49050	151.333	0.758	315.237	-1.22	0.72	0.5	0.61	43.650038	-79.674647	4	3.74	3.87	97.51	AC	1173327
CR	20	410	N_INC	NETWORK	711428	1850	1900	49050	151.613	0.904	315.249	-1.74	0.65	0.58	0.61	43.650358	-79.675077	4.58	3.94	4.26	97.5	AC	1173328
CR	20	410	N_INC	NETWORK	711435	1900	1950	49050	151.849	0.648	315.52	-1.79	0.73	0.53	0.63	43.650679	-79.675505	3.86	4.22	4.04	97.4	AC	1173329

iVision Export

Figure B.1 ARAN's output

Appendix C Average of IRI, MPD, DMI, PCI, and Collisions per Year

Table C.1 Average of IRI, MPD, DMI and PCI by Highway per Year

HWY	Year	Total of LHRS	Length (km)	Mean of Averages			
				IRI	MPD	DMI	PCI
1	2012	51	122.42	1.07	0.9727	10	92
	2013	51	122.42	1.05	0.9182	10	93
	2014	48	120.09	1.07	1.0572	9	87
3	2012	23	109.12	0.99	0.5583	8	82
	2013	31	153.51	1.53	0.9717	8	76
	2014	30	146.27	1.38	1.0649	8	73
6	2012	50	335.94	1.46	0.6212	9	80
	2013	47	334.82	1.41	0.9259	8	77
	2014	48	303.97	2.30	1.0762	8	65
7	2012	70	400.85	1.39	1.2024	9	83
	2013	60	356.85	2.81	1.0798	8	67
	2014	75	412.75	1.59	1.0683	8	68
10	2012	18	110.38	1.50	0.4779	7	66
	2013	15	110.09	1.41	0.8220	8	72
	2014	20	77.48	3.52	1.1228	6	54
11	2013	135	1391.80	1.07	1.2375	8	80
	2014	135	1363.43	1.51	1.2119	8	73
12	2012	19	73.52	1.72	1.1246	9	85
	2013	18	67.62	0.84	1.3891	10	95
	2014	20	67.13	1.38	1.0704	9	86
17	2014	148	1328.78	1.66	1.1475	6	59
21	2012	23	150.35	1.56	0.7294	8	77
	2013	22	147.75	1.22	0.8094	8	79
	2014	23	141.45	1.73	0.4046	8	71
23	2012	8	81.39	1.46	1.3208	8	74
	2013	8	81.39	1.44	1.4561	7	69
	2014	8	81.39	1.25	0.8609	9	83
24	2012	9	45.29	1.89	1.1775	7	63
	2013	9	45.29	2.90	0.8795	8	63
	2014	9	45.29	2.44	1.0781	7	58
26	2012	11	84.92	2.05	0.5070	9	79
	2013	11	84.92	2.51	0.9807	9	75
	2014	11	84.92	2.62	1.1629	6	54
28	2012	18	128.36	1.98	0.8204	7	59
	2013	18	128.36	1.34	0.7634	6	60
	2014	17	126.82	2.53	1.2348	7	58
35	2012	33	145.85	1.28	1.4065	8	71
	2013	34	146.31	1.22	1.4115	7	70
	2014	34	146.31	0.99	1.0834	7	70

41	2012	16	136.71	2.13	0.9056	8	71
	2013	16	136.71	2.29	1.3495	8	71
	2014	16	136.71	1.30	1.3589	7	70
60	2012	23	195.14	1.86	0.9606	8	75
	2013	23	195.14	1.17	1.4099	9	86
	2014	23	195.14	1.83	1.4506	8	71
62	2012	15	131.60	1.36	1.0136	8	76
	2013	15	131.60	1.70	0.9060	8	70
	2014	15	131.60	1.29	1.2035	7	71
63	2012	4	33.50	1.13	0.6018	10	91
	2013	4	33.50	1.15	1.1027	10	91
	2014	4	33.50	1.28	1.2100	8	78
64	2012	11	126.89	1.92	0.7333	7	59
	2013	11	126.89	1.39	1.0915	6	52
	2014	11	126.89	2.47	1.1648	7	60
66	2014	7	71.09	1.31	1.2455	8	79
72	2012	6	68.48	3.89	NA	4	31
	2013	6	68.48	1.01	1.3100	6	63
	2014	6	68.48	1.04	1.4104	5	49
101	2012	23	346.34	1.91	0.1527	8	73
	2013	23	353.94	0.99	0.6558	9	83
	2014	23	351.94	1.60	1.0652	7	63
118	2012	11	91.41	1.43	1.0372	9	88
	2013	11	87.58	1.17	1.0928	10	93
	2014	11	91.41	0.82	1.3396	10	95
141	2012	6	44.38	1.26	0.8743	9	89
	2013	5	43.49	1.22	1.2256	9	89
	2014	6	44.38	1.02	1.2966	8	82
144	2012	10	152.44	2.44	0.5126	8	67
	2013	14	232.54	2.26	0.2865	7	70
	2014	14	232.54	2.13	1.2144	6	52
400	2012	53	221.26	1.17	0.8780	8	76
	2013	53	209.06	1.89	1.2298	8	71
	2014	53	226.37	1.09	1.1391	8	76
401	2013	78	362.31	2.10	1.1822	8	72
	2014	137	615.52	1.66	1.1144	7	69
(NA) = Information not available							

Table C.2 Total Collisions by Highway per Year

HWY	Total Collisions		
	2012	2013	2014
1	3975	4479	2209
3	363	523	292
6	1098	1191	769
7	3356	1639	1136
10	500	503	357
11	2937	1934	NA
12	461	518	258
17	NA	NA	1668
21	300	307	207
23	87	111	92
24	188	174	140
26	291	720	199
28	195	212	151
35	333	370	258
41	122	126	83
60	264	287	225
62	209	293	179
63	60	61	50
64	104	122	30
66	NA	NA	42
72	44	38	28
101	132	131	121
118	136	157	131
141	38	39	33
144	38	260	175
400	3415	2838	2008
401	NA	13338	6574
(NA) = Information not available Total of collisions = 66432			

Appendix D Summary Statistics of the Mean and Variances of SN64R by Highway

Table D.1 Summary of Descriptive Statistics of SN64R by Highway

HWY	Total LHRS	Length (km)	SN64R				
			Min.	Max.	Mean	SD*	N**
1	10	38.56	46	56	52	6.31	95
3	2	19.20	45	52	49	2.12	42
6	10	198.05	39	43	42	3.72	145
7	1	10.70	49	52	51	–	13
9	3	42.80	46	54	51	1.98	52
10	4	38.15	45	47	47	0.82	43
11	13	253.72	52	59	56	1.87	175
17	9	162.77	44	62	58	1.79	102
21	3	42.67	38	42	41	2.01	64
23	1	9.00	42	48	44	2.41	13
26	1	9.70	44	61	54	4.17	18
28	1	10.00	24	51	39	11.24	11
35	4	22.02	50	58	54	3.34	84
40	1	10.08	39	54	49	3.44	13
41	2	18.39	51	57	57	2.13	36
48	1	10.96	48	53	50	1.97	5
60	4	39.95	51	61	54	2.42	70
62	1	7.99	54	60	57	1.94	17
63	1	21.47	54	61	58	2.48	5
64	1	10.20	59	68	61	–	10
66	1	40.20	53	62	58	2.97	11
69	2	20.00	57	62	60	1.68	11
72	1	14.73	56	61	59	1.76	12
89	3	13.40	33	37	36	2.49	66
101	2	41.30	54	62	59	2.01	44
118	1	31.00	57	60	58	1.21	6
124	2	10.20	57	61	59	–	10
141	1	8.00	47	60	57	2.94	18
144	1	17.60	50	61	53	2.78	11
400	3	24.42	47	54	49	2.13	52
401	12	81.36	39	45	41	2.29	121
403	2	14.80	51	55	53	1.02	51
404	1	2.12	45	53	48	2.34	17
409	2	0.72	41	49	46	2.32	18
417	3	50.70	58	62	60	1.13	83
(*) SD = Standard deviation, (**) N = Number of tests.							

Figure D.1 shows a high-low graphic with the ranges of variation of SR64R tests by highway. The graphic shows the upper and lower bounds and means of the of SR64R measured for 110 road segments located on 26 highways. It is observed that approximately 25% of the sample (27 cases) exhibited variances greater than ± 3 units of SN64R and 75% (83 cases) exhibited variances greater than ± 3 units of SN64R. It is also observed that the greatest variation of SN64R were found on highways that exhibited the minimum values of SN64R (HWY 6, 28, 89, and 401).

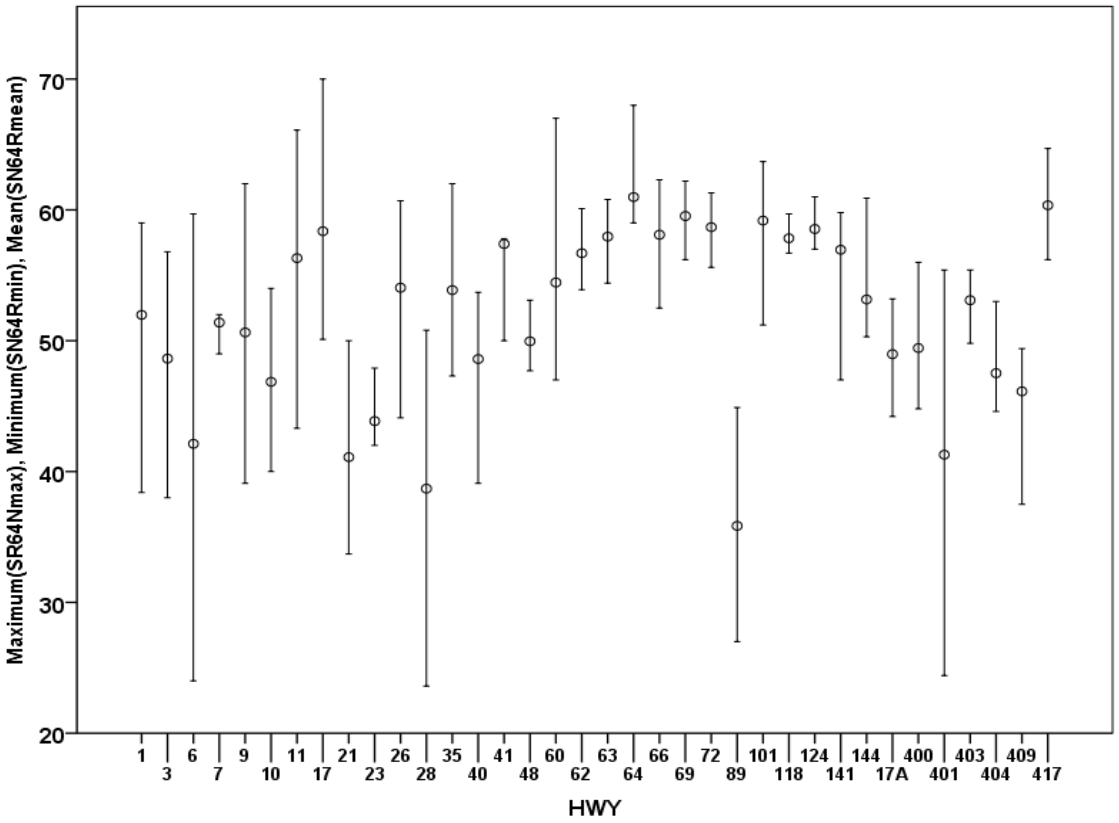

Figure D1. Variance of SR64R by Highway

Appendix E Quadratic Curves of the Relationships between SN64R, MPD, and Pavement Distress

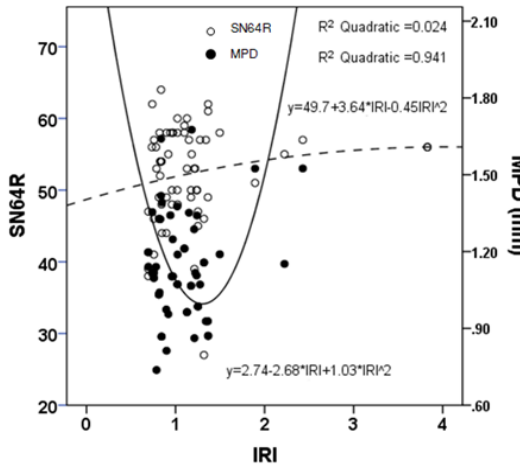

Figure E.1 Relationship between SN64R, MPD, and IRI

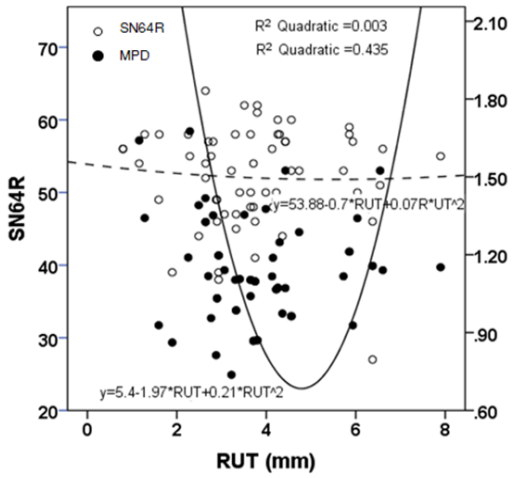

Figure E.2 Relationship between SN64R, MPD, and RUT

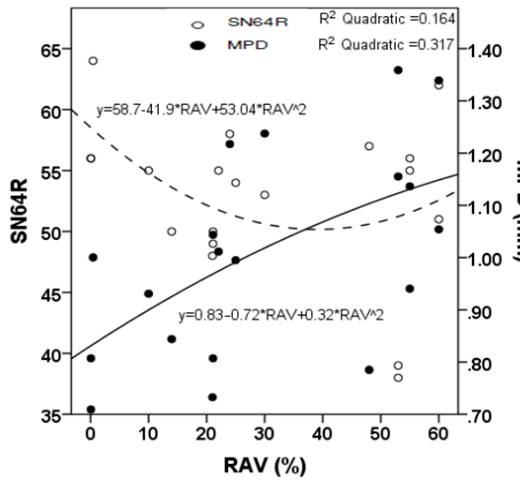

Figure E.3 Relationship between SN64R, MPD, and RAV

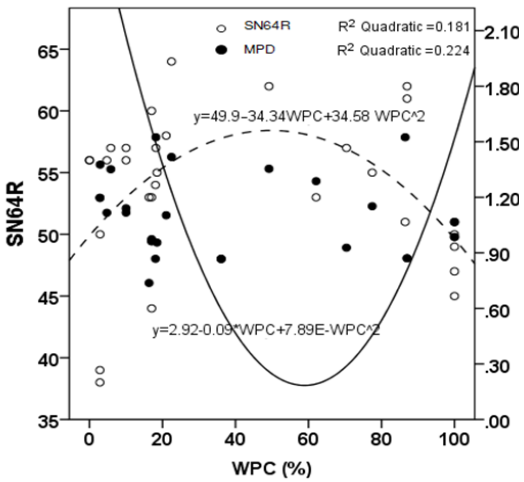

Figure E.4 Relationship between SN64R, MPS, and WPC

Appendix F Nonlinear Regression Analysis of SN64R and Pavement Ages

The relationship between skid resistance and pavement ages was analyzed using piecewise regression. A piecewise regression was selected because it is a nonlinear approach that allows changes in slope without interruption of the line segments, which results a continuous model with structural breaks.

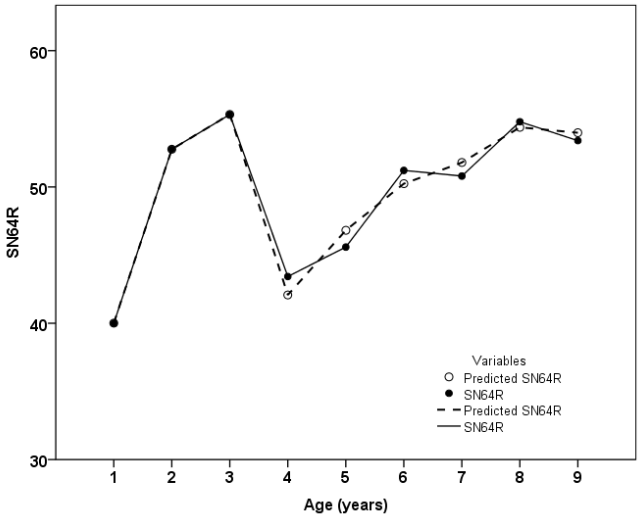

Figure F.1 Piecewise Regression of SN64R and Pavement Ab-section ge

The piecewise approach allowed the inclusion of polynomials of high order and knots, which resulted in an intricate model that describes skid resistance variation over the years. However, piecewise models are not suitable for multivariate modelling because the inclusion of third order polynomials in multivariate regression affect the regression weights of the independent variables and increase errors in the estimated values of the dependent variable (Brauner & Schacham, 1999; Gelman & Imbens, 2018). Further, inferences based on intricate models can be misled (Gelman & Imbens, 2018). Therefore, instead of a single piecewise regression models, the relationship between skid resistance

and pavement age was broken down into two models with polynomials of second order—the first model for pavements three years old or less (new pavements) and the second model for pavement four years old and greater (aged pavements). The polynomials of second order for new and aged pavements are shown on Figure F2 and Figure F3.

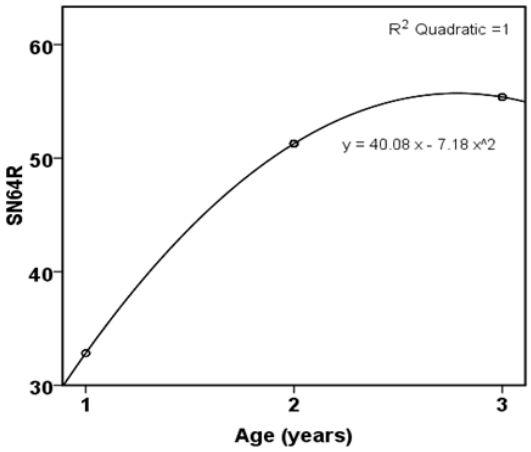

Figure F.2 Polynomial of 2nd Order for New Pavements

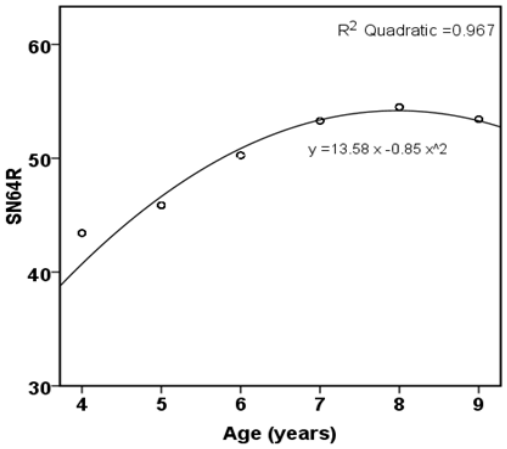

Figure F.3 Polynomial of 2nd Order for Aged Pavements

Appendix G SPSS Outputs for New and Aged Pavements

- **New Pavements**

Table G.1 Model Summary of New Pavements

Model	R	R-Square	Adjusted R-Square	Std. Error of the Estimate
1	0.546	0.299	0.268	6.634
2	0.750	0.563	0.524	5.353
3	0.789	0.623	0.569	5.092
4	0.797	0.635	0.562	5.131
1. Predictors: (Constant), AESAL				
2. Predictors: (Constant), AESAL, Age				
3 Predictors: (Constant), AESAL, Age, RVPC				
4. Predictors: (Constant), AESAL, Age, RVPC, FFi/Co,				
Dependent Variable: SN64R				

Table G.2 ANOVA of Models for New Pavements

Model		Sum of Squares	df	Mean Square	F	p-value
1	Regression	431.081	1	431.081	9.794	0.005
	Residual	1012.359	23	44.016	–	–
	Total	1443.440	24	–	–	–
2	Regression	813.000	2	406.500	14.185	0.000
	Residual	630.440	22	28.656	–	–
	Total	1443.440	24	–	–	–
3	Regression	898.909	3	299.636	11.556	0.000
	Residual	544.531	21	25.930	–	–
	Total	1443.440	24	–	–	–
4	Regression	916.731	4	229.183	8.702	0.000
	Residual	526.709	20	26.335	–	–
	Total	1443.440	24	–	–	–

Table G.3 Coefficients of Models for New Pavements

Model		Unstandardized Coefficients		Standardized Coefficients	p-value	Collinearity Statistics	
		Beta	Std. Error	Beta		Tolerance	VIF
1	Constant	81.43	9.59	–	< 0.001	–	–
	AESAL	-5.31	1.69	-0.55	< 0.05	51.00	1.00
2	Constant	11.94	20.55		0.57	–	–
	AESAL	-2.39	1.58	-0.25	0.14	0.75	1.34
	Age	7.26	1.99	0.59	< 0.001	0.75	1.34
3	Constant	13.84	19.57	–	0.48		
	AESAL	-2.24	1.51	-0.23	0.15	0.74	1.34
	Age	6.97	1.90	0.57	< 0.001	0.74	1.35
	RVPC	2.39	1.32	0.25	0.08	0.98	1.02
4	Constant	13.19	19.74	–	0.51	–	–
	AESAL	-2.30	1.52	-0.24	0.14	0.74	1.34
	Age	7.17	1.93	0.59	< 0.001	0.78	1.37
	RVPC	2.15	1.36	0.22	0.13	0.94	1.07
	FFi/Co	7.03	8.55	0.11	0.42	0.93	1.07

- **Aged Pavements**

Table G.4 Model Summary of Age Pavements

Model	R	R-Square	Adjusted R Square	Std. Error of the Estimate
5	0.763	0.582	0.542	4.674
6	0.864	0.746	0.708	3.731
7	0.884	0.784	0.736	3.548
5. Predictors: (Constant), AESAL, Age				
6. Predictors: (Constant), AESAL, Age, FFi/Co				
7. Predictors: (Constant), AESAL, Age, FFi/Co, RVPC				
Dependent Variable: SN64R				

Table G.5 ANOVA of Model for Aged Pavements

Model		Sum of Squares	df	Mean Square	F	p-value
5	Regression	638.44	2	319.22	14.60	< 0.001
	Residual	458.89	21	21.85	–	–
	Total	1097.33	23	–	–	–
6	Regression	818.87	3	272.95	19.60	< 0.001
	Residual	278.46	20	13.92	–	–
	Total	1097.33	23	–	–	–
7	Regression	858.06	4	214.51	17.03	< 0.001
	Residual	239.27	19	12.59	–	–
	Total	1097.33	23	–	–	–

Table G.6 Coefficients of Model for Aged Pavements

Model		Unstandardized Coefficients		Standardized Coefficients	p-value	Collinearity Statistics	
		Beta	Std. Error	Beta		Tolerance	VIF
5	Constant	86.07	15.81	–	< 0.001	–	–
	AESAL	–5.66	1.13	-0.78	< 0.001	0.82	1.22
	Age	–0.06	0.21	-0.05	0.17	0.82	1.22
6	Constant	67.57	13.63	–	< 0.001	–	–
	AESAL	–3.88	1.03	-0.54	0.001	0.63	1.58
	Age	0.15	0.17	0.11	0.19	0.73	1.37
	FFi/Co	17.89	4.97	0.47	< 0.05	0.76	1.329
7	Constant	78.67	14.40	–	< 0.001	–	–
	AESAL	–4.74	1.09	-0.64	< 0.001	0.50	1.98
	Age	0.05	0.18	0.04	0.17	0.65	1.54
	FFi/Co	15.66	4.89	0.47	< 0.05	0.71	1.41
	RVPC	1.23	0.70	0.22	0.09	0.79	1.26

Appendix H Model Results of Arterial Highways and Freeways

Table H shows a summary of the results of initial attempt of modelling using the dataset that included collision and pavement condition for freeways and arterial highways. The models were tested for five independent variables that included four scaled variables (AADT, Number of Lanes, MPD, and SN) and one categorical variable (PCI).

Table H.1 Summary of Collision Means

Model Specification:

$$\ln(\mu) = \beta_0 + \beta_1 lnAADT + \beta_2 PCI + \beta_3 N°Lanes + \beta_4 lnMPD + \beta_5 SN$$

Collision Class	Variables in the models		Model Goodness of Fit	
	Statistically Significant (p-value ≤ 0.05)	Non–Statistically Significant (p-value > 0.05)	Log Likelihood	AIC
Total collisions	Intercept, AADT	PCI, N° Lanes, SN, MPD	-3561.84	7137.69
PDO	AADT	Intercept, PCI, N° Lanes, SN, MPD	-3196.77	6407.54
Fatal and injury	Intercept, AADT, SN	PCI, MPD, N° Lanes	-1642.653	3299.30
Single vehicle	Intercept, AADT	PCI, N° Lanes, SN, MPD	-2668.78	5351.63
Sideswipe	Intercept, AADT, N° Lanes, SN,	PCI, MPD	-979.88	1973.76
Rear-end	Intercept, AADT, N° Lanes, SN, MPD	PCI	-1487.17	2988.33
Wet	Intercept, AADT	PCI, N° Lanes SN, MPD	-1893.39	3800.79
Dry	Intercept, AADT, N° Lanes	PCI, SN, MPD	-2740.59	5495.19

The results showed that the variable AADT was statistically significant in all models, while the variable PCI and MPD were not statistically significant in the models. This finding indicates that the model specified did not fit the data used. A possible explanation for the lack of fit can be related to data variation due to geometric differences between freeways and arterial highways (e.g., number of lanes, medians) and problems with matching pavement condition measurements and collisions on roads. The pavement condition data have information of the lanes surveyed and direction of traffic, while the collision data did not contain this information.

The problem with coordinating collision and pavement condition in multiple lanes highways may reduce considerably the probability to match satisfactorily collision and pavement condition data. For example, in a four–lane highways the probability to match a collision with the correspondent lane surveyed by ARAN is 25%, while in a two–lane highway the probability increases to 50%. Thus, restricting the study to two–lane highways may increase model accuracy.